DEVELOPING REVERSE GENETIC TOOLS IN WEAKLY ELECTRIC FISH: INVESTIGATING ELECTRIC ORGAN *IN VIVO SCN4AA* FUNCTION THROUGH CRISPR KNOCKOUTS AND MORPHOLINO KNOCKDOWNS

By

Savvas James Constantinou

A DISSERTATION

Submitted to
Michigan State University
in partial fulfillment of the requirements
for the degree of

Zoology- Doctor of Philosophy
Ecology, Evolutionary Biology, and Behavior- Dual Major

2021

ABSTRACT

DEVELOPING REVERSE GENETIC TOOLS IN WEAKLY ELECTRIC FISH: INVESTIGATING ELECTRIC ORGAN *IN VIVO SCN4AA* FUNCTION THROUGH CRISPR KNOCKOUTS AND MORPHOLINO KNOCKDOWNS

By

Savvas James Constantinou

The ability to determine gene function allows research to progress at one of the finest scales in biology and is a goal in electric fish research. Reverse genetics allows researchers to determine gene function and would aid the electric fish community in beginning to answer some of the broadest and most complicated questions in biology such as linking genotype to phenotype and understanding the processes that lead to biological diversity. In this dissertation, I describe the development of two major reverse genetic tools for use in the electric fish system: CRISPR/Cas9 genome editing and morpholinos. To develop these tools, I also produced protocols for *in-vitro* breeding, husbandry, and single-cell embryo microinjections. In the first chapter, I describe *in*-vitro breeding, husbandry, and single-cell embryo microinjections and demonstrate that CRISPR/Cas9 is a promising tool for future electric fish research by targeting nonsense mutations to *scn4aa* in the mormyrid *Brienomyrus brachyistius* and gymnotiform *Brachyhypopomus gauderio*, two independently evolved lineages of weakly electric fish, resulting in a reduction in the electric organ discharge amplitude. In the second chapter, I provide electric fish researchers with a detailed analysis of our many successes and failures applying CRISPR/Cas9 methods to this system and discuss future suggestions on how to best apply them to novel electric fish research. In the third chapter, I describe my efforts to utilize vivo-morpholinos in mormyrid electric fish. While a single early pilot study I performed demonstrated vivo-morpholinos can reduce target gene mRNA levels and cause a phenotypic effect, my efforts to replicate these findings demonstrate inconsistent performance: control vivo-morpholino

and *scn4aa* targeting vivo-morpholino injected fish had indistinguishable effects on electric organ discharge amplitude. Due to additional concerns of toxicity, I suggest morpholinos are not an ideal reverse genetic tool in *Brienomyrus brachyistius* and should only be utilized for future research with caution.

I want to dedicate this work to all the people who supported me and believed in me. I cannot express my gratitude enough to all the friends and colleagues met along the way, my family, and the love of my live, Madi.

ACKNOWLEDGEMENTS

I would like to give special acknowledgements to researchers and individuals who helped me complete this work. I would like to thank Dr. Jason Gallant who helped with project design, analysis, mentorship, and provided tools for EOD capture and analysis and who's laboratory I was a part of since 2015. I would like to specifically mention the technicians that have helped keep fish alive, Katherine Shaw, John Ryan Taylor, and Jared Thompson. Dr. William Pitchers, Colin Diesh, and Dr. Dhruv Sharma were integral to code writing and statistical analysis. Many undergraduates assisted me in data collection for my projects, especially Chapter 3, including Hope Healey, Allison Kwang, Nicole Robichaud, Nicole Thompson, Cassandra Sarria, and Fernando Fernandez. Monica Lucas set the groundwork for developing breeding protocols in the Gallant lab and Dr. Frank Kirschbaum and Linh Nguyen helped to improve squeezing protocols. Microinjection was developed from protocols that Dr. Jose Cibelli and Gabriella Saldana provided to the Gallant laboratory. Vielka Salazar brought *Brachyhypopomus gauderio* to the Gallant laboratory and helped develop the CRISPR protocol. Gallant laboratory members past and present deserve acknowledgements for their assistance throughout my tenure in the Gallant lab and for their constructive feedback including Dr. Sophie Picq, Dr. David Luecke, Mauricio Losilla, and Lauren Koenig. I would also like to thank Dr. Jenette Boughman, Dr. Weiming Li, and Dr. Julia Ganz for their support as my committee and for helping to polish my dissertation.

TABLE OF CONTENTS

LIST OF TABLES

LIST OF FIGURES

KEY TO ABBREVIATIONS

°	Degree
DNA	Deoxyribonucleic acid
MO	Morpholino
CRISPR	Clustered regularly interspaced short palindromic repeats
RNA	Ribonucleic acid
RNAi	RNA interference
dsRNA	Double stranded RNA
siRNA	Small interfering RNA
miRNA	MicroRNA
piRNA	Piwi-interacting RNA
mRNA	Messenger RNA
RISC	RNA-inducing silencing complex
EOD	Electric organ discharge
Na^+	Sodium ion
K^+	Potassium ion
sgRNA	Short guide RNA
gRNA	Guide RNA (also known as sgRNA)
DSB	Double-stranded break
NHEJ	Non-homologous end joining
HDR	Homology directed repair
F_0	The individuals directly injected with CRISPR components; Parental generation

F_1	First filial generation
F_2	Second filial generation
GFP	Green fluorescent protein
CpG	Cytosine followed by guanine nucleotide in the 5’ to 3’ direction
5’	The end of a DNA strand with terminal phosphate group on carbon 5
3’	The end of a DNA strand with a terminal hydroxyl group on carbon 3
UTR	Untranslated region
BLAST	Basic local alignment search tool
PCR	Polymerase chain reaction
bp	Base pair
PAM	Protospacer adjacent motif
µ	Micro-
L	Liter
M	Molar
°C	Degree Celsius
min	Minute
s	Second
dNTP	Deoxynucleoside triphosphate
m	Milli-
n	Nano-
g	Gram
$A_{260/280}$	Ratio of absorbance at 260/280 nanometers

h	Hour
%	Percent
EtOH	Ethanol
UV	Ultraviolet
PVC	Polyvinyl chloride
c	Centi-
S	Siemens
pH	Measure of hydrogen atoms in a solution- specifies acidity or basicity
m	Meter
hpf	Hours post fertilization
SES	Sperm extender solution
IVF	*In vitro* fertilization
dpf	Days post fertilization
pre-mRNA	Precursor mRNA
k	Kilo-
N	Sample size
qPCR	Quantitative PCR
™	Trademark
WT	Wild type
≥	Greater than or equal to
NGS	Next generation sequencing
InDel	Insertion/deletion

TILLING Targeting Induced Local Lesions IN Genomes

INTRODUCTION

Understanding gene function is a problem that, when solved, can help to understand the basic mechanisms of life. Determining what function a stretch of DNA provides an organism is a difficult task that can be accomplished through reverse genetics. In this section I will help the reader to understand the history of functional genetics, what reverse genetics is, and some of the tools utilized to determine the gene function of a targeted genomic region. I briefly introduce electric fish and how studying the electric organ and electric organ discharge has led a community to begin to explore some broad biological phenomena. I end this section by discussing a question in electric fish research that has been left unanswered for decades, and how reverse genetic tools may allow the electric fish community to begin to understand that process. In presenting this information, I demonstrate why I sought to develop reverse genetic tools in electric fish during my dissertation work.

Functional Genomics

History of functional genetics

The goal of functional genetics is to understand the function of single genes and gene variants (Marchetti *et al.*, 2012). There are two major approaches in functional genetics: forward and reverse strategies. Forward genetics is the 'blind' generation of phenotypic variants with a mutagen, and phenotypic variants of interests are then studied to identify which genetic mutations are responsible for the phenotypic changes seen. In reverse genetics, a specific DNA sequence is targeted, the product of that DNA sequence (*e.g.* protein, functional RNA, *etc*) is altered, and the resulting phenotype can be assessed (Hardy *et al.*, 2010). In either strategy, once

a phenotypic change is associated with a particular genomic region, it is possible to assign a function to the DNA sequence.

There is a vast amount of sequencing data available for genomic regions that have no known function. For example, 23%, 40%, and 33% of all kinases, phosphatases, and associated factors, respectively, were ascribed unknown function in the well understood *Drosophila melanogaster* genome as recently as 2020 (Wu *et al.*, 2020). Reverse genetics allows for the possibility of these genes with unknown functions to be assigned a function. Linking gene function to DNA sequence identity results in a positive feedback system in multiple research areas. As the link between sequence data and gene function improves, the refinement of gene discovery (Katz, Baltz and Baltz, 2016; Ramharack and Soliman, 2018), assigning unknown gene function (Rubin *et al.*, 2015), and uncovering cis-regulatory elements (Bartlett *et al.*, 2017) becomes more robust. If more resources are devoted to reverse genetic tools and studies, it will be easier to assign gene functions to novel sequencing data and may eventually improve understanding of even the human genome.

Reverse genetics and forward genetics originally both relied on the same principles but differed in their application. Forward genetics tools produce many random mutations in unspecified regions of the genome. These mutants were often created by chemical mutagens (Brusick, 1983; Crebelli *et al.*, 1986; Wu *et al.*, 2005) or insertional mutagenesis (Parks *et al.*, 2004). Insertional mutagenesis occurs when exogenous DNA enters the genome and disrupts gene function by altering open reading frames or promoters and is generated through transposons and retroviruses which will randomly insert into the genome (Zwaal *et al.*, 1993; Venken and Bellen, 2014). The progeny of the affected individuals is screened for mutations that cause a phenotype, a process that can be tedious and requires a large amount of housing and maintenance

for keeping mutant lines alive. Due to the need for breeding, high throughput screening, and high-resolution sequencing, these tools were reserved for canonical "model organisms" such as *Drosophila*, *Danio*, *Mus*, and *Caenorhabditis elegans* (Cooley, Kelley and Spradling, 1988; Zwaal *et al.*, 1993; Granger, Martin and Ségalat, 2004; Capecchi, 2005; Nord *et al.*, 2006; Duverger *et al.*, 2007; Sivasubbu *et al.*, 2007; Nagayoshi *et al.*, 2008; Amsterdam, Varshney and Burgess, 2011).

The underlying genomic region that was impacted by the mutation is discovered (Amsterdam, Varshney and Burgess, 2011) by identifying where the insertional element is positioned in individuals with a phenotype compared to WT, cloning the flanking genomic DNA, and then identifying the gene from the sequence using a BLAST analysis (Altschul *et al.*, 1997). These untargeted approaches to modifying gene sequence I described above (forward genetics) were applied as a reverse genetics tool: instead of finding mutant phenotypes after mutagenesis and determining where the DNA mutated (forward genetics), DNA would be screened for mutations in a particular region of interest and the phenotype resulting from that mutation was studied (reverse genetics).One hurdle when using insertional mutagenesis or chemically induced mutations in reverse genetics is an incomplete loss of function of the gene of interest; mutagenesis would not often result in a null mutation (Hardy *et al.*, 2010; Kutscher and Shaham, 2014). This complicates downstream applications for assigning function, particularly in non-model organisms where behavior and phenotypes are not well documented and are less easily matched to their underlying genetics. Mutagenesis can also cause mutations in regions of the genome outside the gene of interest and exposed individuals may have no mutagenesis in the region of interest. This is especially problematic from a technical standpoint when testing vertebrate and plant models, which have relatively large genomes compared to organisms like

Drosophila and *C. elegans*; a region of interest is a smaller percentage of the genome when the genome itself is larger and may therefore be harder to target with random insertions or chemical mutagenesis. For example, to ensure that mutations in the gene of interest arose via chemical mutagenesis, a relatively high amount of mutagen had to be used to ensure that at least some of the random insertions would reach the intended target (which is often only a fraction of the entire genome). A high mutagen load causes a high number of mutations to be found outside the gene of interest (Martín *et al.*, 2009). These additional mutations would need to be bred away through outcrossing to isolate individuals with only the mutation of interest who could then be used to produce a stable line. Experiments can be performed to test the function of the targeted regions' gene product(s) after a stable line is produced. Due to difficulties in breeding, husbandry, and performing insertional mutagenesis, non-model organisms were not able to easily be studied through this approach.

To better understand forward and reverse genetics consider a theoretical laboratory that is investigating coloration and patterning in zebrafish at the genetic level (Figure 1). A forward genetics approach would try to produce mutants with a coloration/patterning phenotype and then find the mutated region of DNA responsible for inducing the phenotype. For example (Figure 1A), a forward genetic approach would cause mutations (through chemical mutagenesis or UV radiation) in the germ line of F_0 individuals. Breeding the mutated F_0 and interbreeding the F_1 progeny will result in some F_2 mutants. Of those mutants, by chance, some will have mutations in coloration or patterning that produce a visible phenotype. Those coloration/patterning mutants are then genotyped to uncover the genetic region that is mutated, relative to WT. To isolate the genetic region that is mutated there are multiple approaches including microarrays (Stickney *et al.*, 2002; Jones *et al.*, 2007; Maydan *et al.*, 2009), SNP mapping (Wicks *et al.*, 2001; Stickney *et*

al., 2002), and more commonly, whole-genome sequencing (Sarin *et al.*, 2008; Doitsidou *et al.*, 2010; Zuryn *et al.*, 2010; Obholzer *et al.*, 2012; Sanchez *et al.*, 2017).

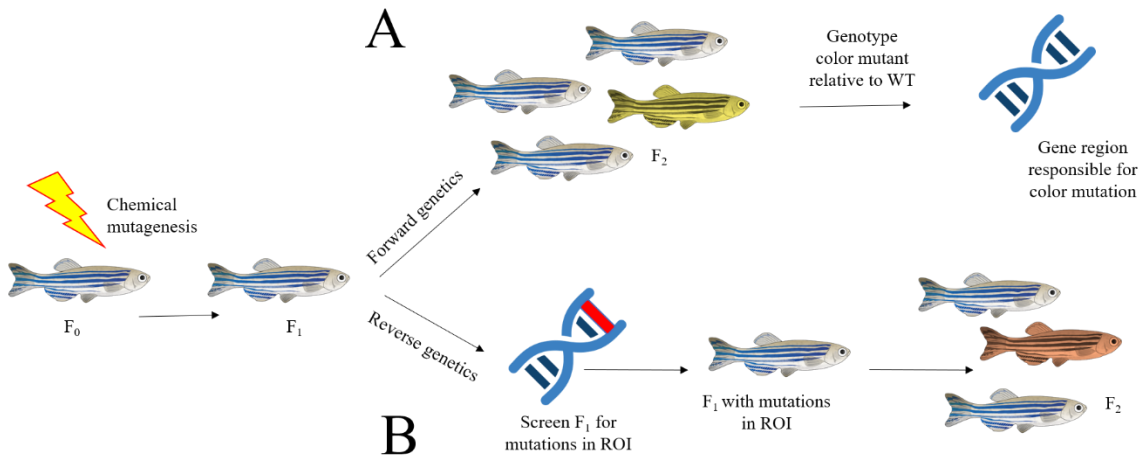

Figure 1: Forward vs reverse genetics. Schematic highlighting the differences and similarities between a forward genetics approach (A) and an early reverse genetics approach (B). In this example, the genetics underlying zebrafish coloration is determined through forward and reverse genetic approaches. In forward genetics, a particular mutant phenotype is produced and the gene region responsible is uncovered (A). In reverse genetics, a particular genomic region is mutated and phenotypes resulting from the mutation are characterized. ROI- Region of interest, WT- Wild type.

A reverse genetics approach would attempt to produce individuals with mutations in a particular genomic region of interest (like a gene) and determine if coloration/patterning mutant phenotypes are present when that region of interest is mutated. For example (Figure 1B), early reverse genetic studies would follow similarly to the forward genetics approach given above; the germlines of F_0 individuals are mutated via chemical or UV radiation to produce F_1 progeny. The F_1 progeny can then be screened to look for mutations in the region of interest through methods like PCR (Jansen *et al.*, 1997; Edgley *et al.*, 2002; Hardy *et al.*, 2010) or TILLING (Targeting Induced Local Lesions IN Genomes) (McCallum *et al.*, 2000; Colbert *et al.*, 2001; Till *et al.*, 2003). Once F_1 progeny are identified that carry mutations in the region of interest, they can be

interbred and F_2 progeny can be screened for non-WT coloration/patterning phenotypes. If any exist, then the region of interest is involved in coloration/patterning in some capacity.

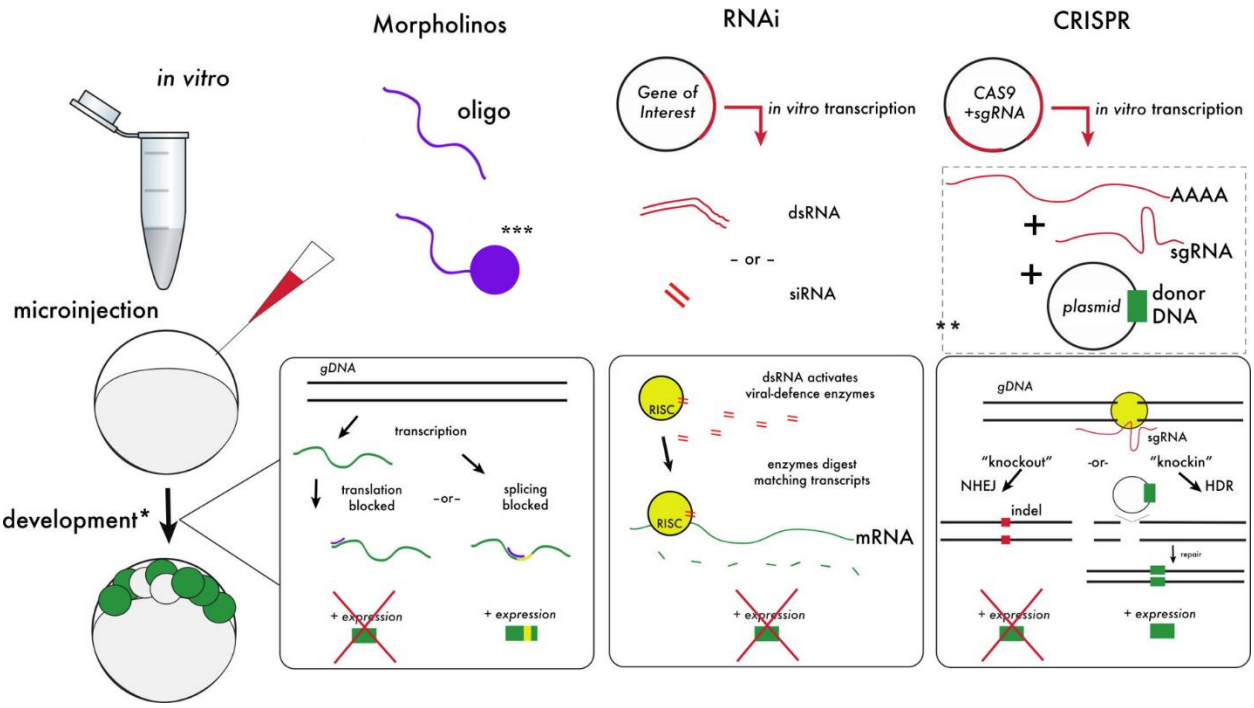

Figure 2: Three common reverse genetics tools. Simplified cartoon illustrations of the mechanisms of Morpholinos (including vivo-morpholinos), RNAi, and CRISPR for modifying phenotype. See text for more comprehensive explanations. RISC-RNA-induced silencing complex. * Knockdown utilizing morpholinos and RNAi can also occur in adult tissues over time. ** CRISPR can also be performed via *in vitro* transcription of just sgRNA and subsequent injection of the sgRNA/Cas9 enzyme complex. *** Vivo-morpholinos are represented with a circle showing the delivery motif. Reprinted and modified with permissions (Pitchers *et al.*, 2016).

The stochastic nature of early forward/reverse genetic tools (Figure 1) was a major impediment to the discovery of gene function. It was not until the late 1990s (Fire *et al.*, 1998) that the first tool, RNA interference (RNAi), would arise that would address many of the issues associated with stochasticity in insertional mutagenesis by utilizing a site directed model. Site directed models cause mutations to arise at specific sites on the genome that are targeted in some way. RNAi, Morpholino (MO), and CRISPR/Cas9 mutagenesis (Clustered Regularly Interspaced Short Palindromic Repeats paired with Cas9 endonuclease) are three reverse genetics tools

(Figure 2) commonly utilized in research settings. Reverse genetic tools can target the genome (*e.g.* insertional mutagenesis, CRISPR) or the transcriptome (*e.g.* RNAi, MOs). While there are additional reverse genetic tools available (like Tol2 transposase), I will focus on RNAi (briefly), MOs, and CRISPR and how these three tools fit different needs.

RNAi

RNAi (RNA interference) is historically the first reverse genetics tool created to address the non-specific nature of previous tools. RNAi was coined as a phrase after feeding bacteria expressing dsRNA against the *C. elegans* gene *unc22* to *C. elegans* and then seeing a phenotypic effect (Fire *et al.*, 1998); RNAi was later discovered to be the same process described as co-suppression nearly a decade earlier in plants (Napoli, Lemieux and Jorgensen, 1990). The RNAi system takes advantage of intrinsic pathways in eukaryotic cells thought to function endogenously in immune response (Fritz, Girardin and Philpott, 2006; Wang *et al.*, 2006; Y. Li *et al.*, 2013) and gene regulation (Lee, Feinbaum and Ambrost, 1993; Palatnik *et al.*, 2003).

As a reverse genetics tool, RNAi is used to transiently knockdown gene expression. RNAi is performed by introducing dsRNA, or noncoding RNAs (siRNA, miRNA, piRNA) specific to the gene of interest into an organism/cell. When the endogenous RNAi pathway is activated, the introduced dsRNA is cut by the enzyme Dicer into small pieces, generating many different siRNAs that target the entire dsRNA sequence. The siRNA is separated into single strands that the cell uses as target sequences that will be complementary to endogenous mRNA. The RNA-inducing silencing complex (RISC) then forms around the single stranded siRNAs and destroys any endogenous RNA that matches in sequence to the siRNAs generated by Dicer or delivered through microinjection (Kim, Han and Siomi, 2009; Alagia and Eritja, 2016), thus knocking down protein expression and altering phenotype (Figure 2- See RNAi). As RNAi

became a more widespread tool, RNAi components were manufactured that allowed for more precise temporospatial control such as light-activated morpholinos and convergent transcription constructs (Tang *et al.*, 2007; Andrews *et al.*, 2014), further refining the tool and increasing the ability to identify gene function.

A major restriction of RNAi as a tool is the level of efficacy in various model and non-model organisms. While many plant and invertebrate systems and most cell cultures respond well to RNAi, vertebrates, especially *Xenopus* and zebrafish (Eisen and Smith, 2008), often show less effectiveness, or none at all *in vivo*, and present with increased off-target effects compared to other organisms.

Morpholinos

To overcome the ineffectuality of RNAi in *Xenopus* and zebrafish, Phosphorodiamidate morpholino oligomers (MOs) were developed. MOs were found to be amendable for knockdown use in a wide variety of organisms; the journal *Genesis* had a full issue (30(3), July 2001) with 28 papers that described this tool use in various organisms. The main advantages of MOs were the ability to use them in these model organisms that were not amenable to RNAi and their capacity to induce phenotypic change via protein knockdowns which target different cellular mechanisms than RNAi ('Targeting zebrafish', 2000).

MOs are small (~25 bp) oligomers with a morpholine ring in the backbone (Figure 3). MOs bind through complementary base pairing ('antisense') to specific RNA sequences, thereby interrupting post-transcriptional processing using an antisense technology (Moulton, 2016). Using MOs, knockdown of the targeted gene product can be achieved (Figure 2- See Morpholinos) by physically blocking the translation of the targeted RNA sequence (translation blocking) or by blocking the spliceosome and altering mRNA splicing (splice blocking).

Translation blocking MOs bind to the 5’ UTR or at the translational start site of the gene of interest (Eisen and Smith, 2008). The mechanism of protein knockdown is initiated when the MO binds to the mRNA of the gene of interest at the 5’ UTR or translational start site. The mRNA bound MO physically blocks the translation initiation complex from forming or scanning properly when bound in the 5’ UTR; subsequently, the large ribosomal subunit is unable to complex with the translation initiation complex and begin translation. The lack of translation stops new protein production, causing any wild type proteins to eventually be destroyed based on the intrinsic protein turnover rate, and results in phenotypes with varying severity (Rana *et al.*, 2006). As the mechanism of translation blocking MOs causes a decrease in protein levels, antibody-based assays are ideal to verify translation blocking MO-induced phenotypes.

Splice blocking MOs are designed to sit across intron/exon boundaries of pre-mRNA. Introns are canonically removed from pre-mRNA before mature mRNA is produced and able to be translated in a process known as splicing. If an MO is bound to both an intron and exon, normal splicing cannot occur and mRNA either retains the intron or removes the exon (Draper, Morcos and Kimmel, 2001; Gebski *et al.*, 2003). The loss of an exon from the mRNA results in a protein that is often missing a functional subunit or misfolds. When an intron is retained in the mRNA, it can alter protein function or proper protein folding and may also lead to truncated proteins via an in-frame stop codon (Morcos, 2007). Intron retention can also lead to mRNA degradation through nonsense-mediated decay (Ward *et al.*, 2014). Any altered proteins generated from MO use are unable to function as they would normally, and the lack of wild type protein produces an altered phenotype.

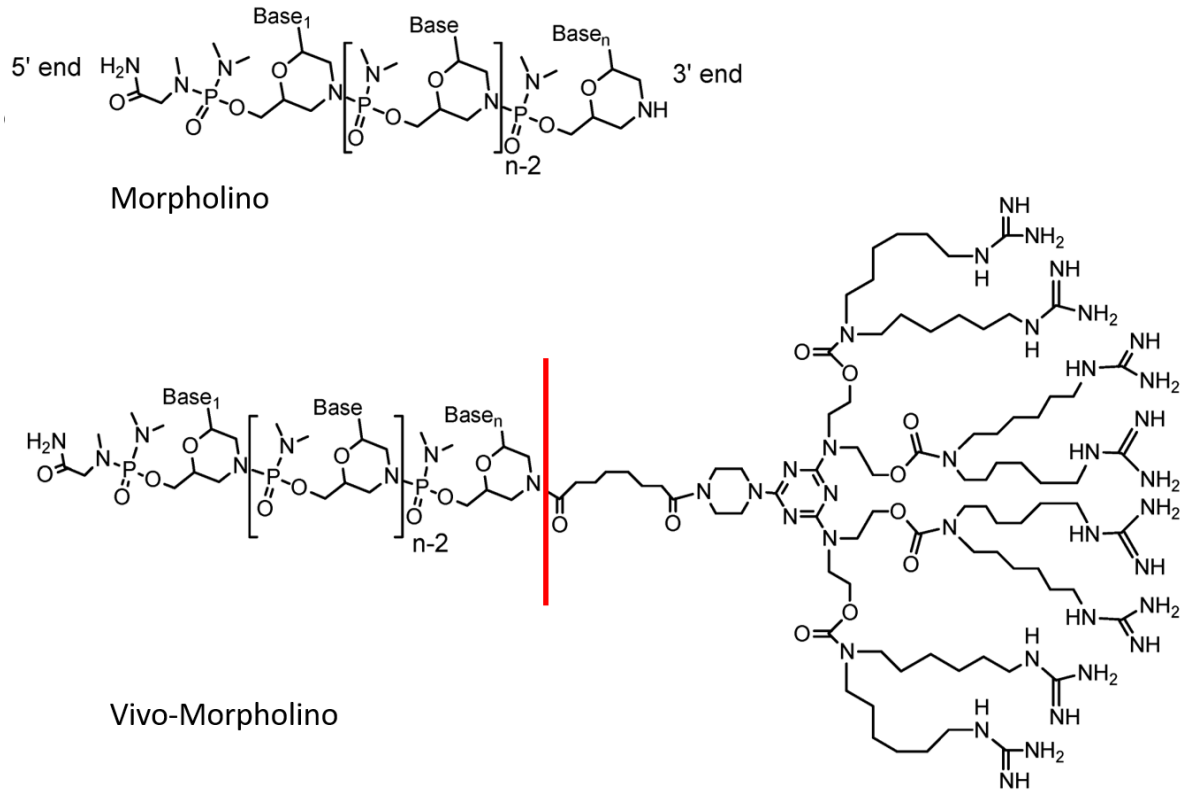

Figure 3: Morpholino schematic. Illustration demonstrating the structure of morpholinos and vivo-morpholinos. The delivery motif of the vivo-morpholino is to the right of the red line and is what separates a vivo-morpholino from a standard morpholino. Modified from (Moulton and Shan, 2009).

MOs can be injected into single cell/developing embryos or adult tissues without permanent effect. Regardless of the type of MOs used, eventually the MOs will lose effect as they are destroyed by the cell. 'Scrambled' MOs which do not target any sequence, are used to control for the presence of MO oligomers that have no target-specific effects. Vivo-MOs (Figure 3) are synthesized with a carrier subunit that can pass cell membranes (Morcos, Li and Jiang, 2008). This carrier subunit allows for delivery to target cells after intramuscular, intravascular, or intraperitoneal injections (Notch *et al.*, 2011; Kotb *et al.*, 2016; Schulman *et al.*, 2016), and even into developing fish embryos with a bath immersion (Wong and Zohar, 2015). Modifications to the MO subunits can generate a tool for inducible gene knockdowns (Shestopalov, Pitt and Chen, 2012; Yamazoe *et al.*, 2012), providing extra specificity and control; *e.g.*, fluorescein-tagged

morpholinos can be visualized as well as electroporated (Hyde, Godwin and Thummel, 2012). Correctly identifying targets for MO loss of function requires access to sequence data, either the coding sequence (translation-blocking morpholinos) or an annotated genome (to identify splice-blocking targets).

CRISPR/Cas9

MOs and RNAi function on similar principles by causing knockdown of protein levels through transiently faulting the translation process. Canonically these methods are for use in an individual and are not heritable over generations. As discussed above, while these can be useful attributes in certain circumstances, they also lead to limitations in use. CRISPR addresses some of these limitations.

CRISPR varies from RNAi and MO mainly in the mode of action. CRISPR allows genomic modifications (generally as disruptions to the native gene sequence, but also allows for insertions of exogenous DNA) acting at the DNA level. As the genome of the target is modified, these results are permanent in all affected cells and have the capacity for generational inheritance if gametes are modified. CRISPR can still be used to modify individuals to allow for direct phenotyping; however, the potential for heritability allows for the generation of stable mutant lines relatively easily, as well as in non-model organisms, where standard methods for generating mutant lines, such as Cre-*loxP* in mice (Kim *et al.*, 2018), are unavailable. CRISPR seems to also be a tool that can be used in nearly every system tested to date; delivery of the constructs to the nucleus is the major hurdle for most non model organisms. While not exhaustive, researchers have reported success using CRISPR in the pea aphid (Le Trionnaire *et al.*, 2019), butterfly species (Mazo-Vargas *et al.*, 2017; Zhang, Mazo-Vargas and Reed, 2017; Matsuoka and Monteiro, 2018), ant species (Friedman, Gordon and Luo, 2017; Trible *et al.*, 2017; Favreau *et*

al., 2018), beetle species (Gilles, Schinko and Averof, 2015; Farnworth *et al.*, 2020; Gui *et al.*, 2020), bee and wasp species (Roth *et al.*, 2019; Benetta *et al.*, 2020; Chaverra-Rodriguez *et al.*, 2020; Değirmenci *et al.*, 2020; Chen *et al.*, 2021), a lizard (Rasys *et al.*, 2019), rice (Bi and Yang, 2017; Farhat *et al.*, 2019), wheat (Kim, Alptekin and Budak, 2018; Sánchez-León *et al.*, 2018), the thale cress (Fauser, Schiml and Puchta, 2014; Miki *et al.*, 2018), maize (Char *et al.*, 2017; Chilcoat, Liu and Sander, 2017), soybean (Chilcoat, Liu and Sander, 2017; J. Liu *et al.*, 2019), zebrafish (Hwang *et al.*, 2013; Jao, Wente and Chen, 2013; Auer *et al.*, 2014; Irion, Krauss and Nusslein-Volhard, 2014; Shah *et al.*, 2015; Burger *et al.*, 2016; Hua *et al.*, 2017), mouse (Yen *et al.*, 2014; Hashimoto and Takemoto, 2015; Qin *et al.*, 2015; Singh, Schimenti and Bolcun-Filas, 2015; Jung *et al.*, 2017), rat (D. Li *et al.*, 2013), sheep (Crispo *et al.*, 2015), pig (Xie *et al.*, 2020; Xu *et al.*, 2020), *Toxoplasma gondii* (Jacot and Soldati-Favre, 2020), cow (De Oliveira *et al.*, 2019; Savy *et al.*, 2020), and human cells (Artegiani *et al.*, 2020; Lu *et al.*, 2020; Nakazawa *et al.*, 2020).

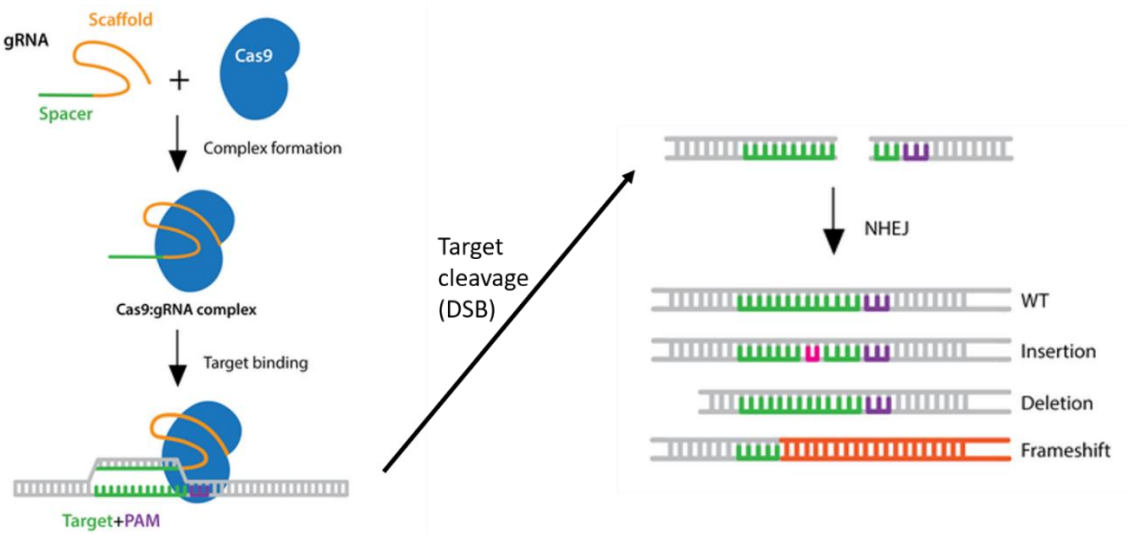

Figure 4: CRISPR/Cas9 knockouts. Illustration demonstrating the mechanism by which CRISPR/Cas9 causes InDels. The gRNA complexes with the Cas9 and is injected. The gRNA binds to the DNA and the Cas9 sits at the PAM site. The DNA is broken 3 bases upstream of the PAM and the cell repairs the break, often causing InDels which can result in frameshift mutations. Modified from Addgene.org CRISPR guide.

For CRISPR/Cas9 to be performed (Figure 4), a short guide RNA (sgRNA) is produced in the laboratory that is complementary to a given DNA sequence of interest. The sgRNA complexes with a Cas9 endonuclease and the complex then bind to the DNA sequence where the Cas9 will cause a double-stranded break (DSB) precisely 3 bases upstream of the PAM sequence. The cell will attempt to repair the DSB using the non-homologous end joining (NHEJ) pathway, causing insertions or deletions at the DSB site. Addition of a template with homologous arms spanning the DSB site can be utilized in the homology-directed repair pathway (HDR) and allow DNA insertions (Figure 2- See CRISPR). InDels (insertations or deletations) are produced to generate loss of function, whereas HDR is mainly used in gain of function studies.

Researchers can begin to study how novel genes/gene products confer fitness advantages that may eventually lead to processes like speciation. To understand how a novel protein gives an advantage, the function of that protein needs to be considered within a living organism. Through NHEJ repair, InDels often cause loss of function when in the coding region of a gene (Wang *et al.*, 2014). CRISPR thereby serves as a primary tool for generating F_0 individuals lacking a specific gene. The ability for individuals injected with CRISPR components to have precise genomic mutants is a strength (Jao, Wente and Chen, 2013; Ablain *et al.*, 2015; Wu *et al.*, 2020), as traditional breeding methods to generate mutants do not produce mutants until the F_2 generation.

HDR allows researchers to develop a wide range of studies to determine gene function. Adding reporter constructs to allow visualization of an endogenous gene expression is a key use of CRISPR-mediated HDR. Reporter constructs are DNA sequences that add some detectable unit to the DNA sequence of interest, generally in the form of a linked fluorescent protein. It is

possible to design a construct that contains the gene of interest (with modifications to the CRISPR site to protect against CRISPR/Cas9 cleavage of the donor template), followed by a 2A peptide sequence upstream of a fluorescent protein such as GFP. That construct can then be used in HDR following a Cas9 induced DSB to introduce the designed sequence into the genome. Using this design, the endogenous gene product will be generated, the 2A sequence will self-cleave (Kim *et al.*, 2011) and the GFP protein will also be produced. In utilizing this methodology, the endogenous gene product attains several traits/attributes: it is present at the wildtype levels, timing, and location, has no change in function (no change in shape due to a tethered GFP or a tag addition), and colocalizes with GFP, which can then be visualized. Understanding the temporospatial distribution of a gene product can add insights into its function and role in the evolution of an organisms' phenotype, such as investigating the gene *dachshund2* in arachnids and understanding its role in the formation of the patella, a derived leg structure compared to other arthropod legs (Turetzek et al., 2016) but CRISPR/Cas9 HDR has been performed in other species as well (Auer *et al.*, 2014; Jung *et al.*, 2017; Zhang and Reed, 2017; Liu *et al.*, 2018).

CRISPR is an ever evolving tool; modifications to the Cas9 enzyme allow many additional applications (Adli, 2018). Cas9 has been genetically altered to have tethered proteins attached to it while also losing endonuclease activity, allowing the CRISPR/Cas9 complex to guide proteins to a DNA sequence of interest without causing a DSB (Ran *et al.*, 2013; Fauser, Schiml and Puchta, 2014; Li *et al.*, 2014; Tsai and Joung, 2016). Cas9 tethered proteins, such as transcriptional activators and repressors, can test promoter function under various conditions or genetic backgrounds (Barrangou and Doudna, 2016). A Cas9/sgRNA complex lacking endonuclease activity can also be used to physically bind a DNA sequence, stop any complexing

of the DNA sequence of interest with native proteins, and cause disruption of normal transcription factor binding, DNA modifications, DNA packaging, *etc* (Gilbert *et al.*, 2013; Qi *et al.*, 2013). Like the tethered activators and repressors described above, methyltransferase (Khan *et al.*, 2018) and acetyltransferase (Hilton *et al.*, 2015; Shrimp *et al.*, 2018) can be tethered to Cas9 and directed to particular CpG/histone sites respectively. In addition to these modifications, CRISPR has already been shown to be involved in chromatin imaging and topology, specific base editing, and RNA targeting (Adli, 2018).

RNAi, MOs, and CRISPR have opened the door for the exploration of deep biological questions through non-model organisms (Goldstein and King, 2016; Russell *et al.*, 2017). The idea that model organisms could be adapted to answer any question due to sheer resources and data depth is now able to be challenged with the adaptiveness of MOs, RNAi, and CRISPR. The approach of finding the model that best fits the biological question at hand (Dietrich *et al.*, 2020) is newly accessible with reverse genetic tools. Functional genomics allows natural systems to be leveraged, providing a breadth of investigative inquiry that model organisms cannot assess.

Electric Fish

Electric fish background

Electric fish are characterized by the ability to produce bursts of electricity from a derived, specialized organ that functions solely to produce electricity. There are 6 lineages of electric fish (Figure 5) that have all independently evolved electrogenesis and which span both marine and freshwater environments and include teleosts and non-teleosts (Pitchers *et al.*, 2016). Some electric fish, like the electric eel, are strongly electric and produce electric organ discharges (EODs) that function in predation and defense (Macesic and Kajiura, 2009; Catania, 2019).

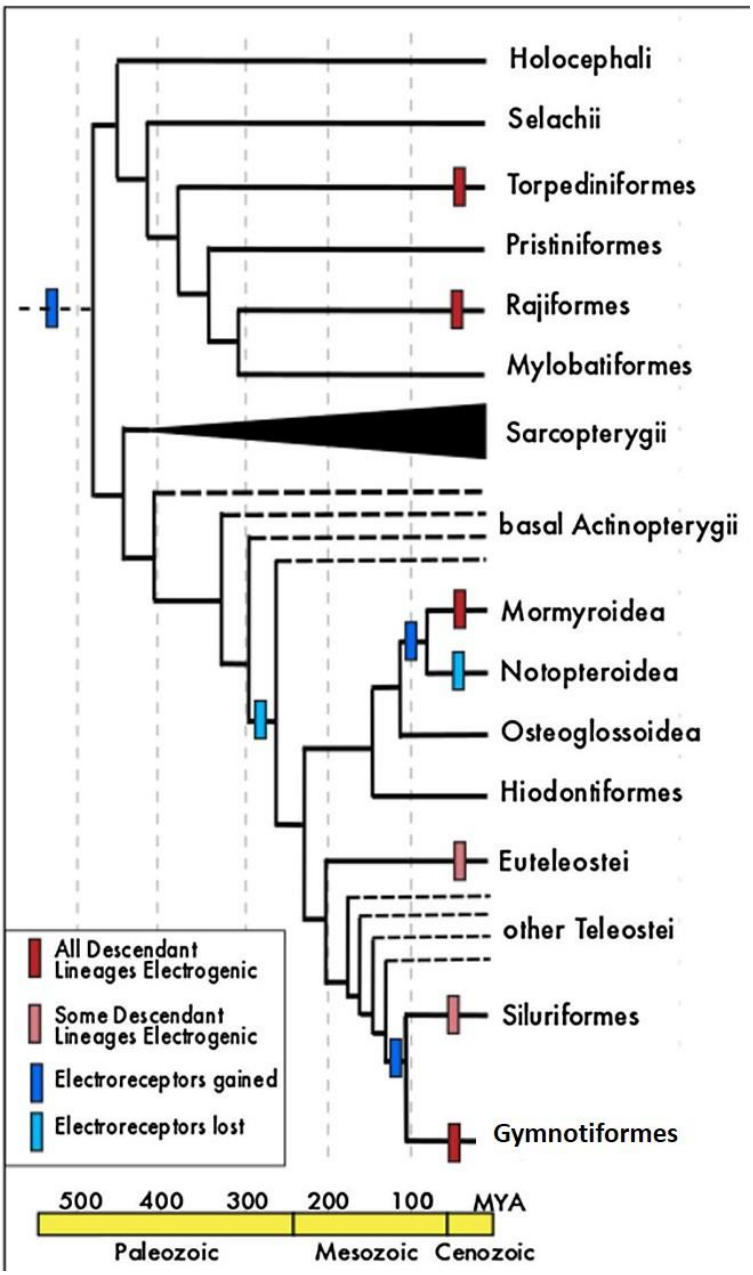

Figure 5: Electrogenesis phylogeny. Phylogeny demonstrating the 6 lineages of electric fish. Electroreception is also depicted. Modified from (Pitchers *et al.*, 2016).

The vast majority of electric fish are known as weakly electric fish and produce voltages undetectable without specialized electroreceptors (Baker, Modrell and Gillis, 2013). These low voltage EODs are used for active electrolocation. EODs are emitted from the electric organ and are modulated when they interact with objects in the environment in characteristic ways, depending on how well the object conducts electricity. The subsequent distortions are detected

by electroreceptors and processed in the brain against the expected EOD shape, allowing the fish to process its external environment (von der Emde, 1999; Alves-Gomes, 2001). The EODs of weakly electric fish are also used in communication between individuals and to differentiate between species (Bass, 1986; Kawasaki, 2009).

The numerous convergent features between independent groups and evolutionary novelties within electric fish groups have captivated the research community for decades. Since the first discovery of weakly electric fish low voltage EODs (Lissmann, 1951), a vast breadth of knowledge has been gained, not only about electric fish biology, but also about evolution of development (Cuellar, Kim and Unguez, 2006; Modrell and Baker, 2012; Gallant *et al.*, 2014), systems and circuits neuroscience (Heiligenberg, 1991; Bell *et al.*, 1997; Kawasaki, 1997; Carl D Hopkins, 1999), cellular physiology (Markham, Kaczmarek and Zakon, 2013; Ban, Smith and Markham, 2015), ecology and energetics (Salazar and Stoddard, 2008; Gavassa and Stoddard, 2012; Salazar, Krahe and Lewis, 2013; Lewis *et al.*, 2014; Sinnett and Markham, 2015), behavior (Hopkins and Bass, 1981; Arnegard, Jackson and Hopkins, 2006), and macroevolution (Crampton, 1998; Sullivan *et al.*, 2004; Arnegard *et al.*, 2010).

Electric fish provide a natural experiment in the evolution of novel organ systems, speciation, and convergent evolution. The most well studied electric fish groups, the weakly electric African Mormyridae, and South American Gymnotiformes, are a striking example of convergent evolution from the anatomical and behavioral level, down to the level of gene expression (Zakon *et al.*, 2006; Markham, 2013; Gallant *et al.*, 2014; Thompson *et al.*, 2014). There is a wealth of physiological, neuronal, and ecological information collected about these species (Alves-Gomes, 2001; Baker, Modrell and Gillis, 2013; Carlson and Gallant, 2013; Markham, 2013; Pitchers *et al.*, 2016; Crampton, 2019; Gallant, 2019).

Need for functional genetics in electric fish

The electric fish research community has collected a considerable amount of information on the phenotypic variation of electric fish spanning multiple levels of biological analysis. More recently, genomic and transcriptomic resources have been generated to describe genomic variation (Gallant *et al.*, 2014; Lamanna, Kirschbaum and Tiedemann, 2014; Lamanna *et al.*, 2015; Salisbury *et al.*, 2015; Traeger *et al.*, 2015a; Pinch *et al.*, 2016; Swapna *et al.*, 2018). Application of genomic data allows for a wide diversity of future research avenues in electric fish (Pitchers *et al.*, 2016; Gallant and O'Connell, 2020) such as determining function of electric organ specific genes (Constantinou *et al.*, 2019).

By utilizing genomic resources to identify gene targets for reverse genetic studies, the gene involvement at a molecular level can be added to the models currently discovered through electric fish research in the fields mentioned above (Hopkins and Bass, 1981; Heiligenberg, 1991; Kawasaki, 1997; Bell *et al.*, 1997; Crampton, 1998; Carl D Hopkins, 1999; Sullivan *et al.*, 2004; Arnegard, Jackson and Hopkins, 2006; Cuellar, Kim and Unguez, 2006; Salazar and Stoddard, 2008; Arnegard *et al.*, 2010; Modrell and Baker, 2012; Gavassa and Stoddard, 2012; Markham, Kaczmarek and Zakon, 2013; Salazar, Krahe and Lewis, 2013; Lewis *et al.*, 2014; Gallant *et al.*, 2014; Sinnett and Markham, 2015; Ban, Smith and Markham, 2015).

It is possible through reverse genetics to identify genes that control phenotypes that drive the ecology and evolution of electric fishes. There are some topics in weakly electric fish research that can progress rapidly using reverse genetic tools. The development of electric organs presents one well-studied topic that highlights the need for reverse genetic tools to progress further.

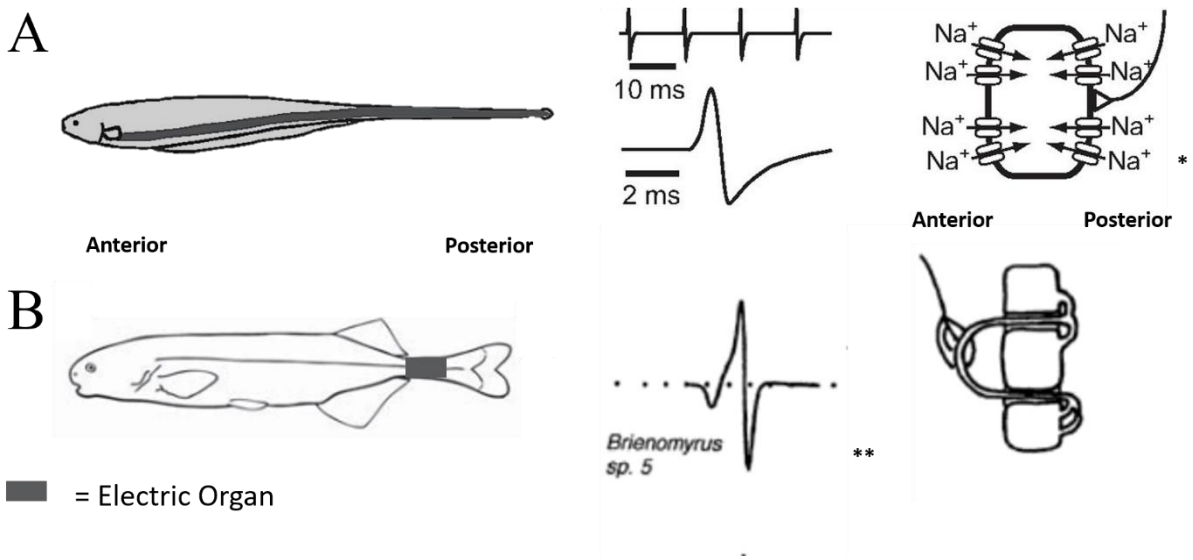

Figure 6: Electric organs, EODs, and electrocytes. The location of the adult electric organ, the waveform of the adult EOD, and the electrocyte anatomy are shown for *B. gauderio* (A) and *B. brachyistius* (B). *B. gauderio* is a pulse type gymnotiform and a series of EODs is shown with the 10 ms scale and a single EOD is shown in the 2 ms scale. *Modified from (Salazar, Krahe and Lewis, 2013). ** Modified from (C D Hopkins, 1999).

Electrocytes are the functional cells of the electric organ that allow EODs to provide the signal for electroreception and supports the electrocommunication abilities of the weakly electric fish (Figure 6). There is decades old research investigating the development of the electric organ in mormyrids and gymnotiformes; however, this research investigates morphology/anatomy/physiology (Kirschbaum and Westby, 1975; Kirschbaum, 1977; Denizot *et al.*, 1978; Westby and Kirschbaum, 1978a, 1978b; Kirschbaum and Schwassmann, 2008; Nguyen *et al.*, 2017; Gallant, 2019). Highlighting the lack of molecular data concerning embryonic electric organ development, there is only a single piece of published literature, other than my own (Constantinou *et al.*, 2019), that touches on the molecular mechanisms or players involved in embryonic electric organ development (Alshami *et al.*, 2020) and discusses expression of *Pax7*, *actin*, *Myosin*, *alpha-tubulin,* and neurons in the nerve cord.

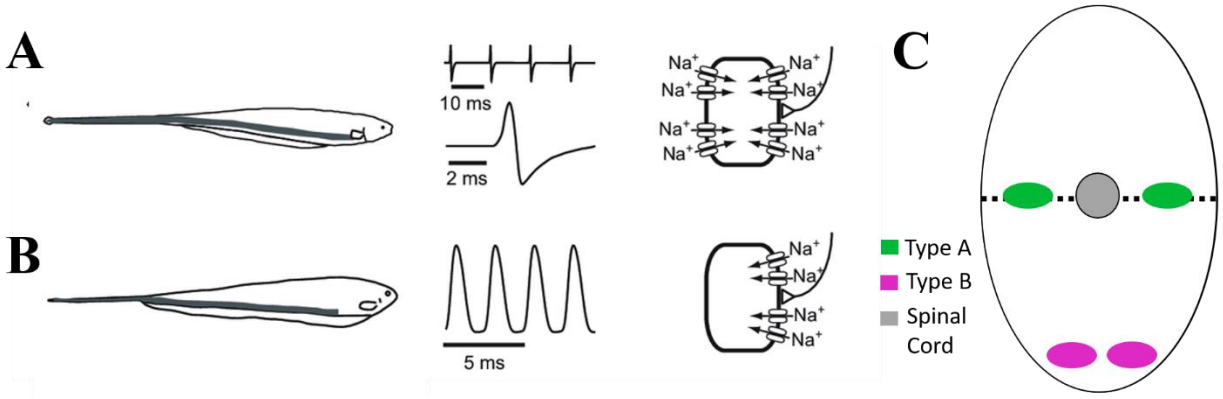

Figure 7: Wave vs pulse type gymnotiformes. *Brachyhypopomus gauderio* is a pulse type gymnotiform which has delays between EODs, has a biphasic EOD, and an electrocyte with two excitable faces (A). An *Eigenmannia* species demonstrates wave type gymnotiformes which has no delay between EODs, has a monophasic EOD, and an electrocyte with one excitable face (B). (C) Cross section of a developing body cavity from a juvenile gymnotiform is shown. The dotted line represents the midline, above (dorsal) sits epaxial muscle and below (ventral) sits hypaxial muscle. The location where Type A electrocytes (wave type gymnotiformes) arise from is shown in green lateral to the spinal cord (gray circle). The location where Type B electrocytes (pulse type gymnotiformes) arise is shown in purple in the ventral hypaxial muscle. Na^+- Sodium ion. Figure modified from (Salazar, Krahe and Lewis, 2013; Gallant, 2019).

There is a significant amount of variability in electric organ development across electric fishes as exemplified in the Gymnotiformes. Gymnotiformes are composed of two major groupings, the pulse and wave types, which vary in the frequency of the electric organ discharge. Wave types produce a constant sinusoidal waveform as EODs are constantly produced, while the pulse types vary the time between each EOD (Figure 7). The development of the electric organs varies between these two groups with wave type fish having “Type A” electrocytes (Figure 7B) and pulse type fish having “Type B” electrocytes (Figure 7A) (Kirschbaum and Schwassmann, 2008). The body regions from which these cells originate, and the morphology seen during development (Figure 7C), suggest that “Type A” electrocytes derive from transdifferentiation of skeletal muscle (or at least from differentiated myotubes containing sarcomeric proteins), whereas “Type B” electrocytes develop from a non-differentiated, muscle stem cell-like progenitor (Kirschbaum and Schwassmann, 2008).

It appears that generally, electrocytes form in a similar way to skeletal muscle as electrocytes are modified skeletal muscle cells (Gallant, 2019). Electrocytes form via fusion of precursor cells and then expression of electrocyte specific genes which is also accompanied by downregulation of skeletal muscle transcripts/proteins in "Type A" electrocytes (Baillet-Derbin, 1978; Unguez and Zakon, 2002). The exceptions to this rule are the adult neurogenic electric organs of the *Apternotids* which derive from neurons and not skeletal muscle (Kirschbaum, 1983; Kirschbaum and Schwassmann, 2008).There seems to be some variability in the expression of yet unknown electrocyte specific genes during development as fishes with "Type A" electrocytes have distinct and separate adult and larval electric organs (Kirschbaum and Schwassmann, 2008) and "Type B" electrocyte fishes have a single organ which changes complexity in developmental time and space (Franchina, 1997). For example, *B. gauderio*, with "Type B" electrocytes, have an electric organ which has monophasic EOD producing, cuboidal electrocytes (generated as larvae) in the anterior and biphasic EOD producing, cigar shaped electrocytes (generated after a certain size in development) throughout the rest of the body and into the posterior tail tip (Franchina, 1997)

Without understanding what genes are involved in development, where and when they are expressed, and how they function, development can only be explored to a certain depth. It may be possible to understand how pulse vs wave type electrocytes develop, how larval vs adult electric organs arise, and how skeletal muscles are reprogramed into electrocytes by uncovering the genes and their functions that drive these processes through reverse genetic methods. Using reverse genetics may uncover what gene networks are involved in electrocyte development and how those genes function, providing insights into how electric organs arose and how they might be modified during development to assist in speciation events.

I present the following three chapters to investigate the plausibility of reverse genetic tools in weakly electric fish. In Chapter 1, I develop husbandry and CRISPR/Cas9 protocols for two species of distantly related electric fish and produced representative results of *scn4aa* knockdown utilizing those protocols and methods. In Chapter 2, I discuss progress made following Chapter 1's publication in producing F_0 *scn4aa* mutants, including the development of growth curves, verification of an adult mutant with an EOD amplitude reduced phenotype, and exploration of husbandry and breeding practices. I also explore pitfalls and suggestions in a "Call to the Efish Community" concerning breeding, husbandry, and CRISPR/Cas9 future applications in other laboratories. Lastly, in Chapter 3, I investigate the possibility of vivo-morpholinos as a reverse genetic tool in mormyrids including potential toxic effects, reliability, and efficacy of phenotypic knockdown. To accomplish this I investigate, *scn4aa* targeting vivo-morpholinos, molecular verification of vivo-morpholino knockdown, and the ideal injection location. Reverse genetic tools will be a rich source of future research in electric fish, given certain considerations and suggestions laid out from my research.

CHAPTER 1

Silencing the spark: CRISPR/Cas9 genome editing in weakly electric fish[1]

Abstract

Electroreception and electrogenesis have changed in the evolutionary history of vertebrates. There is a striking degree of convergence in these independently derived phenotypes, which share a common genetic architecture. This is perhaps best exemplified by the numerous convergent features of gymnotiforms and mormyrids, two species-rich teleost clades that produce and detect weak electric fields and are called weakly electric fish. In the 50 years since the discovery that weakly electric fish use electricity to sense their surroundings and communicate, a growing community of scientists has gained tremendous insights into evolution of development, systems and circuits neuroscience, cellular physiology, ecology, evolutionary biology, and behavior. More recently, there has been a proliferation of genomic resources for electric fish. Use of these resources has already facilitated important insights with regards to the connection between genotype and phenotype in these species. A major obstacle to integrating genomics data with phenotypic data of weakly electric fish is a present lack of functional genomics tools. We report here a full protocol for performing CRISPR/Cas9 mutagenesis that utilizes endogenous DNA repair mechanisms in weakly electric fish. We demonstrate that this protocol is equally effective in both the mormyrid species *Brienomyrus brachyistius* and the gymnotiform *Brachyhypopomus gauderio* by using CRISPR/Cas9 to target InDels and point mutations in the first exon of the sodium channel gene *scn4aa*. Using this protocol, embryos

[1] This work was published in The Journal of Visualized Experiments (Constantinou *et al.*, 2019).

from both species were obtained and genotyped to confirm that the predicted mutations in the first exon of the sodium channel *scn4aa* were present. The knock-out success phenotype was confirmed with recordings showing reduced electric organ discharge amplitudes when compared to uninjected size-matched controls.

Video Link

The video component of this article can be found at https://www.jove.com/video/60253/

Introduction

Electroreception and electrogenesis have changed in the evolutionary history of vertebrates. Two lineages of teleost fish, osteoglossiformes and siluriformes, evolved electroreception in parallel, and five lineages of teleosts (Gymnotiformes, Mormyridae, and the genera Astroscopus, Malapterurus, and Synodontis) evolved electrogenesis in parallel. There is a striking degree of convergence in these independently derived phenotypes, which share a common genetic architecture (Zakon *et al.*, 2006; Arnegard *et al.*, 2010; Gallant *et al.*, 2014).

This is perhaps best exemplified by the numerous convergent features of gymnotiforms and mormyrids, two species-rich teleost clades, which produce and detect weak electric fields and are called weakly electric fish. In the 50 years since the discovery that weakly electric fish use electricity to sense their surroundings and communicate (Lissmann, 1951), a growing community of scientists has gained tremendous insights into evolution of development (Cuellar, Kim and Unguez, 2006; Modrell and Baker, 2012; Gallant *et al.*, 2014), systems and circuits neuroscience (Heiligenberg, 1991; Bell *et al.*, 1997; Kawasaki, 1997; Carl D Hopkins, 1999), cellular physiology (Markham, Kaczmarek and Zakon, 2013; Ban, Smith and Markham, 2015), ecology and energetics (Salazar and Stoddard, 2008; Gavassa and Stoddard, 2012; Salazar, Krahe and

Lewis, 2013; Lewis *et al.*, 2014; Sinnett and Markham, 2015), behavior (Hopkins and Bass, 1981; Arnegard, Jackson and Hopkins, 2006), and macroevolution (Crampton, 1998; Sullivan *et al.*, 2004; Arnegard *et al.*, 2010).

More recently, there has been a proliferation of genomic, transcriptomic, and proteomic resources for electric fish (Mate, Brown and Hoffman, 2011; Gallant *et al.*, 2014; Lamanna, Kirschbaum and Tiedemann, 2014; Lamanna *et al.*, 2015; Salisbury *et al.*, 2015; Traeger *et al.*, 2015b; Pinch *et al.*, 2016; Swapna *et al.*, 2018). Use of these resources has already produced important insights regarding the connection between genotype and phenotype in these species (Zakon *et al.*, 2006; Arnegard *et al.*, 2010; Futuyma, 2013; Gallant *et al.*, 2014; Thompson *et al.*, 2014; Swapna *et al.*, 2018). A major obstacle to integrating genomics data with phenotypic data of weakly electric fish is a present lack of functional genomics tools (Pitchers *et al.*, 2016).

One such tool is the recently developed Clustered Regularly Interspaced Short Palindromic Repeats paired with Cas9 endonuclease (CRISPR/Cas9, CRISPR) technique. CRISPR/Cas9 is a genome editing tool that has entered widespread use in both model (Liang *et al.*, 2015; Jung *et al.*, 2017; K. Liu *et al.*, 2019) and non-model organisms (Crispo *et al.*, 2015; Zu *et al.*, 2016; Sun *et al.*, 2017) alike. CRISPR/Cas9 technology has progressed to a point where a laboratory capable of basic molecular biology can easily generate gene-specific probes called short guide RNAs (sgRNAs), at a low cost using a non-cloning method (Gagnon *et al.*, 2014). CRISPR has advantages over other knockout/knockdown strategies, such as morpholinos (Kok *et al.*, 2015; Morcos, Vincent and Moulton, 2015), transcription activator-like effector nucleases (TALENs), and zinc finger nucleases (ZFNs) which are costly and time-consuming to generate for every target gene.

The CRISPR/Cas9 system functions to create gene knockouts by targeting a specific region of the genome, directed by the sgRNA sequence, and causing a double-stranded break. The double-stranded break is detected by the cell and triggers endogenous DNA repair mechanisms preferentially using the non-homologous end joining (NHEJ) pathway. This pathway is highly error-prone: during the repair process, the DNA molecule will often InDels at the double stranded break site. These InDels can result in a loss of function due to either (1) shifts in the open reading frame, (2) insertion of a premature stop codon, or (3) shifts in the critical primary structure of the gene product. In this protocol, we utilize CRISPR/Cas9 editing to target point mutations in target genes using the NHEJ in weakly electric fish species. While simpler and more efficient than other techniques, this method of mutagenesis is expected to result in a range of phenotypic severities in F_0, which is attributed to genetic mosaicism (Yen *et al.*, 2014; Singh, Schimenti and Bolcun-Filas, 2015; Mianné *et al.*, 2017; Mehravar *et al.*, 2019).

Selection of organisms

For the purposes of facilitating future studies on the comparative genomics of weakly electric fish, a representative species for both gymnotiforms and mormyrids for protocol development needed to be selected. Following discussions during the 2016 Electric Fish meeting in Montevideo, Uruguay, there was community consensus to utilize species that already could be bred in the laboratory and that had genomic resources available. The gymnotiform *Brachyhypopomus gauderio* and the mormyrid *Brienomyrus brachyistius* were selected as species that fit these criteria. In both species, natural cues to induce and maintain breeding conditions are easy to mimic in captivity. *B. gauderio*, a gymnotiform species from South America, has the advantage of low husbandry requirements: fish can be kept at relatively high density in relatively small (4 L) tanks. *B. gauderio* also has fast generational turnover under

captive conditions. Under laboratory conditions, *B. gauderio* can develop from egg to adult in about 4 months.

B. brachyistius, a species of mormyrid fish from West-Central Africa, breeds readily in captivity. *B. brachyistius* is readily available through the aquarium trade, has been widely used in many studies, and now has several genomic resources available. Their life cycle spans 1−3 years, depending on laboratory conditions. Husbandry requirements are somewhat more intensive for this species, requiring moderately sized tanks (50−100 L) due to their aggression during breeding.

Laboratories studying other species of electric fish should be able to easily adapt this protocol if the species can be bred, and single cell embryos can be collected and reared into adulthood. Housing, larval husbandry, and *in vitro* fertilization (IVF) rates will likely change with other species; however, this protocol can be used as a starting point for breeding attempts in other weakly electric fish.

An ideal gene target for proof of concept: *scn4aa*

Weakly electric mormyrid and gymnotiform fish generate electric fields (electrogenesis) by discharging a specialized organ, called the electric organ. Electric organ discharges (EODs) result from the simultaneous production of action potentials in the electric organ cells called electrocytes. EODs are detected by an array of electroreceptors in the skin to create high-resolution electrical images of the fish's surroundings (von der Emde, 1999). Weakly electric fish are also capable of detecting features of their conspecifics' EOD waveforms (Hopkins and Bass, 1981) as well as their discharge rates (Carlson, 2009), allowing EODs to function additionally as a social communication signal analogous to birdsong or frog vocalizations (Hopkins, 1988).

A main component of action potential generation in the electrocytes of both mormyrid and gymnotiform weakly electric fish is the voltage-gated sodium channel NaV 1.4 (Zakon *et al.*, 2006). Non-electric teleosts express two paralogous gene copies, *scn4aa* and *scn4ab*, coding for the voltage-gated sodium channels NaV 1.4 (Thompson *et al.*, 2014). In both gymnotiform and mormyrid weakly electric fish lineages, *scn4aa* has evolved rapidly and undergone numerous amino acid substitutions that affect its kinetic properties (Arnegard *et al.*, 2010). Most importantly, *scn4aa* has become compartmentalized in both lineages to the electric organ (Zakon *et al.*, 2006; Arnegard *et al.*, 2010). The relatively restricted expression of *scn4aa* to the electric organ, as well as its key role in the generation of EODs, makes it an ideal target for CRISPR/Cas9 knockout experiments, as it has minimal deleterious pleiotropic effects. Because weakly electric fish begin discharging their larval electric organs 6-8 days post fertilization (dpf), targeting of *scn4aa* is ideally suited for rapid phenotyping following embryo microinjection.

Protocols

Selecting sgRNA targets

NOTE: A protocol is provided for manual design of sgRNAs in step “Design sgRNA targets”. This was utilized for *scn4aa* target selection. An additional protocol is provided to facilitate this process (step “Perform automated design of sgRNA targets”) using the EFISHGENOMICS web portal. It is advised that users select step “Perform automated design of sgRNA targets”), which features several automated ‘checks’ to ensure success in designing sgRNAs for custom targets.

Design sgRNA targets

For generating sgRNA guide oligos, it is best to target exon 1, or other 5’ exons. The 5’ UTR can be targeted; however, it is best to target the 5’ coding sequence. Utilizing

genomic information is preferable, but it is possible to develop successful sgRNAs using transcriptome data. Annotations of intron/exon boundaries (genomic data) or exon/exon boundaries are preferable.

Candidate genomic sequences from are searched for putative target sequences that match the pattern 5'-N(18)-NGG-3'. This can be automatically performed using desktop sequence analysis software, custom scripts, or through manual inspection of sequences.

Sequences can be prioritized for on-target activity (Doench *et al.*, 2014). Additionally, target sequences may be evaluated by a BLAST search against genomic/transcriptomic databases for off-target binding.

Ensure that standard PCR primers can be generated that flank the target sequence. Primers should be at least 20 base pairs (bp) from either side of the cut site (three bases upstream of the NGG sequence). Ideally, the PCR product should be 150−200 bp.

Design oligomers meeting the above criteria using the below template, which includes a T7 promoter (5' of N_{18}) and a complementary region (3' of N_{18}) for annealing to the constant oligomer (see below): 5'-TAATACGACTCACTATAGG-**N_{18}**-GTTTTAGAGCTAGAAATAGCAAG-3'

NOTE: The **N_{18}** sequence does not include the NGG protospacer adjacent motif (PAM) sequence. Do not include this in the oligomer.

Order the constant oligomer (Table 1 in Chapter 2) that will be used to synthesize all sgRNAs, oligomers for sgRNA targets, and PCR primers as standard desalted

oligomers from an oligonucleotide production service. Oligomers and PCR primers may be ordered as standard desalted oligomers, no additional purification is necessary.

Perform automated design of sgRNA targets

Using genomic data, select a target gene. Transcriptome data could be used instead when exon/intron boundaries are known. Targets can be identified using the EFISHGENOMICS portal (http://efishgenomics.integrativebiology.msu.edu). The ideal target will be within exon 1; however, other 5' exons and the 5' UTR can be considered.

Once the target sequence is identified, load the freely available EFISHGENOMICS CRISPR web tool (http:// efishgenomics.integrativebiology.msu.edu/crispr_tool/). This web tool uses a customized version of the CRISPOR algorithm for target generation (Haeussler *et al.*, 2016; Concordet and Haeussler, 2018).

In the box for **Step 1**, enter the name of the sequence and enter the target's sequence into the appropriate box.

Select the appropriate genome that the sequence derives from. Presently, genomic data is available for *B. brachyistius* and *B. gauderio*. Genome sequences are not required for use of this tool but are useful in assessing potential unwanted off-target effects.

Select the appropriate PAM. The 20 bp-NGG PAM is recommended, though there are several additional PAM motifs to choose from, depending on the Cas9 protein used.

A report will be generated with the location of the target sequence in the genome with suggested guide sequences. Select three targets with low predicted off-target effects, high

specificity scores, and high efficiency scores. The highest scoring guide sequences are highlighted with green on the left-hand side. Yellow and red highlighted guide sequences should be avoided, if possible.

Clicking on selected target sequences generates a comprehensive CRISPOR report. Key information from these reports is for “T7 in vitro expression from overlapping oligonucleotides”. From this report, extract the following information: recommended sgRNA oligos, PCR primers for the target site, and a constant oligomer that will be used to synthesize all sgRNAs.

Order the selected oligomers from an oligonucleotide production service. Oligomers and PCR primers may be ordered as standard desalted oligomers, no additional purification is necessary.

Generate sgRNA

Anneal oligomers in PCR tube: add 1 µL of 100 µM constant oligomer, 1 µL of 100 µM sgRNA specific oligomer, and 8 µL of nuclease-free H_20

Anneal oligomers in a thermocycler with the following program: heat at 95°C for 5 min, cool to 85°C at -2°C/s, cool to 25°C at 0.1°C/s, and hold at 4°C.

To generate sgRNA template, add 2.5 µL of dNTP mix (10 mM), 2 µL of 10x buffer, 0.5 µL of T4 DNA polymerase, and 5 µL of nuclease-free H_2O to the annealed oligomers. Incubate for 20 min at 12°C.

Purify template using a PCR clean up column per the manufacturer’s instructions.

Elute in 20–30 µL. Use a spectrophotometer to estimate concentration and purity. The template should be 100–200 ng/µL and 1.8–1.9 $A_{260/280}$.

Verify via an agarose gel by running 1–5 µL. The dominant band should be 120 bp. See Figure 8A for representative results.

Store gel-verified sgRNA template at -20°C (long term) or 4°C (short term, 1–4 weeks).

Transcribe sgRNA using T7 RNA transcription kit by adding to a 1.5 mL microcentrifuge tube at room temperature 8 µL of dNTP mix (equal volumes all 4 dNTPs), 2 µL of 10x buffer (room temperature), 2 µL of T7 RNA polymerase, 100−200 ng of sgRNA template, and nuclease-free H_2O to 20 µL total volume. Spin to collect at the bottom. Incubate for 2–4 h at 37°C.

Add 1 µL of DNase and incubate an additional 15 min at 37°C.

Clean up sgRNA by adding 1 µL of glycogen, 30 µL of nuclease-free H_2O, 30 µL of 5 M ammonium acetate and 180 µL of 100% EtOH to transcribed sgRNA. Mix well and incubate at least 20 min at -80°C (until frozen) or at -20°C overnight. Centrifuge at 4°C for 15 min at maximum speed.

Remove and discard supernatant without disturbing the pellet, and wash with 1 mL of RNase-free 70% EtOH chilled at -20°C. Spin an additional 5 min at maximum speed at 4°C.

Remove and discard the supernatant without disturbing the pellet, and air-dry the pellet for 5 min.

Resuspend in 30 µL of nuclease-free H_2O and determine purity and yield using UV spectroscopy (minimum yield of 200 ng/µL).

Verify the presence of sgRNA on an RNase-free gel. The sgRNA appears between 50 and 150 bp as two bands due to the secondary structure (Figure 8B).

Aliquot into 3 µL and store at -80°C.

Validate cutting efficiency *in vitro*

Extract genomic DNA from the target species using a commercial DNA extraction kit. Fin clippings can be used without having to sacrifice the fish because the tissues are regenerated.

Amplify the target DNA region using the primers designed as described earlier using standard PCR. Verify the product by gel electrophoresis. Sequencing the fragment to ensure the proper region is being amplified is suggested, but not necessary. Representative results are shown in Figure 9 (*scn4aa* template).

Clean up the PCR fragment with an established laboratory or company protocol.

Store the amplified DNA at -20 °C. Consider separating it into aliquots to reduce freeze-thaw cycles.

Determine the required amounts and volumes of each component. Consider running negative controls (excluding either sgRNA or Cas9) and a positive control (a previously tested sgRNA that cleaves its target PCR amplified DNA) if available, as well as a concentration series of the sgRNA.

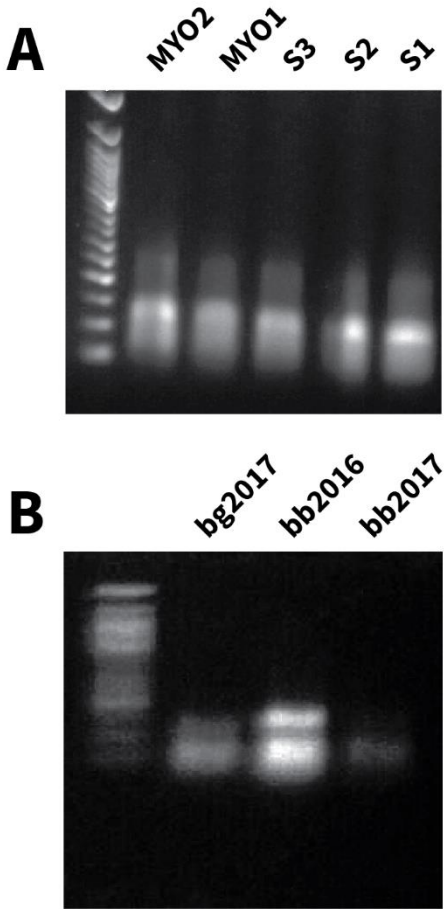

Figure 8: sgRNA template synthesis and transcription- Gel images of **(A)** sgRNA template synthesis; labels correspond to different sgRNAs for *myod* (MYO2, MYO1) and three sgRNAs for *scn4aa* (S1-S3). After annealing the oligomers, a ~120 bp template is produced. **(B)** Gel image of sgRNA transcription, for three sgRNAs for *B. gauderio* (bg2017) and two for *B. brachyistius* (bb2016,2017). sgRNA will appear as 2 bands due to secondary structure and will be between 50-150 bp when using a dsDNA ladder.

Set up the reaction mixture below in the specified order in a PCR tube at room temperature, adding the sgRNA and Cas9 protein last for best results: 50–100 ng of target DNA PCR product, 1 µL of 10x buffer 3, 1 µL of 10x Bovine Serum Albumin (0.1 g/mL), 50–200 ng of Cas9 protein (1 mg/mL, 150 ng suggested), and 30–200 of ng sgRNA (100 ng suggested).

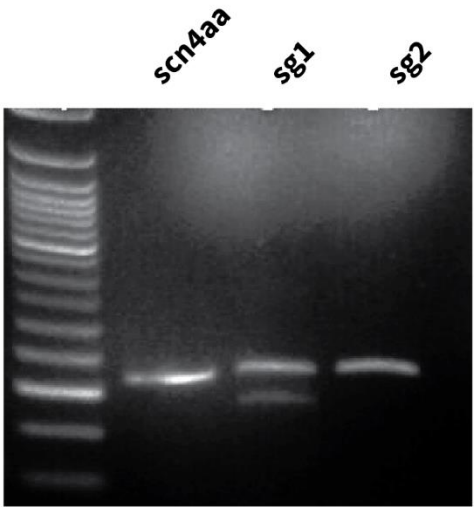

Figure 9: *In vitro* CRISPR assay- Representative gel image of successful (sg1) and unsuccessful (sg2) *in vitro* CRISPR assay. An equivalent amount of template without CRISPR components is shown in *scn4aa* lane. Note the duplicate bands in sg1 that represent that cutting has occurred.

Incubate the reaction at 37 °C for 1 h and then at 65 °C for 10 min to inactivate Cas9 protein.

Run the entire sample on a 2%–3% agarose gel (expected band sizes between 30–200 bp) along with positive and negative controls. Successful cleavage may show some of the PCR product but will also have two smaller bands representing the PCR fragment cut in two. Representative results are shown in Figure7.

Obtaining embryos

NOTE: Obtaining embryos of weakly electric fish can be challenging. Careful monitoring of water quality, adequate time for fish care, and regular feeding are key to a successful breeding program. Fish must first be conditioned for several weeks for reproduction (Kirschbaum, 1975) as described below. Following this, a protocol augmenting natural gametogenesis for use in natural spawning and artificial insemination are presented. Natural spawning is equally effective

for *B. brachyistius and B. gauderio*, and squeezing and *in vitro* fertilization have only been performed in *B. gauderio*.

Conditioning

Keep *B. brachyistius* in couples/small groups (100–150 L tanks) or in very large tanks (2 males and 5–6 females in approximately 475 L tank), as they become very aggressive under breeding conditions. There should be at least 1–2 PVC tubes per fish to be used as shelter (Figure 10A, B).

B. gauderio can be reared at much higher density. Keep up to eight individuals in a 100 L tank (2 males and 6 females). There should be at least 1 PVC tube per fish to be used as shelter. Adding tangled yarn increases enrichment and hiding spots. Add 50 mL centrifuge tubes with 1 cm diameter holes drilled into them to the top of the tank to allow adults to spawn naturally into the tubes (Figure 10C).

During the breeding season, feed fish daily fresh blackworms supplemented with frozen bloodworms. The food can be enriched with vitamins and supplements, if desired.

House fish normally in a relatively high conductivity (300–600 µS), pH balanced solution. During the breeding season, gradually lower the conductivity by at least half over the course of 1–3 weeks to induce gonad recrudescence and spawning. Lower conductivity by daily additions of reverse osmosis water, keeping close attention to pH when conductivity is low (pH <6 becomes problematic).

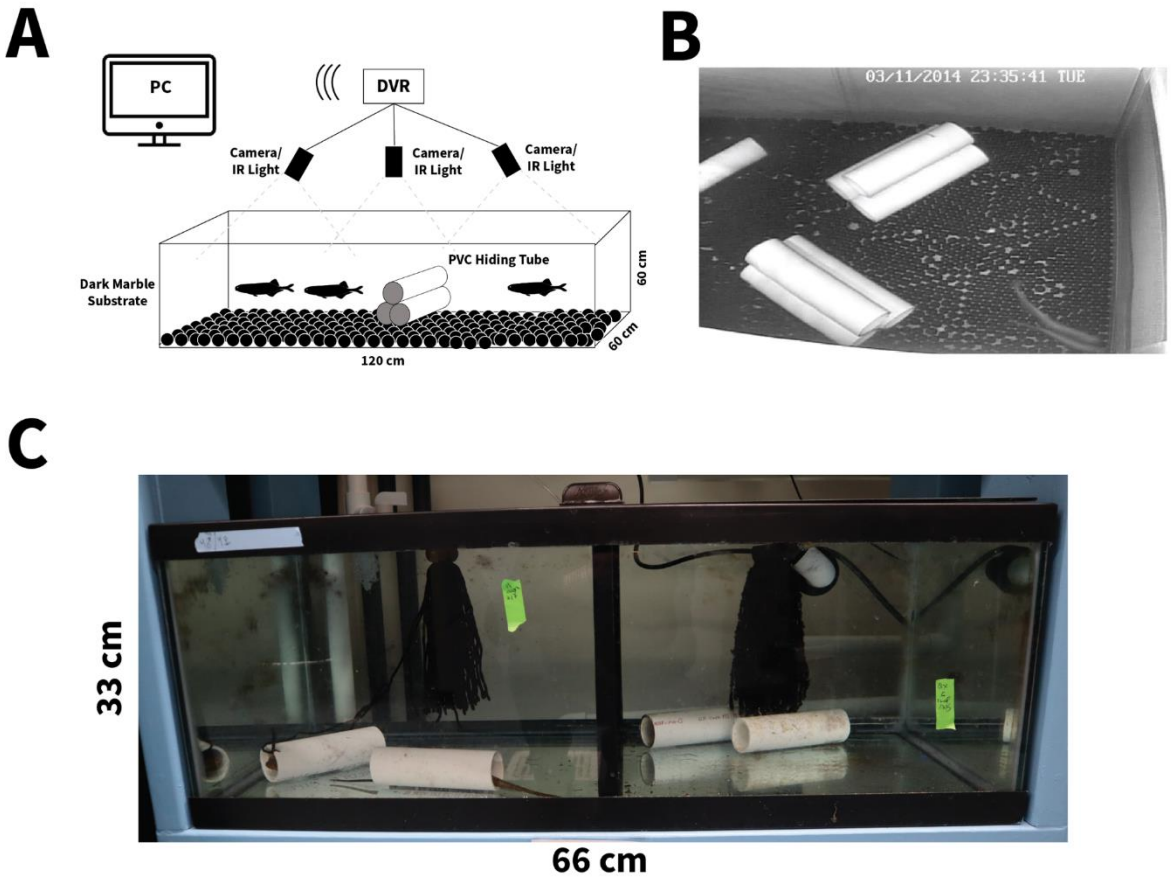

Figure 10: Breeding tank setups for weakly electric fish. (A) Schematic of the typical setup for wireless video monitoring of spawning behavior. Three commercially available CCTV cameras (Swann, Inc.) capable of producing infrared light are aimed at the top of the water and connected to a digital video recorder (DVR). Video is monitored in real time for spawning behavior in an adjacent room from a network connected computer (PC). (B) Spawning behavior captured with such a setup in *B. brachyistius*. (C) A typical breeding setup for *B. gauderio* with PVC hiding tubes and yarn mops.

Breeding conditions can be kept for around 1-2 months in *B. gauderio* and 3−5 months in *B. brachyistius* with egg production tapering off over time. After this time, return fish to high conductivity slowly over 1-3 weeks. Keep another ~3 months at high conductivity before being exposed to breeding conditions again.

Spawning agent injections

1. Identify female fish in breeding conditions that appear gravid (Figure 11). *B. brachyistius females* will have swollen bellies and appear deep bodied (Figure 11A); in *B. gauderio* the female will have swollen gonads just caudal to the vent (Figure 11B). Males generally do not have an issue producing sperm. However, larger males are preferred due to the larger sperm volume collected.

   NOTE: Spawning agent is a commercial hormone mix that facilitates maturation of gametes and coordinates spawning. If the fish has been injected with spawning agent in the past, allow for >4 weeks of rest and ample feeding between injections. We suggest injecting at least 2 males and 4–5 females to ensure a few clutches of eggs and plenty of sperm.

Anesthetize fish in MS-222 (0.4 g/3 L) for a few minutes, until the fish is not able to keep its posture, is immobile, but continues to have opercular movement (Stage II in Iwama, McGreer and Pawluk, 1989).

Weigh the fish (g) to calculate spawning agent amount, (0.5 µL/ g) + 0.5 µL. The extra 0.5 µL accounts for pipetting errors.

Add the spawning agent to 4x volumes of buffer (1x Phosphate Buffered Saline) in a PCR tube and mix well. The solution will become cloudy. It helps to dispense the spawning agent onto thermoplastic and then use a pipette to measure the calculated dose. The spawning agent is viscous, so be sure to dispense the entire dose and be careful with pipetting.

Pipette the injection solution onto thermoplastic and draw into a precision glass syringe, avoiding air bubbles. We recommend a 28 gauge, 19–25 mm length, beveled needle.

Inject the solution into the dorsal trunk muscle at a smooth rate. Let the needle sit for 2–4 s and then remove. Immediately put fish into fresh system water for recovery.

Figure 11: Breeding males and females. (A) *Brienomyrus brachyistius* and (B) *Brachyhypopomus gauderio*. Both species are sexually dimorphic and easily distinguished visually when sexually mature. Both females are gravid in these photos, exhibiting characteristically swollen bellies that are full of ripe eggs.

After approximately 24 h prepare for collection of embryos (see below). Gather all necessary materials including what is needed for single cell microinjection (see below).

Obtain embryos through natural spawning

House spawning, agent-injected adults (step 4.2) in large 450 L tanks. The most effective sex ratios have typically been 1–2 males and 3–4 females with adequate hiding places made from PVC tubes, and dark marble substrate on the tank bottom to prevent egg consumption. Marbles are typically more important for *B. brachyistius* than *B. gauderio*, which prefer to deposit their sticky eggs in crevices or 50 mL centrifuge tubes as described above.

Place fish in a reverse light cycle to match nighttime spawning to regular lab working hours. Using an off-the-shelf consumer grade security system, monitor fish using infrared illumination to minimize disturbance from a remotely connected PC (Figure 10).

The fish will spontaneously spawn during the dark photoperiod approximately 24 h post the spawning agent injection.

When spawning begins, collect eggs hourly while the spawning behavior occurs. In *B. brachyistius*, collect eggs using a small-diameter siphon over a fine cotton mesh net to minimize damage to the freshly spawned eggs. Collect *B. gauderio* eggs from 50 mL centrifuge tubes or tank substrate. Work efficiently with minimal disturbance to spawning fish by using a head lamp with a low-intensity red light. As first cleavage occurs approximately 1 h post fertilization (hpf), a large portion of eggs will be suitable for single cell microinjection.

Proceed immediately to microinjection (see below).

Squeeze males for *in vitro* fertilization of *B. gauderio*

Prepare the sperm extender solution (SES) as described in The Zebrafish Book (Westerfield, 2000): 10 mM HEPES, 80 mM KCl, 45 mM NaCl, 45 mM sodium acetate, 0.4 mM $CaCl_2$, and 0.2 mM $MgCl_2$.

Anesthetize fish in MS-222 (0.4 g/3 L) for a few minutes, until the fish is not able to keep its posture, is immobile, but continues to have opercular movement (Stage II-Iwama, McGreer and Pawluk, 1989). Place 500 µL aliquots of SES into ice.

Dry hands and fish thoroughly, especially around the head and vent. Place ventral side up, anterior to the left (for right-handed individuals) in a polystyrene foam/sponge holder covered in an MS-222 soaked, damp paper towel. The head should be as parallel with the table as possible.

NOTE: Steps below should be done as quickly as possible, and the fish should only be out of water for 30–60 s.

Apply pressure in the caudal to rostral direction with light squeezing medially over the gonads towards the vent. The fish may expel waste. Be careful to clean the vent with a delicate task wipe if any waste is expelled. Do not collect waste with sperm. Depending on the size of the male, 10-60 µL is common.

Using a micropipetter with a tip, carefully collect the sperm as it is squeezed from the male in 50 µL increments. Place sperm directly into 500 µL aliquots of SES on ice. It can be helpful to have another researcher assist in collecting sperm while the other squeezes. Sperm should be used as soon as possible, but remains viable for at least 1 h.

Immediately after collecting, put fish into fresh system water for recovery. The fish should only be out of water for 30–60 s.

Squeeze females for *in vitro* fertilization of *B. gauderio*

Anesthetize fish in MS-222 (0.4 g/3 L) for a few minutes, until the fish is not able to keep its posture, is immobile, but continues to have opercular movement (Stage II-Iwama, McGreer and Pawluk, 1989). Place polytetrafluoroethene sheet on workstation.

NOTE: Sections below should be done as quickly as possible, and the fish should only be out of water for 30–60 s.

Dry hands, tools, polytetrafluoroethene sheet, and fish thoroughly, especially around the head and vent. Place on side with head facing anterior (for right-handed individuals).

Apply pressure in the caudal to rostral direction with light squeezing medially over the gonads towards the vent. The fish may expel waste. Be careful to clean the vent with a delicate task wipe if any waste is expelled. Depending on the size of the fish, 20–150 eggs is common. Using a polytetrafluoroethene coated spatula/tool carefully collect eggs as they are squeezed from the cloaca. Quickly move eggs to a small Petri dish and cover. Make sure the eggs remain dry during this process. Alternatively, after squeezing, touch the egg mass to the base of a small Petri dish or to the polytetrafluoroethene sheet as they are expelled from the female.

Immediately after collecting, put the fish into fresh system water for recovery.

Perform egg fertilization for *in vitro* fertilization of *B. gauderio*.

Add 100 µL of well-mixed sperm in SES (see below) directly over the egg mass.

Add 1 mL of system water (filtered through a 0.22 µm filter) and mix well for 30–60 s.

Add an additional 1–2 mL system water (leave some space in the Petri dish) and place in incubator. Record time of *in vitro* fertilization (IVF) on Petri dish and move to a 29 °C incubator. Set a 50 min timer to check progress of development (*e.g.*, formation of the single cell at the animal pole, see Figure 13). During this time, prepare materials for microinjection.

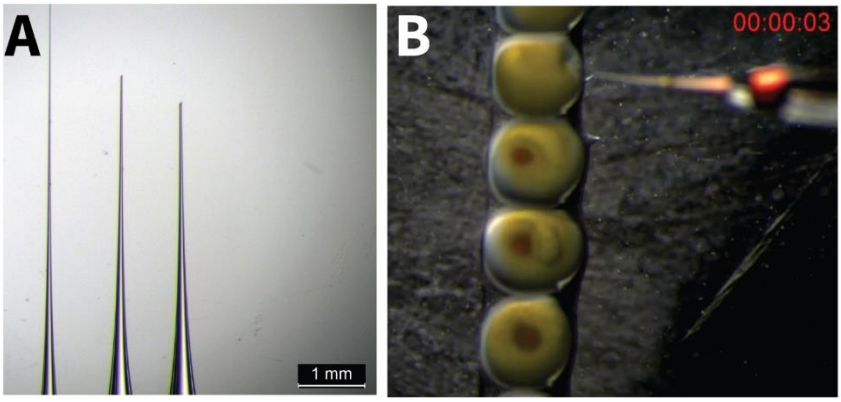

Figure 12: Microinjection- (A) Glass capillary needle tips must be broken to deliver an appropriate microinjection volume. The tip on the left is unbroken. The middle and right tips are broken with a slightly angled bevel to pierce the egg chorion. (B) Eggs are lined against a glass slide (1%–10% phenol red is included as a tracer to visualize the delivery of the injection) and injected with glass capillary needles

Single cell microinjection

Pull microinjection needles prior to spawning agent injections or natural spawning. Use a borosilicate glass capillary with a filament (outer diameter 1.0 mm, inner diameter 0.58 mm, 10 cm length) and a needle puller to pull microinjection needles. Prepare 2–4 needles per planned treatment injection.

NOTE: Backloading needles with a filament are preferred because the filament wicks the solution towards the tip and eliminates bubbles. However, needles without a filament can be used and frontloading should have no effect on the outcome. The needle should have a

long, but sturdy taper. Use the needle pulling program with the following specifications as a starting point: heat = 500; Pull = 70; Velocity = 70; and Time = 100. Representative needle morphologies are shown in Figure 12A.

Prepare injection solution and prepare needle

Add 0.9 µL of sgRNA and 0.9 µL of Cas9 enzyme (1 mg/mL) to 0.2 µL of 10% or 100% phenol red (for 1% and 10% final phenol red concentration, respectively) in a PCR tube. Mix well and let sit on ice 2−5 min to allow sgRNA and Cas9 to complex. Calculate the final concentration of sgRNA, Cas9, and phenol red in the injection solution.

NOTE: If there are issues with needle clogging or cutting efficiency using the above recipe, it may be useful to use a 1x final concentration salt/buffer mix to stabilize Cas9 and prevent needle clogging.

Use a microloader pipette tip to backload the 2 µL of solution into the microinjection needle. Expel the liquid as close to the tip as possible.

Load needle into micromanipulator and set pressure settings (start with 775 injection pressure, 0.1−0.2 s, and 8-12 compensation pressure).

Under the scope, use a pair of fine forceps to break the needle tip at a beveled angle. Break towards where the taper of the needle starts to have rigidity. It is best to break closer to the tip, test the size of the injection solution and then break further if necessary. The bore of the needle should remain as small as possible while maintaining a rigid taper (Figure 12A).

Use mineral oil and a micrometer to measure the size of the injection solution. 1–2 nL is typically used; 0.1 mm diameter is 0.5 nL.

Adjust the needle tip or pressure settings to get an injection volume within specifications.

Identify developing zygotes and prepare injection stage

Set up the injection stage. Take a 100 mm diameter Petri dish. Invert the bottom and place under the inverted top. Place a glass microscope slide within the inverted top.

Note: Depending on how your micromanipulator is mounted to the scope, the added height from the inverted base may be unnecessary.

Look at the developing eggs and identify presumed fertilized zygotes 50–60 min after IVF. The animal pole will begin to form and there will be an excess of small fat droplets around the yolk/animal cell interface (Figure 13).

Collect 10–20 eggs with as little water as possible using a plastic transfer pipette (cut the tip slightly to allow eggs to pass) and place onto the edge of the slide. Water will be wicked under the slide and pull eggs against the edge.

Use a delicate task wipe and gently press the slide to remove excess water and allow the eggs to firmly adhere to the edge of the slide. There should be just enough water to keep the eggs moist while maintaining little standing moisture to avoid egg movement during injection.

Inject directly into single cell

Align the eggs against the slide vertically, perpendicular to the approaching needle (Figure 12B).

Using the micromanipulator, position the needle against the chorion. At roughly a 45° angle, insert the needle into the chorion, and then into the single cell. It can be helpful to enter the single cell through the yolk. Moving both the injection stage with the free hand and the micromanipulator may provide more control over the injection process (Figure 12B).

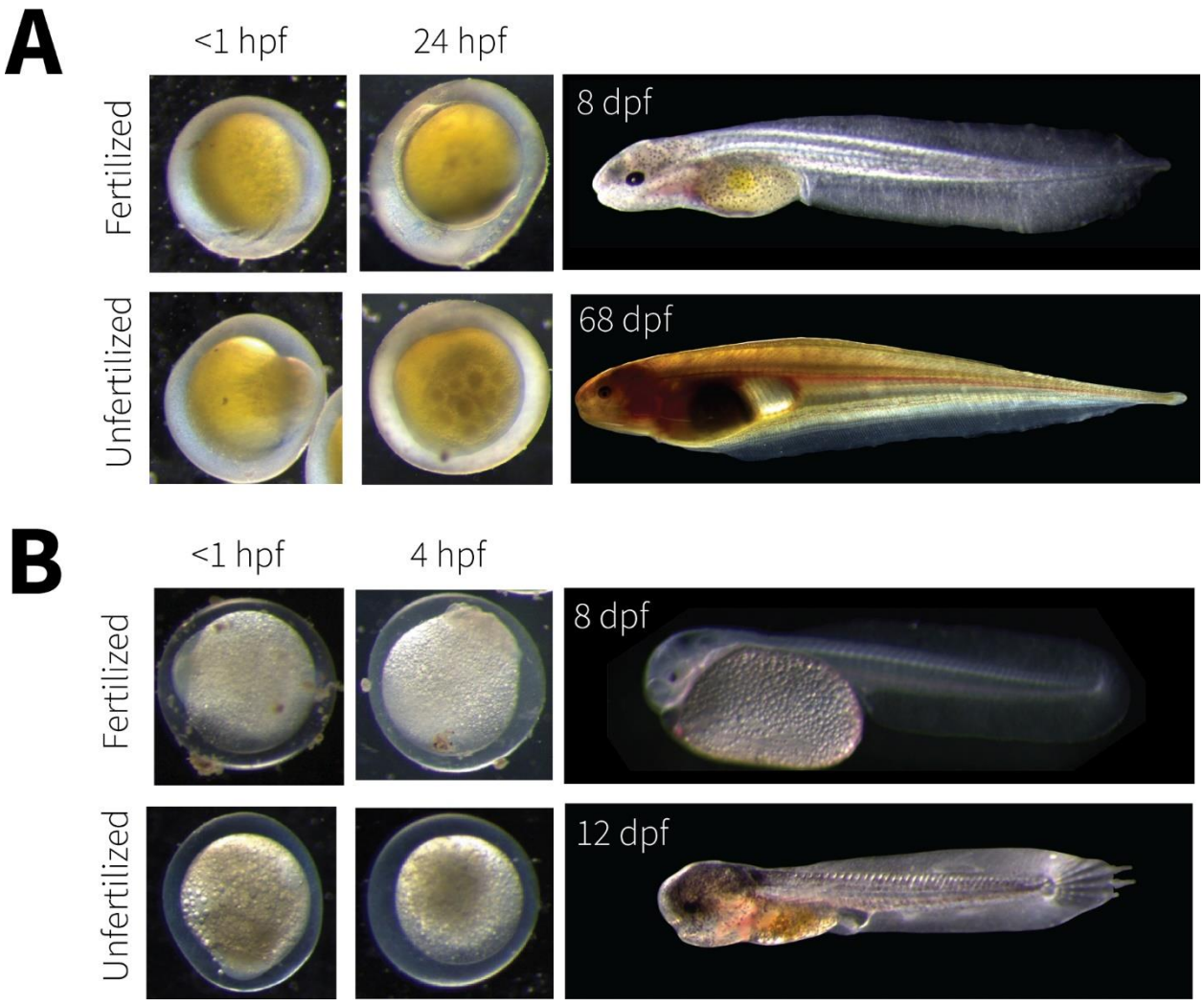

Figure 13: Developmental stages- (A) *Brachyhypopomus gauderio* and (B) *Brienomyrus brachyistius*. All eggs are assumed fertilized. Between 12−24 hours post fertilization embryos are visible in viable eggs, otherwise eggs exhibit degradation. Several divisions appear to take place on egg activation, regardless of fertilization. Unfertilized eggs exhibit unusual patterns of cleavage that are much more symmetrical in fertilized eggs.

Inject sgRNA/Cas9/phenol red solution into the single cell. Carefully remove the needle. Proceed to the next egg and repeat previous steps until all eggs are injected.

Remove any eggs broken during injection with fine forceps. Use 0.22 µm of filtered system water in a squirt bottle to gently remove eggs from the injection stage into a new 100 mm diameter Petri dish.

Repeat above steps until all eggs have been injected or have developed to the two-cell stage. Make sure to set aside approximately 20 presumed fertilized eggs as a no-injection control to determine fertilization rates and injection success per treatment ideally. For larger clutches use uninjected embryos that have developed to the two-cell stage, and for smaller clutches set aside presumed fertilized eggs.

Additionally, consider a sgRNA/injection control by injecting 15–25 embryos with Cas9 complexed with an sgRNA against a gene that is not present in the genome. The GFP gene recommended for wild type embryos.

Record the number of eggs, parents, IVF time, and date on each Petri dish. Include sgRNA target or label as uninjected. Move to a 29°C incubator.

Animal Husbandry

Care for eggs

Check egg viability 4–6 h following injections.

Record the number of dead eggs, as well as any that are unfertilized. The unfertilized eggs will arrest around the eight-cell stage and have a rosette pattern of the cells at the animal pole (Figure 13). Depending on number of dead eggs and amount of egg debris

in the water, remove at least 50%–80% of the water and replace with filtered system water. It can be helpful to scrub the bottom of the Petri dish if a cellular debris film or biofilm forms.

For the next 2–3 days, check eggs 1–2x daily. Repeat steps above each time the eggs are checked.

After 2−3 days the larvae will hatch. Remove all egg casings as they hatch. Gentle pipetting can help to free half-hatched larvae.

Care for larvae

Check 1−2x daily. Record and remove any dead larvae. remove at least 50%–80% of the water and replace with filtered system water. It can be helpful to scrub the bottom of the Petri dish if a cellular debris film or biofilm forms.

From 6–14 dpf, feed vinegar eels to the larvae. A slight excess of food is good, because the vinegar eels will remain alive in the dish. Add vinegar eels each time the dish is checked and cleaned as mentioned previously.

From 11–14 dpf, add 5–10 freshly hatched *Artemia* per larvae in addition to vinegar eels and when cleaned as mentioned previously. During this time, the larvae will learn to eat the free swimming *Artemia*.

At 15 dpf, move larvae to egg cups (see note below) in a tank with flowing water, filtration, and aeration. There should be no more than approximately 25 embryos per cup. Continue to add both vinegar eels and 15−30 freshly hatched *Artemia* per larvae from days 15–18. Clean Petri dish piece daily and use a pipette to remove masses of

dead *Artemia*.

Note: Egg cups are plastic cups with a mesh netting on the bottom. A 100 mm Petri dish top/bottom can be added to the bottom of the egg cup to help stop food from falling through the mesh. Egg cups allow the fish to be housed in a larger volume of water for water quality reasons, while maintaining discrete groups.

From days 18–30, feed only freshly hatched *Artemia*. Increase the feeding amount as the fish grow and if tail biting or high aggression is seen.

After approximately 30 days, move fish to 10 L (2.5 gallon) tanks, approximately 25 individuals per tank. Make sure there is filtration, aeration, and places for hiding. Consider cylindrical biofiltration media and small diameter PVC tubes.

Feed freshly hatched *Artemia* and blackworms from approximately 30–45 days onwards. Maintain standard cleaning and water changes for the tank (i.e., at a minimum ~10%–20% water change per 1 week).

After ~45 dpf, feed only blackworms until ~60 dpf.

After ~60 dpf, move cohorts of approximately 15 fish to 40 L (10 gallon) tanks and begin adult husbandry procedures. Add PVC tubes and a yarn “mop” (a mass of brown yarn tied together around a cork) for hiding places (Figure 10C). Fish should be nearing breeding size after approximately 3−4 months post fertilization for *B. gauderio* and after about 1 year for *B. brachyistius*.

Care for adults

Feed fish daily with enough blackworms so that a small amount of blackworms are present at the next feeding. This *ad libitum* feeding allows maximal growth.

A few times a week, it can be helpful to supplement the blackworm feeding with bloodworms.

Clean tanks every 2–4 weeks with a 20%–30% water change. If the yarn mop gets full of biofilm/algae, rub it clean under RO water.

Representative Results

The sgRNA target sites were identified within exon 1 of *scn4aa* in both *B. gauderio* and *B. brachyistius* as described. The sgRNAs were generated as described. Following successful sgRNA selection and synthesis (Figure 8), *in vitro* cleavage was tested (Figure 9). The sgRNAs demonstrating *in vitro* cutting were then selected for single cell microinjections.

Adult fish were conditioned for reproduction, then injected with a spawning agent and subsequently squeezed (*B. gauderio*) for IVF as described or allowed to spawn naturally (*B. brachyistius*) as described. These efforts yielded single cell embryos for microinjection in both species. As described, 1.5−2.0 nL of the *scn4aa* sgRNA/Cas9/phenol red complex (65-190 ng/uL sgRNA, 450 ng/uL Cas9, 1%−10% phenol red, final concentrations) was injected at the one-cell stage. Eggs from the same clutch were used as uninjected controls. All embryos were cared for as described. Following IVF, 40%–90% of eggs were fertilized, and 70%–90% of embryos survived to hatching following injection.

About 75% of fish survived to 6−11 dpf and were then phenotyped. Larval fish were placed into a 35 mm Petri dish embedded in a larger dish with Sylgard immobilized Ag/Cl recording electrodes (Figure 14A). Embryo movement was restricted using 3% agarose molds made with system water and cut to fit the embryo (Figure 14B). The same recording chamber was used for both species and the same agarose mold was used among species comparisons. Embryos were recorded for 60 s, which is sufficient to capture hundreds of EODs. Age and size-matched uninjected controls were selected for comparison. At this time point, 10%–30% of surviving embryos show a reduced amplitude EOD. Embryos displaying a reduction in EOD amplitude with no obvious morphological defects and control uninjected whole embryos were digested for DNA extraction and subsequent PCR of the *scn4aa* target site. There was often a range of penetrance of the phenotype, with some individuals having a stronger reduction in EOD amplitude than others.

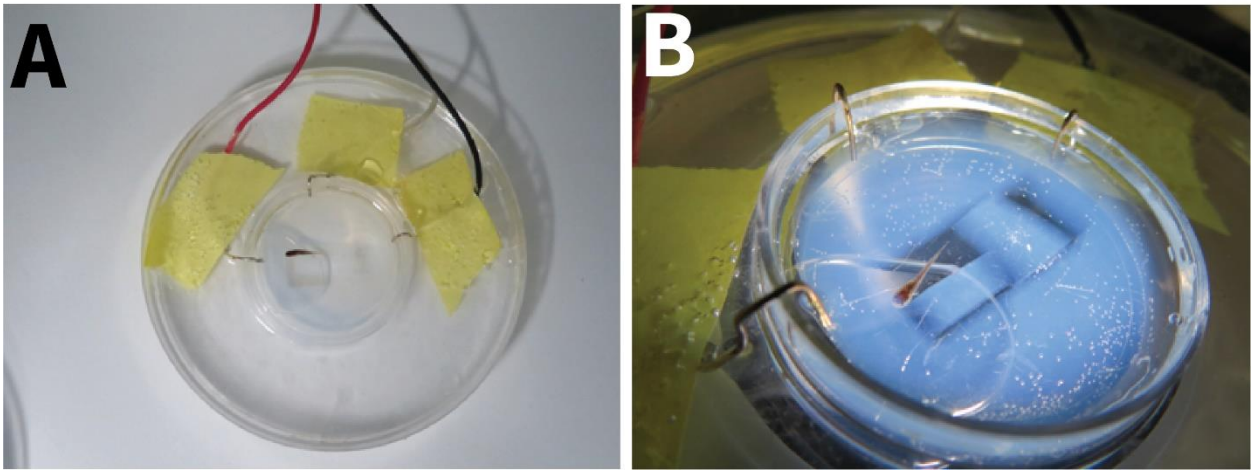

Figure 14: Photograph of larval recording chamber- (A) The electrodes are embedded within Sylgard but extend into the 35mm dish containing an embryo restricted via a 3% agarose mold. (B) Higher magnification image highlighting the restricted movement of the embryo due to agarose. Note the pieces of agarose that can be removed as the embryo changes size. The *B. gauderio* embryo shown is facing the positive electrode.

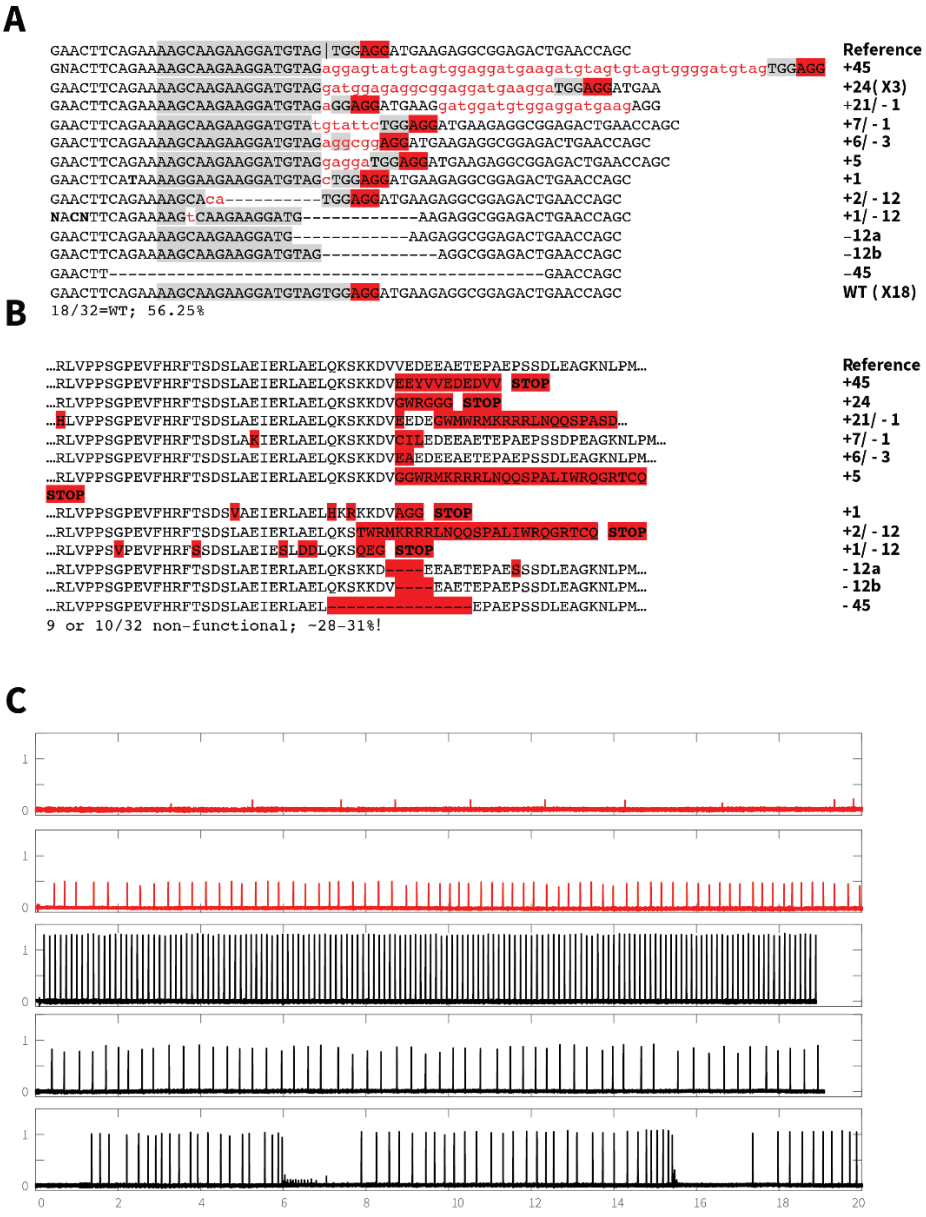

Figure 15: CRISPR/Cas9 induced mutations in *Brachyhypopomus gauderio*- (A) Thirty-two clone sequences from genomic DNA of Cas9-induced mutations in a single *scn4aa* targeted F_0 *B. gauderio embryo* (11 dpf). The reference sequence is underlined with the sgRNA target site highlighted in gray, the protospacer-adjacent motif (PAM) sequence highlighted in red, and the Cas9 cut site marked with "|". The change from the expected wild type sequence is given and the number of clones for each sequence is given in parenthesis. (Abbreviations: + = insertion, - = deletion, ± = InDel) Any non-CRISPR associated sequence dissimilarities are bolded. Figure modeled after (Jao, Wente and Chen, 2013). (B) Amino acid sequence predicted from sequenced clones of *scn4aa* knockdown *B. gauderio* from (A). Cas9-induced changes from the wild type sequence are highlighted in red and the nucleotide-induced change number is given. (C) Twenty-second electrical recordings from five size-matched larvae, all recorded 6 dpf in the same recording chamber. Gain settings are identical for all traces. Traces in red are from *B. gauderio*

Figure 15 (cont'd)

larvae with confirmed mutations (one individual shown in Figure 15A, B above), traces in black are from uninjected *B. gauderio* larvae. Overall, CRISPR/Cas9 editing of *scn4aa* showed a reduction in EOD amplitude, though the effect was heterogeneous.

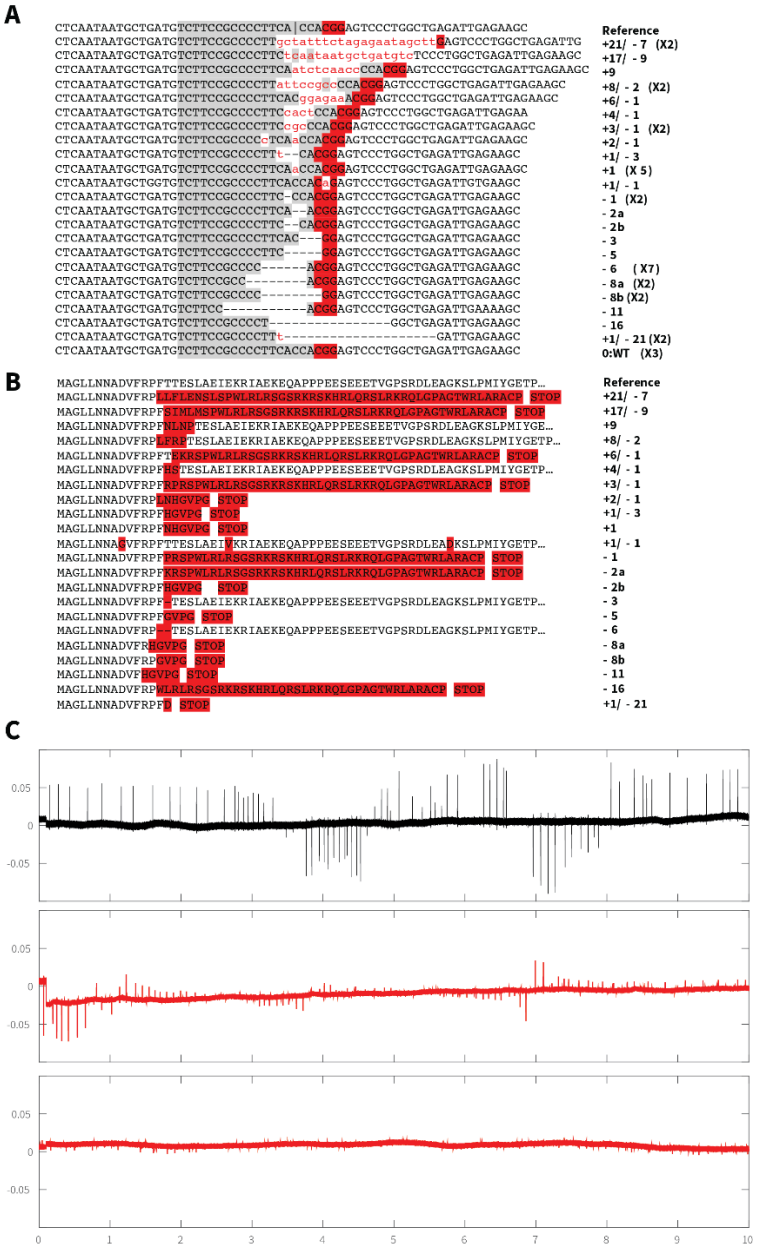

Figure 16: CRISPR/Cas9 induced mutations in *Brienomyrus brachyistius*- (A) Forty-two clone sequences from genomic DNA of Cas9-induced mutations in a single *scn4aa* targeted F_0 *B. brachyistius* embryo (11 dpf). The reference sequence is underlined with the sgRNA target site highlighted in gray, the protospacer-adjacent motif (PAM) sequence highlighted in red, and the Cas9 cut site marked with "|". The change from the expected wild type sequence is given and the number of clones for each sequence is given in parenthesis. (Abbreviations: + = insertion,

Figure 16 (cont'd)

- = deletion, ± = InDel) Any non-CRISPR associated sequence dissimilarities are bolded. Figure modeled after (Jao, Wente and Chen, 2013). (B) Amino acid sequence predicted from sequenced clones from *scn4aa* knockdown *B. brachyistius* in (A). Cas9-induced changes from the wild type sequence are highlighted in red and the nucleotide induced change number is given. (C) Ten second electrical recordings from four size-matched larvae, all recorded 10 dpf in the same recording chamber. Gain settings are identical for all traces. Traces in red are from *B. brachyistius* larvae with confirmed mutations (one individual shown in Figure 16A, B above), traces in black are from uninjected *B. brachyistius* larvae. Overall, CRISPR/Cas9 editing of *scn4aa* showed a reduction in EOD amplitude, though the effect was heterogeneous. Inverted EODs are from the fish changing orientation during the recording. No difference is discernible between experimental fish and controls despite this.

After PCR clean up and cloning, 30+ clones from each embryo were selected for Sanger sequencing. CRISPR/Cas9 induced mutations were identified in *B. gauderio* (Figure 15A, B) and *B. brachyistius* (Figure 16A, B) individuals with strong EOD amplitude reduction (Figure 15C and Figure 16C, respectively), where uninjected controls had only reference genotypes. Visualization of EOD amplitude between confirmed mutants ("CRISPR") and age/size matched uninjected controls demonstrated that both *scn4aa* mutant *B. brachyistius* (Figure 17A) and *B. gauderio* (Figure 17B) embryos had significantly lower EOD amplitude than controls ($p < 2.2 \times 10\text{-}16$, Welch two-sample t-test). CRISPR/Cas9 targeting of *scn4aa* was successful in both *B. brachyistius* and *B. gauderio* and implicate *scn4aa* in the larval/early electrocyte discharge in both species.

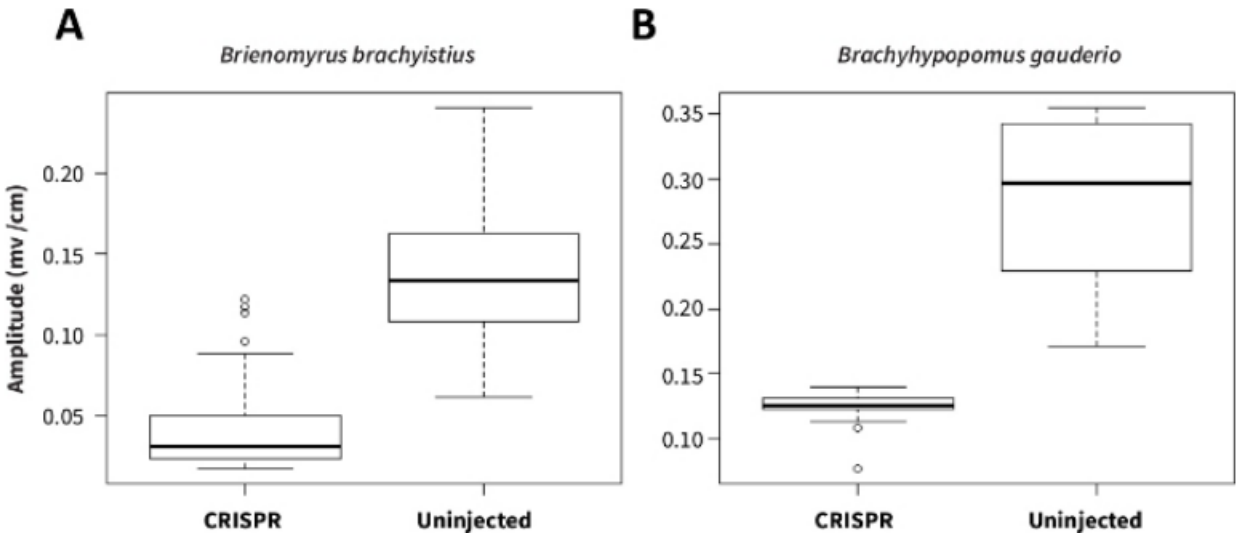

Figure 17: Average EOD amplitude of CRISPR and uninjected size/age matched siblings- (A) EOD amplitude of *B. brachyistius* larvae at 10 dpf. Recorded with a gain of 100, CRISPR EODs (*N* = 56) from two individuals, uninjected EODs (*N* = 114) from three individuals. (B) EOD amplitude of *B. gauderio* larvae at 6 dpf. Recorded with a gain of 500, CRISPR EODs (*N* = 34) from two individuals, uninjected EODs (*N* = 148) from three individuals. Amplitude of CRISPR fish was significantly less than uninjected controls ($p < 2.2 \times 10\text{-}16$, Welch two-sample t-test). All individuals were recorded with the recording chamber described in Figure 14.

CHAPTER 2

Abstract

Although there is overlap in the biological mechanisms responsible for reverse genetic knockdowns, delivery into novel organisms and development of the components that create specificity require experimentation and optimization. Before tools can be used to answer questions related to biology and gene function, the tools must be verified to work in the target species (recall the lack of RNAi in *Xenopus* and zebrafish, explained in the Introduction). Single cell embryos must be generated to perform efficient, whole organism, CRISPR/Cas9 genomic modifications. The previous chapter outlined a protocol that was developed for husbandry, breeding, and CRISPR/Cas9 in a gymnotiform, *Brachyhypopomus gauderio*, and a mormyrid, *Brienomyrus brachyistius* (Constantinou *et al.*, 2019). This chapter is a "Call to the Efish Community" where I discuss the application of the protocols from Chapter 1 for husbandry and CRISPR/Cas9 gene editing in new laboratories. I also make suggestions for future development and refinement of these protocols in electric fish species based on information collected while troubleshooting the protocols developed in Chapter 1. I intended to utilize the CRISPR/Cas9 protocols developed (Constantinou *et al.*, 2019) to establish mutant adults as founders for future mutant *scn4aa* stable lines and to document how the EOD changes over development when there is a suspected *scn4aa* mutation. However, these experiments were unable to be performed due to time constraints as well as safety considerations concerning laboratory work during the 2020-2021 Sars-CoV-2 pandemic as the Gallant laboratory shut down March 2020 and ceased all breeding programs during this time.

Introduction

CRISPR/Cas9 as a reverse genetic tool

Over the last 10-15 years, a tool amendable to reverse genetics has emerged that has already significantly changed the course of evolutionary studies. This tool is known as CRISPR/Cas9 genome modification. Clustered regularly interspaced short palindromic repeats (CRISPR) originated as a microbial defense system in bacteria (Horvath and Barrangou, 2010) and has since been optimized and utilized in a research setting (Jinek *et al.*, 2012). Prior to the utilization of the CRISPR/Cas9 system, it was difficult to study DNA function due to the inability to produce specific DNA sequence change(s) reliably and accurately in a cost and time effective way. Understanding the types of questions that can be asked through CRISPR by modifying the genome, is paramount to understanding the importance of developing this tool in electric fish.

CRISPR has already been demonstrated to broaden the understanding of novel traits, like the electric fish electric organ (Constantinou *et al.*, 2019). Through CRISPR-mediated loss of function, an elastin gene has been implicated in the development of the teleost specific bulbous arteriosus (Moriyama *et al.*, 2016), a structure that has been implicated in increased fitness of teleosts (Grimes and Kirby, 2009). Additional works have used CRISPR in a similar context to examine the role of genome duplication in neofunctionalization (Prince and Pickett, 2002) and can be used to explore novel protein function in complex organs (Gregory, 2008).

The arrival of CRISPR has allowed researchers to investigate many aspects of evolutionary biology beyond the sequence level. Specifically how a gene sequence leads to novel proteins, directs the amount and temporospatial distribution of gene products, and regulates in

direct response to the environment can be explored (Moriyama *et al.*, 2016). The usefulness of the CRISPR/Cas9 toolbox is highly promising, especially when considering the range of applications, Cas9 mutants, and the relative ease and low cost of this technology.

Electric fish breeding & husbandry history

To easily target the entire genome of an entire organism, it is best to modify the DNA during the single-cell stage. DNA within the nucleus of the first cell of a zygote will replicate to produce the DNA in all the cells of the adult body; a single modification event in a zygote could affect all the cells of an individual. To best utilize CRISPR as a tool, single-cell embryos must be able to be reliably collected, produced, or harvested. Although weakly electric fish (Gymnotiformes and Mormyridae) had been studied since the 1950's (Lissmann, 1951), it was not until the mid-1970's that breeding and developmental work were possible. Dr. Frank Kirschbaum is responsible for developing protocols to breed weakly electric fish in the laboratory, and has successfully done so in a number of species (see Kirschbaum and Schugardt, 2002; Schugardt and Kirschbaum, 2004; Kirschbaum and Schwassmann, 2008; Kirschbaum *et al.*, 2016; Nguyen *et al.*, 2017.

Dr. Kirschbaum began the work of breeding electric fishes by looking at the animals' natural lifecycle: Mormyridae and Gymnotiformes were thought to breed during the rainy season as females caught during that time have well-developed gonads and underdeveloped gonads during the dry season (Okedi, 1970; Hopkins, 1974). Kirschbaum first attempted to get these fishes to breed (Kirschbaum, 1975) by simulating a rainy season in the laboratory; the water levels were raised, the pH and conductivity dropped, the light cycle maintained, and rain was simulated. Under these conditions, the mormyrid *Pollimyrus isidori* began breeding in the lab after ~9 weeks and laid eggs in small clutches about a week apart.

In subsequent breeding attempts with *P. isidori*, it was found that a relative conductivity change (reducing the conductivity by about half) alone was sufficient for gonad recrudescence and senescence (Kirschbaum, 1987; Kirschbaum and Schugardt, 2002; Schugardt and Kirschbaum, 2004). The ionic composition of the water does not seem to have an effect on breeding; as long as the conductivity was decreased, the fish would spawn independent of the change in total hardness and carbonate hardness (Kirschbaum, 1987).

Artificial insemination can help reduce the difficulties that arise with collecting electric fish eggs at the one-cell stage from natural spawning events; eggs need to be collected hourly from breeding tanks and can disrupt fish subsequent spawns in that evening. It is much easier to introduce CRISPR components to the one cell stage via microinjection when the first cell formation can be timed by controlling fertilization. Gonadotropin Releasing Hormone can induce ovulation and sperm production, is available commercially as Ovaprim, and has been demonstrated to function in electric fish (Kirschbaum *et al.*, 2016). About 24 hours after administration of the hormone, sperm and eggs can be expressed and fertilized *in vitro*, adding another layer of control to the production of single-cell embryos for CRISPR.

Selection of gene target

Given the known links between ion channels, EODs, and selective forces on the EOD, modifications to genes that disrupt the EOD can be easily tested for function, and ultimately contribute to a deeper understanding of evolution. By creating mutants with specific mutations and a known phenotypic change to the EOD, theories about how EODs influence the evolution of electric fish, like through sexual selection (Curtis and Stoddard, 2003), can be tested directly. A clear “proof of concept” gene target for establishing reverse genetic tools in electric fish are

ion channels. One ion channel is the perfect target for electric fish, a voltage gated Na^+ channel NaV 1.4 encoded by the *scn4aa* gene.

scn4aa is the gene of electric fish that has garnered the most attention. *scn4aa* is expressed almost exclusively in the electric organ and *scn4ab* is expressed exclusively in muscle (Zakon *et al.*, 2006; Arnegard *et al.*, 2010). Positive selection has been identified in *scn4aa* in regions that change the channel kinetics by altering the speed at which the channel can open and close (Zakon *et al.*, 2006, 2008; Arnegard *et al.*, 2010; Paul *et al.*, 2016), suggesting NaV 1.4 has an effect on EOD shape and the rate at which EODs can be discharged. Evidence for this claim came when the EODs of *Sternopygus*, a wave type Gymnotiform, were shown to decrease in amplitude when electrocytes were bathed in the sodium channel disruptor tetrodotoxin (Ferrarla, Mcanelly and Zakon, 1995); however, these and other experiments suggesting *scn4aa* functions in generating the EOD amplitude (Shenkel and Sigworth, 1991; Ferrari and Zakon, 1993; Markham *et al.*, 2009), were done *in vitro* on dissected electric organs in culture. No functional tests have been done *in vivo* to verify the function of *scn4aa*, although the evidence from ion channel kinetics and *in vitro* studies suggest Nav 1.4 is the main ion channel responsible for electric organ discharge amplitude (Figure 6).

If *scn4aa* functions *in vivo* as the data collected thus far suggests, one would expect that electric organs with *scn4aa* disrupted through reverse genetic tools would express fewer functional Nav 1.4 proteins on the membrane faces and reduce the amplitude of the EOD. If fewer Na^+ ions can enter the electrocyte, the amplitude of the EOD would decrease, with a complete knockout being unable to evoke any EODs (unless there are other ion channels that contribute to producing the EOD). *scn4aa* was therefore selected as a target for reverse genetic

tool optimization given the straightforward assumptions of *scn4aa* function, and the low pleiotropic effects of *scn4aa.*

Methods

Larval measurements

Larvae length was measured using LAS v4.9 software on a photograph taken by Leica dissecting scope Mz10f that was calibrated with a micrometer. Larvae were placed directly onto a raised petri dish with minimal water to immobilize them for the photograph. The length was calculated by measuring through the body center from mouth to the tail tip from a photograph taken by the microscope.

Genotyping

DNA was extracted from the whole larva or adult tail tips using DNeasy Blood and Tissue Kit (QIAGEN) as per the manufacturer's instructions. gDNA was amplified surrounding the sgRNA target site using OneTaq (NEB) and standard cycling parameters suggested by the manufacturer. T_m was calculated using the NEB T_m calculator. PCR amplicons were verified by size using gel electrophoresis. Gels were made using 1% agarose, run at 100-140 volts and DNA ladders (50 bp and 100 bp; NEB) were used to verify size. Sequences are given in Table 1 and a schematic of where sgRNA and primers bind in exon 1 of *B. brachyistius* (Figure 18A) and *B. gauderio* (Figure 18B) is given in Figure 18.

The amplicons were then cloned into pSC-A-amp/kan vectors and transformed into bacteria using the StrataClone PCR kit (Agilent) as per the manufacturer's instructions. Colony PCR was performed on blue/white screened colonies using universal M13 F and R primers to

linearize clones. Linearized clones were purified and then sequenced at the Michigan State University genomics core via Sanger sequencing.

Genotyping was also completed on PCR amplicons via Paired-End Illumina sequencing through GENEWIZ. A 165 bp amplicon was generated using Bg Exon1 primer pairs (Table 1) which bind in Exon 1. Samples were prepared according to the instructions for "Amplicon-EZ" given by GENEWIZ.

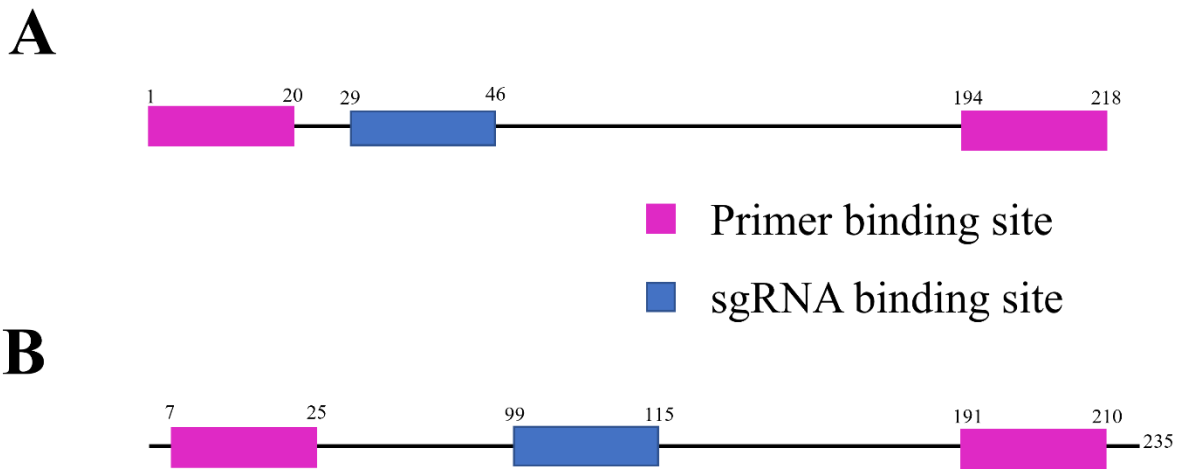

Figure 18: PCR primer and sgRNA binding sites. Exon 1 of *scn4aa* is shown for *B. brachyistius* (A) and *B. gauderio* (B). The PCR primer binding sites are given in purple and indicate how much of exon 1 is targeted and at what position relative to the start codon at 1. All of exon 1 is amplified in *B. brachyistius* (A) and nearly all of exon 1 is amplified in *B. gauderio* (B). The sgRNA binding site, and the location where CRISPR/Cas9 induced mutations should be found, is given in blue and indicate what position the sgRNA binds relative to the start codon at 1. 5' is to the left and 3' is to the right.

EOD recordings and analysis

Electric organ discharge (EOD) recordings were performed using bipolar silver chloride coated silver wire electrodes, amplified (bandwidth= 0.0001-50 kHz) with a bioamplifier (BMB 200), and digitized at a 100 kHz sampling rate. Custom software, d2d_EOD, developed by Dr. Jason Gallant, was developed to take recordings. Larval recordings were taken in a larval

recording chamber: a 35 mm Petri dish embedded in a larger dish with Sylgard immobilized Ag/Cl recording electrodes (Figure 14). Larval movement was restricted using 3% agarose molds made with system water and cut to fit the larvae (Figure 14B). The same recording chamber was used for both species and the agarose mold was kept moist in system water and replaced every few weeks. Adults were recorded in a 5-gallon tank within a recording chamber (Figure 26) which limited the movement of the fish and stabilized recording electrodes. 30 second to 2.5 minute recordings were taken. EOD recordings were analyzed by custom MATLAB code developed by Dr. Jason Gallant.

Generating growth curve

Individuals from a pool of 5-20 wild type fish were randomly sampled with replacement (Davies and Ratcliffe, 1994). Sampling with replacement means that in subsequent measurements it is possible that the same individual was measured again later in time as the wild type population was not followed at the individual level. Lengths and EOD amplitude was measured as described previously in the Methods and were used to generate a growth curve.

Statistics

Statistics were performed in R and reported in the body of the text. Code can be found at https://github.com/savvasjconstantinou/Chapter2 and in Appendix B.

Table 1: Sequences used in CRISPR procedures.

Description	**Sequence**
Constant oligomer	5'-AAAAGCACCGACTCGGTGCCACTTTTTCAAGTTGA-TAACGGACTAGCCTTATTTTAACTTGCTATTTCTAGCTCTAAAAC-3'

Table 1 (cont'd)

Target oligomer backbone (GG-N18, no PAM)	5'-TAATACGACTCACTATAGG-N18-GTTTTAGAGCTAGAAATAGCAAG-3'
Target oligomer backbone (N20, no PAM)	5'-TAATACGACTCACTATAG-N20-GTTTTAGAGCTAGAAATAGCAAG-3'
Brienomyrus brachyistius	
scn4aa Bb sgRNA target (N18, with PAM)	5'-TCTTCCGCCCCTTCACCACGG-3'
scn4aa Bb sgRNA oligomer (GG-N18)	5'-TAATACGACTCACTATAGGTCTTCCGCC-CCTTCACCAGTTTTAGAGCTAGAAATAGCAAG-3
scn4aa Bb PCR primer (218 bp)	
scn4aa _bb_exon1_F	5'-ATGGCCGGCCTTCTCAATAA-3'
scn4aa _bb_exon1_R	5'-TCTTCCAGGGGAATATTCATAAACT-3'
Brachyhypopomus gauderio	
scn4aa Bg sgRNA target (N17, with PAM)	5'- CAAGAAGGATGTAGTGGAGG-3'
scn4aa Bg sgRNA oligomer (GG-N17)	5'-TAATACGACTCACTATAGGCAA-GAAGGATGTAGTGGGTTTTAGAGCTAGAAATAGCAAG-3
scn4aa Bg PCR primer pair (204 bp)	
scn4aa _bg_exon1_F	5'-CGCCTTGTCCCTCCTTCAG-3'
scn4aa _bg_exon1_R	5'-ATCTTCAGGTGGCTCTCCAT-3'

See Figure 18 for a schematic of where primers and sgRNA bind in exon 1.

Results and Discussion: A Call to the Efish Community

The promise for understanding electric fish species at the molecular level rests partially on the ability to identify gene functions, ideally *in vivo*. Understanding the function of genes that are involved in EOD production can provide insights into electric fish biology. The evolutionary

history of the electric organ and EOD (Patterson and Zakon, 1997; Carl D Hopkins, 1999; Alshami *et al.*, 2020), the complex behaviors seen in electrosensing (von der Emde and Fetz, 2007; Gottwald *et al.*, 2018) and electrocommunication (Alves-Gomes, 2001; Smith, Schniederjan and Nguyenkim, 2013), and species diversification through EOD shape (Stoddard, 2002; Swapna *et al.*, 2018), are all mediated through molecules which are encoded in the genome. CRISPR/Cas9 could be a tool to identify EOD gene function in electric fish and holds promise for use in these non-model organisms. CRISPR/Cas9 is a powerful tool that has been added to the toolbox of techniques that electric fish researchers have at their disposal (Constantinou *et al.*, 2019). The ability to determine gene function through site directed mutagenesis *in vivo* will allow a wide array of electric fish researchers to better understand electric fish and generalizable biological processes through the well-established electric fish model systems.

In creating a protocol for CRISPR/Cas9 in both lineages of weakly electric fish, one major goal was accessibility. While incorporating molecular biology into research plans is increasing popular, there are still many research laboratories that lack training and equipment to perform advanced techniques. The protocol I designed attempted to use low cost, basic equipment, reagents, and kits that, with training, are accessible to even undergraduate researchers. While accessibility allows for more research groups to bring CRISPR/Cas9 into their laboratories, it is at the expense of ideal conditions. This “Call to the Community” section will help electric fish researchers to understand and avoid difficult situations that arise during design and execution of CRISPR/Cas9 mutagenesis and will present some considerations for future laboratories that intend to incorporate CRISPR/Cas9 mutants into their discoveries. Now that CRISPR/Cas9 is verified to be possible, the community must share both positive and

negative observations moving forward to facilitate throughput of generating genetic mutants through CRISPR/Cas9.

Breeding and husbandry

The first major consideration for researchers planning on bringing the CRISPR/Cas9 genome editing technique into their laboratories is breeding and husbandry. While a number of electric fish species have now been bred in the laboratory (see Kirschbaum and Schugardt, 2002; Schugardt and Kirschbaum, 2004; Kirschbaum and Schwassmann, 2008; Kirschbaum *et al.*, 2016; Nguyen *et al.*, 2017 for lists of electric fish species successfully bred in captivity), many species are still not able to be bred robustly. The need for copious amounts of single-cell embryos (Table 2, Table 3) requires researchers to have a well-established breeding colony, especially if the collection of single-cell embryos requires natural spawning. Thousands of eggs were produced for developing the breeding, husbandry, and CRISPR/Cas9 protocols in *B. brachyistius* and *B. gauderio* (Table 2, Table 3). We began injecting *B. brachyistius* embryos in September 2016 and *B. gauderio* embryos in February 2017. The final *B. brachyistius* egg collection was July 2017 and the final *B. gauderio* squeezings were performed in late October 2019. There was a decrease in the number of gametes and fertilized *B. gauderio* embryos produced in fall/winter 2018 and into 2019; however, see below for additional information on how fertilization rates were improved after 2019. Given how many eggs were required to produce the few verified mutants that were generated, increasing success in generating viable embryos is a must and some ideas are given below.

I was able to increase success in generating embryos through a few manipulations during protocol development. Both using Teflon coated tools on eggs during *in vitro* fertilization (Hagedorn and Carter, 2011) and limiting handling of eggs by expressing them directly into the

petri dish, anecdotally appeared to increase fertilization rates. Squeezing eggs directly into water, even if sperm is immediately available, is not ideal. It may cause premature activation of eggs, resulting in reduced sperm movement through the micropyle and decreased fertilization rates (Amanze and Iyengar, 1990).

An alteration to the Chapter 1 protocol and consideration to increase fertilization rates is to change the timing of squeezing. Instead of squeezing males first and storing sperm in sperm extender solution (SES), the Gallant laboratory has anecdotally demonstrated increased fertilization rates in *B. gauderio* by first squeezing a clutch of eggs from a female into a dry dish, then squeezing sperm from a male and directly fertilizing the eggs with the sperm while adding system water. If researchers are familiar with squeezing gametes, and especially if there are two people working together, the SES is unnecessary and using fresh-squeezed sperm would likely increase fertilization rates. Alternatively, it may be necessary to determine a different composition of the SES that the sperm is stored in to maximize the usefulness of the SES while limiting any reduction in fertilization rates (Matthews *et al.*, 2018; Beirão *et al.*, 2019).

Another consideration for improving embryo production is scheduling of Ovaprim injections. While I did not explicitly test the effect of multiple Ovaprim injections over time, nor the effect of the length of intervals between Ovaprim injections, there is a possibility that administration of Ovaprim may reduce natural spawning frequency in *B. gauderio* (Figure 19). There is variability in the number of natural spawning events seen in different groups of breeding individuals during the summer 2018 breeding season. During the summer 2018 breeding season, there is a decrease in the number of natural spawning events. There may be a reduction in natural spawning events after beginning Ovaprim injections and squeezing the next day; however, the data collected cannot be used to confirm this possibility as tanks without Ovaprim were not

included. It is unclear if Ovaprim hormonally reduces natural spawning frequency, if the stress and physical toll of squeezing reduces natural spawning frequency, or if there is not an effect and the reduction in spawning events is normal given the amount of time that has passed over the course of the breeding season (Kirschbaum, 1987; Kirschbaum and Schugardt, 2002).

The effects of Ovaprim vary among fish species. Ovaprim can increase the production of eggs in many species and allows manual stripping of gametes (Nguyen *et al.*, 2017; Nuraini *et al.*, 2017; Zadmajid *et al.*, 2017; Brzuska, 2021). Ovaprim has also been shown to reduce egg quality (Brzuska, 2021) and, depending on dose, can reduce fertilization rates (Mylonas, Hinshaw and Sullivan, 1992; Mylonas and Zohar, 2007; DiMaggio, Broach and Ohs, 2013) and alter the number of spawning events following injection (DiMaggio, Broach and Ohs, 2013). The interval between sperm collection can have an effect on sperm quality in other species (Suquet *et al.*, 1992; Cejko *et al.*, 2018; Diogo *et al.*, 2019). While there did not seem to be a decrease in sperm quality or quantity with 1 week between Ovaprim injections and squeezing in *B. gauderio* males, allowing 2-4 weeks between Ovaprim and squeezing in weakly electric fish males may be ideal to minimize stress and potential damage to the fish as well as increase sperm volume.

Harvesting eggs hourly in breeding pairs/groups is labor-intensive and may stress actively breeding pairs. Even though I was unable to produce viable gametes from squeezing *B. brachyistius*, it is possible in mormyrids (communications to Gallant laboratory from Dr. Frank Kirschbaum) and would be an ideal method for producing timed single-celled embryos for other mormyrid researchers to limit problems with naturally spawning embryo collection. Moving forward as an Efish community, research is required to investigate the effects of Ovaprim and squeezing frequency on spawning intervals, egg and sperm viability, and for determining

species-specific doses and between-Ovaprim intervals to maximize gamete output while maintaining gamete quality and reducing harm to parent fishes.

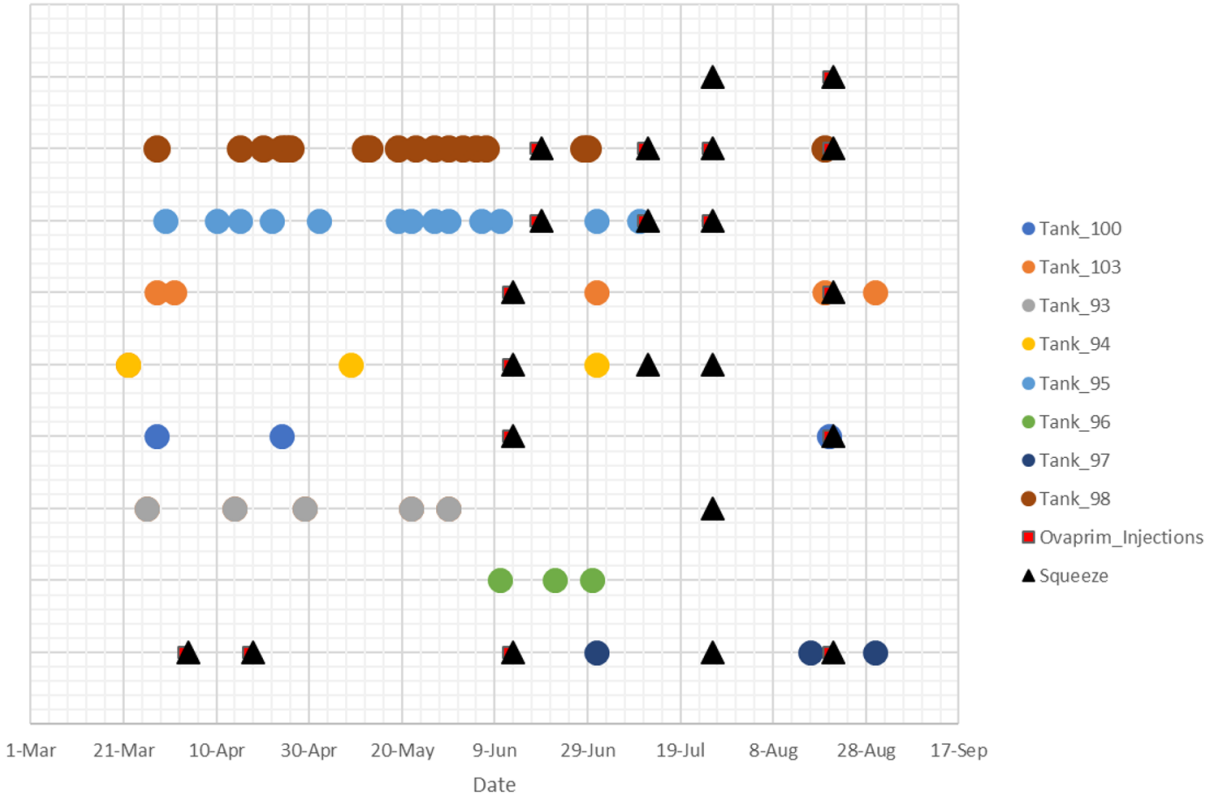

Figure 19: Summer 2018 *Brachyhypopomus gauderio* natural spawning events- The natural spawning events for different breeding groups of *B. gauderio* over the 2018 Summer breeding season are shown. Conductivity was dropped at the beginning of March. Colored circles indicate natural spawning events, Ovaprim injections are displayed as a red square and squeezing events are marked with a black triangle. The top line of data represents a tank that did not breed. Over the breeding season there is a decrease in the number of natural spawning events and there may be reduced spawning following Ovaprim injections.

Table 2: Fate of eggs produced during husbandry, breeding, and CRISPR/Cas9 experiments in *Brienomyrus brachyistius*.

9-12-2016	
Number of eggs collected/squeezed	110
Number of CRISPR/Cas9 injected eggs	78
Number of collected/squeezed eggs that survive 24 hours	25
% of collected/squeezed eggs that survive 24 hours	22.73
Number of embryos that survive 14 days	0

Table 2 (cont'd)

% of collected/squeezed eggs that survive 14 days	0
Number of deformed embryos	4
Number of embryos that demonstrated potentially reduced EOD amplitude	0
Number of individuals with confirmed CRISPR/Cas9 mutagenesis	0
9-19-2016	
Number of eggs collected/squeezed	132
Number of CRISPR/Cas9 injected eggs	92
Number of collected/squeezed eggs that survive 24 hours	54
% of collected/squeezed eggs that survive 24 hours	40.91
Number of embryos that survive 14 days	14
% of collected/squeezed eggs that survive 14 days	10.61
Number of deformed embryos	13
Number of embryos that demonstrated potentially reduced EOD amplitude	2
Number of individuals with confirmed CRISPR/Cas9 mutagenesis	1
9-26-2016	
Number of eggs collected/squeezed	322
Number of CRISPR/Cas9 injected eggs	224
Number of collected/squeezed eggs that survive 24 hours	118
% of collected/squeezed eggs that survive 24 hours	36.65
Number of embryos that survive 14 days	0
% of collected/squeezed eggs that survive 14 days	0
Number of deformed embryos	10
Number of embryos that demonstrated potentially reduced EOD amplitude	0
Number of individuals with confirmed CRISPR/Cas9 mutagenesis	0
10-3-2016	
Number of eggs collected/squeezed	277
Number of CRISPR/Cas9 injected eggs	169
Number of collected/squeezed eggs that survive 24 hours	105
% of collected/squeezed eggs that survive 24 hours	37.91
Number of embryos that survive 14 days	1
% of collected/squeezed eggs that survive 14 days	0.36
Number of deformed embryos	1
Number of embryos that demonstrated potentially reduced EOD amplitude	0
Number of individuals with confirmed CRISPR/Cas9 mutagenesis	0
10-24-2016	
Number of eggs collected/squeezed	488
Number of CRISPR/Cas9 injected eggs	263
Number of collected/squeezed eggs that survive 24 hours	147
% of collected/squeezed eggs that survive 24 hours	30.12
Number of embryos that survive 14 days	10

Table 2 (cont'd)

% of collected/squeezed eggs that survive 14 days	2.05
Number of deformed embryos	31
Number of embryos that demonstrated potentially reduced EOD amplitude	5
Number of individuals with confirmed CRISPR/Cas9 mutagenesis	0
7-24-2017	
Number of eggs collected/squeezed	244
Number of CRISPR/Cas9 injected eggs	143
Number of collected/squeezed eggs that survive 24 hours	14
% of collected/squeezed eggs that survive 24 hours	5.74
Number of embryos that survive 14 days	1
% of collected/squeezed eggs that survive 14 days	0.41
Number of deformed embryos	1
Number of embryos that demonstrated potentially reduced EOD amplitude	1
Number of individuals with confirmed CRISPR/Cas9 mutagenesis	0
Totals	
Number of eggs collected/squeezed	**1573**
Number of CRISPR/Cas9 injected eggs	**969**
Number of collected/squeezed eggs that survive 24 hours	**463**
% of collected/squeezed eggs that survive 24 hours	**29.43**
Number of embryos that survive 14 days	**26**
% of collected/squeezed eggs that survive 14 days	**1.65**
Number of deformed embryos	**60**
Number of embryos that demonstrated potentially reduced EOD amplitude	**8**
Number of individuals with confirmed CRISPR/Cas9 mutagenesis	**1**

Deformed embryos are scored at 3 dpf when WT embryos hatch and are well formed. %-percentage.

Table 3: Fate of eggs produced during husbandry, breeding, and CRISPR/Cas9 experiments in *Brachyhypopomus gauderio.*

2-28-2017	
Number of eggs collected/squeezed	N/A
Number of CRISPR/Cas9 injected eggs	N/A
Number of collected/squeezed eggs that survive 24 hours	≥2
% of collected/squeezed eggs that survive 24 hours	N/A
Number of embryos that survive 14 days	≥1
% of collected/squeezed eggs that survive 14 days	N/A
Number of deformed embryos	N/A
Number of embryos that demonstrated potentially reduced EOD amplitude	2
Number of individuals with confirmed CRISPR/Cas9 mutagenesis	1

Table 3 (cont'd)

6-19-2018	
Number of eggs collected/squeezed	253
Number of CRISPR/Cas9 injected eggs	76
Number of collected/squeezed eggs that survive 24 hours	36
% of collected/squeezed eggs that survive 24 hours	14.23
Number of embryos that survive 14 days	11
% of collected/squeezed eggs that survive 14 days	4.35
Number of deformed embryos	4
Number of embryos that demonstrated potentially reduced EOD amplitude	0
Number of individuals with confirmed CRISPR/Cas9 mutagenesis	0
7-12-2018	
Number of eggs collected/squeezed	780
Number of CRISPR/Cas9 injected eggs	218
Number of collected/squeezed eggs that survive 24 hours	52
% of collected/squeezed eggs that survive 24 hours	6.67
Number of embryos that survive 14 days	36
% of collected/squeezed eggs that survive 14 days	4.62
Number of deformed embryos	10
Number of embryos that demonstrated potentially reduced EOD amplitude	3
Number of individuals with confirmed CRISPR/Cas9 mutagenesis	0
7-26-2018	
Number of eggs collected/squeezed	52
Number of CRISPR/Cas9 injected eggs	32
Number of collected/squeezed eggs that survive 24 hours	6
% of collected/squeezed eggs that survive 24 hours	11.54
Number of embryos that survive 14 days	1
% of collected/squeezed eggs that survive 14 days	1.92
Number of deformed embryos	2
Number of embryos that demonstrated potentially reduced EOD amplitude	1
Number of individuals with confirmed CRISPR/Cas9 mutagenesis	1
8-21-2018	
Number of eggs collected/squeezed	323
Number of CRISPR/Cas9 injected eggs	137
Number of collected/squeezed eggs that survive 24 hours	7
% of collected/squeezed eggs that survive 24 hours	2.17
Number of embryos that survive 14 days	4
% of collected/squeezed eggs that survive 14 days	1.24
Number of deformed embryos	1
Number of embryos that demonstrated potentially reduced EOD amplitude	0
Number of individuals with confirmed CRISPR/Cas9 mutagenesis	0

Table 3 (cont'd)

10-24-2018	
Number of eggs collected/squeezed	162
Number of CRISPR/Cas9 injected eggs	4
Number of collected/squeezed eggs that survive 24 hours	0
% of collected/squeezed eggs that survive 24 hours	0
Number of embryos that survive 14 days	0
% of collected/squeezed eggs that survive 14 day	0
Number of deformed embryos	0
Number of embryos that demonstrated potentially reduced EOD amplitude	0
Number of individuals with confirmed CRISPR/Cas9 mutagenesis	0
2-8-2019	
Number of eggs collected/squeezed	202
Number of CRISPR/Cas9 injected eggs	150
Number of collected/squeezed eggs that survive 24 hours	92
% of collected/squeezed eggs that survive 24 hours	45.54
Number of embryos that survive 14 days	57
% of collected/squeezed eggs that survive 14 days	28.22
Number of deformed embryos	18
Number of embryos that demonstrated potentially reduced EOD amplitude	27
Number of individuals with confirmed CRISPR/Cas9 mutagenesis	0
7-30-2019	
Number of eggs collected/squeezed	70
Number of CRISPR/Cas9 injected eggs	25
Number of collected/squeezed eggs that survive 24 hours	26
% of collected/squeezed eggs that survive 24 hours	37.14
Number of embryos that survive 14 days	3
% of collected/squeezed eggs that survive 14 days	4.29
Number of deformed embryos	9
Number of embryos that demonstrated potentially reduced EOD amplitude	0
Number of individuals with confirmed CRISPR/Cas9 mutagenesis	0
8-6-2019	
Number of eggs collected/squeezed	656
Number of CRISPR/Cas9 injected eggs	246
Number of collected/squeezed eggs that survive 24 hours	35
% of collected/squeezed eggs that survive 24 hours	5.34
Number of embryos that survive 14 days	9
% of collected/squeezed eggs that survive 14 days	1.37
Number of deformed embryos	0
Number of embryos that demonstrated potentially reduced EOD amplitude	2
Number of individuals with confirmed CRISPR/Cas9 mutagenesis	0

Table 3 (cont'd)

10-24-2019	
Number of eggs collected/squeezed	196
Number of CRISPR/Cas9 injected eggs	84
Number of collected/squeezed eggs that survive 24 hours	1
% of collected/squeezed eggs that survive 24 hours	0.51
Number of embryos that survive 14 days	0
% of collected/squeezed eggs that survive 14 days	0
Number of deformed embryos	0
Number of embryos that demonstrated potentially reduced EOD amplitude	0
Number of individuals with confirmed CRISPR/Cas9 mutagenesis	0
Totals	
Number of eggs collected/squeezed	**2694**
Number of CRISPR/Cas9 injected eggs	**972**
Number of collected/squeezed eggs that survive 24 hours	**257**
% of collected/squeezed eggs that survive 24 hours	**9.54**
Number of embryos that survive 14 days	**122**
% of collected/squeezed eggs that survive 14 days	**4.53**
Number of deformed embryos	**44**
Number of embryos that demonstrated potentially reduced EOD amplitude	**35**
Number of individuals with confirmed CRISPR/Cas9 mutagenesis	**2**

Deformed embryos are scored at 3 dpf when WT embryos hatch and are well formed. %- percentage.

To generate stable mutant lines or study phenotypes in F_0 crispants, one needs to be able to rear the embryos to adulthood, or at least until the age that is appropriate for the gene/behavior that is under study. Raising weakly electric fish requires laboratories to establish methods that are viable for their space, food sources, and labor. There are large losses of individuals, especially after 24 hours (mostly due to unfertilized eggs) and around 14 dpf when embryos begin exogenous feeding (Sifa and Mathias, 1987). I was unable to accurately determine rates of death as unfertilized embryos were not differentiated until 24 hpf. Understanding the development and housing requirements for the electric fish species under study should be well understood before any mutants are produced. This is especially important as crispants may be

deficient due to the mutations they carry, so they may require additional care and attention during growth depending on what phenotype arises from the mutation.

It is important to consider housing and feeding requirements for improving the survival of electric fish embryos. The Gallant lab uses a dedicated breeding room with tanks designed for rearing embryos (see Chapter 1). The design allows water to flow across the eggs and has a large volume to absorb any spikes in ammonium. Eggs were also successfully reared in large petri dishes in an incubator (~29°C) with daily water changes until hatching, or just prior to exogenous feeding, as done with other electric fish species previously (Nguyen *et al.*, 2017). We also used a commercial Zebrafish housing rack from Aquaneering Inc to rear fish a few days after hatching and into exogenous feeding and their juvenile stage. The commercial rack system was advantageous for work with crispants as cohorts could be separated physically during phenotyping or for different age groups (food sources would differ) while allowing shared water parameters.

While time-consuming, 2X daily monitoring of eggs until hatching helps increase survival rates as dead, dying, and fungal infected eggs can be identified and removed. Removal of dead eggs to reduce fungal infections is especially important when rearing in petri dishes vs a flow-through system (water movement via pumping water or through aeration), as water flow helps reduce fungal infections (Rach, Marks and Dawson, 1995; Small, 2006). Treatment with chemicals (Schreier, Rach and Howe, 1996; Sudova *et al.*, 2007; Whipps and Kent, 2019) can reduce fungal and bacterial infections from arising, and can be used to treat eggs that have been exposed to fungal infections from dead/dying members of the clutch. While I did not extensively explore the use of these chemicals and their effects on egg health nor fungal infection rates, using 10 uL/L of 0.1% methylene blue on eggs did not appear to have any toxic effects.

Exogenous feeding is a critical step in development for fishes (Sifa and Mathias, 1987). Providing the proper food source in early development to allow fish the opportunity to learn to hunt and feed is necessary to reduce die-off around 10-14 dpf in weakly electric fish. Freshly hatched *Artemia* are a widely used food source for many species of cultured fish (Bengtson, Léger and Sorgeloos, 1991; Sorgeloos, Dhert and Candreva, 2001; Dhont *et al.*, 2013; Tye *et al.*, 2015) and were a successful first food choice in *B. brachyistius* and *B. gauderio* as well as other electric fish species (Nguyen *et al.*, 2017). The size of freshly hatched *Artemia* is just small enough for electric fish larvae that begin to feed exogenously; however, the use of a smaller first food source may increase survival during the exogenous feeding critical period. A colony of vinegar eels, *Turbatrix aceti* (Brüggemann, 2012; Kolesnik *et al.*, 2019), was maintained and used as a first food source provided a day or two before freshly hatched *Artemia*. The nematodes were seen in the stomach of fry, suggesting they were being consumed. Rotifers as a first food source was explored early in development of husbandry protocols. A polyculture with a marine rotifer (Best *et al.*, 2010; Lawrence *et al.*, 2016) was attempted with *B. brachyistius* larvae; however, the larvae all died within 2 days of the polyculture. It is unclear if the death was a result of the culture method as no individuals from the cohort were reared outside the polyculture. Future explorations into polyculture with a freshwater rotifer (to reduce any acclimation to salinity/conductivity for the embryos and rotifers necessary for polyculture with the marine rotifer) may be worth testing.

Phenotyping crispants

Many electric fish researchers are interested in the EOD. I expect that many of the first mutants generated through CRISPR/Cas9 in the electric fish community will have a gene mutated that is thought to be involved in the EOD. As such, a baseline of how the EOD behaves

over developmental time is crucial to phenotype potential crispants who may have EOD alterations. The end goal of establishing breeding and husbandry techniques in a new laboratory or species depends on the gene(s) that are going to be mutated. For example, if one wants to see the effect of a particular gene on the EOD, how the EOD changes over developmental time needs to be well understood to phenotype potential crispants as they develop. How the EOD changes over time is especially important given the differences in larval and adult EODs that exists in many electric fish species (Westby and Kirschbaum, 1977, 1978; Franchina, 1997; Kirschbaum and Schwassmann, 2008; Kirschbaum and Denizot, 2011; Schwassmann, Assunção and Kirschbaum, 2014; Kirschbaum *et al.*, 2016; Nguyen *et al.*, 2017, 2020). The length of the embryo was a better predictor for the EOD amplitude than age, so researchers must make sure to record embryo length when establishing wild type developmental standards.

To identify potential crispants phenotypically, I produced a growth curve of wild type *B. gauderio* that correlated body length with EOD amplitude during early development (Figure 20). Comparison of potential crispant fish to the WT amplitude using body size and a linear model provides a means for identifying potential *scn4aa* crispants by comparing EOD amplitude at a particular size to the wild type standard (Iovine and Johnson, 2000). Ideally, a single data point can help to identify if a potential crispant shows evidence of reduced amplitude by using the linear model predicted from the wild type growth and determining if the point falls outside the confidence interval (provided that the individual is not deformed).

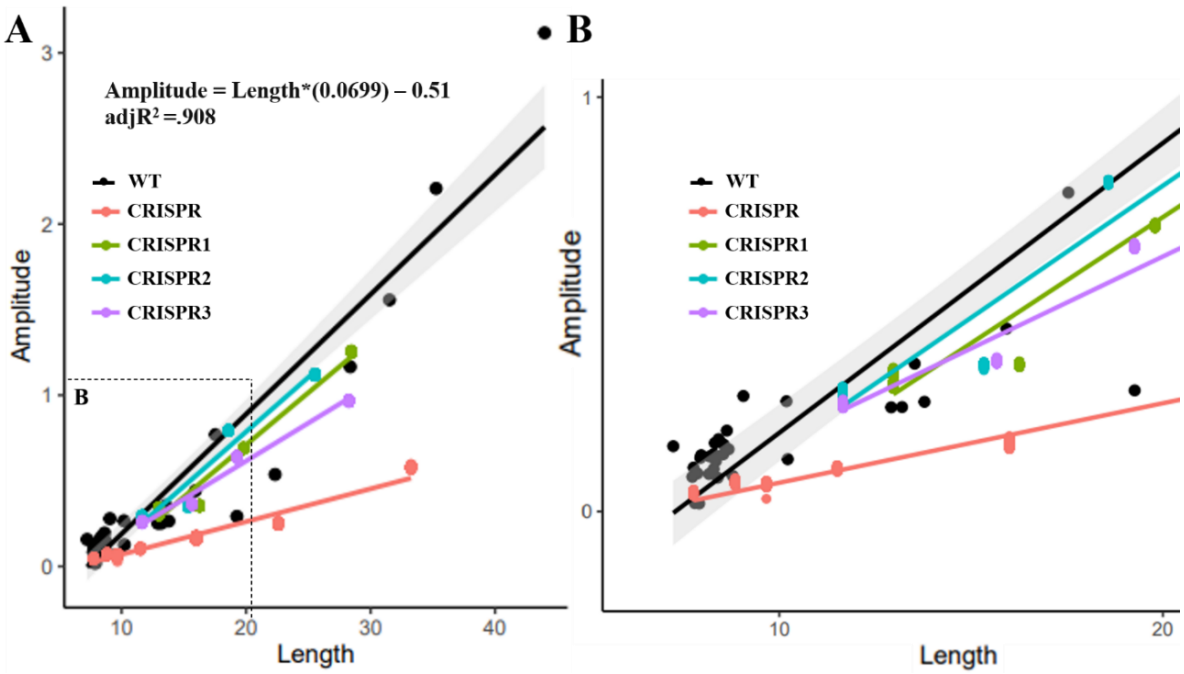

Figure 20: Juvenile *B. gauderio* EOD amplitude changes with body size- EOD amplitude (arbitrary units) is plotted against total body length (mm) for growing *B. gauderio* larvae. A) Wild type (WT) are from a random collection of individuals whereas the CRISPR fishes follow a particular potential *scn4aa* crispant individual over time. Each point represents >290 individual EODs where most time points *N*=~1000. A one-way linear regression of length~amplitude is shown for each crispant and for WT which also displays 95% confidence intervals. B) Enlargement from area denoted by dotted lines in A; during early development it is more difficult to predict potential crispants. There is little variance in EOD amplitude of small WT fishes and the predictive power for mutants increases when multiple length and amplitude measures are taken over time, especially if the embryo is measured past 15-20 mm.

Potential *B. gauderio* crispant individuals (*N*=4) and uninjected wild type siblings (*N*=20) were monitored throughout early development and into adulthood. The potential crispant fishes demonstrated a reduced EOD amplitude compared to wild type fish (Figure 20A). Linear regression analysis was used to generate a model to significantly predict amplitude in wild type fish based on size. The results of the regression indicated that wild type amplitude can be predicted from length (in mm) by the formula: Amplitude = Length*(0.0699) – 0.51 ($adjR^2$ =.908, $F(1,35)=357.8$, $p<.001$). The linear regression of any given crispant's amplitude during growth falls outside of the confidence interval of the wild type growth predicted by the

model (Figure 20), suggesting that these four crispants have a reduced EOD amplitude compared to wild type and may be mutated at the *scn4aa* locus. CRISPR1-3 have a mild EOD amplitude reduction compared to WT and CRISPR has a severely reduced EOD amplitude compared to CRISPR1-3 or WT.

A constraint of the model is that at early time points there is less ability to accurately predict if a crispant is showing a phenotype. This is due in part to the low amplitude variance seen among wild type fish when they first begin the EOD at around 7-8 mm (Figure 20B). The model is better able to predict if a fish is showing a mutant phenotype from length when the amplitude is measured at multiple sizes, especially if the data is for fish of ~20-40 mm in length. Future explorations of electric fish EOD ontogeny should increase the number of individuals and have a large enough pool of individuals to reduce the possibility of sampling the same individual at successive time points.

Genotyping crispants

When selecting sgRNA targets (Chapter 1), the ability for the target region to be amplified by PCR and sequenced must be tested. In my experience, it was not ideal to submit PCR sequences using the primer that amplified the amplicon; looking at chromatograms, it was difficult to determine if a specific mutation had taken place and the identity of the mutant sequence was hard to predict, although some bioinformatic tools do exist (Brinkman *et al.*, 2014). Cloning avoids this problem by sequencing individual PCR amplicons and is a widespread method for genotyping crispants (Yang *et al.*, 2013; Irion, Krauss and Nusslein-Volhard, 2014; Li *et al.*, 2014; Markert *et al.*, 2016). However, cloning becomes much more labor-intensive than directly submitting PCR samples and requires experience with microbiology in addition to somewhat specialized equipment to produce a sterile field, sterile tools, and

incubation for the transformants. Additionally, while Sanger sequencing is relatively cheap, sequencing 30+ clones to estimate CRISPR efficiency is already a few hundred dollars (between $3.50-$7 per sequence at the Michigan State University Genomics Core), not including cloning and transformation costs, and can become difficult to manage when genotyping multiple crispant individuals. The genotyping method presented in the protocol of cloning PCR amplified gDNA and sequencing transformants (Constantinou *et al.*, 2019), while effective (Figure 21) is more labor intensive than sequencing a PCR product directly.

The crispant individual that exhibited the most striking EOD amplitude reduction throughout early development (Figure 20, "CRISPR") matured and at 16.5 months of age I extracted genomic DNA from the electric organ by removal of the tail tip. The sgRNA target site was amplified, cloned, and sequenced, as described for *B. gauderio* and *B. brachyistius* embryos in Chapter 1. 35/38 (92.1%) of sequenced clones exhibited CRISPR associated mutations at the *scn4aa* sgRNA cut site (Figure 21A) and 32/38 (84.21%) of sequenced clones would result in a non-functional protein if translated and produced *in vivo* (Figure 21B). The protein structure for Nav1.4a is given and exon 1, where CRISPR/Cas9 induced mutations are present, is highlighted (Arnegard *et al.*, 2010; Widmark *et al.*, 2011; Paul *et al.*, 2016). Frameshift mutations and STOP codons induced in exon 1 from CRISPR/Cas9 mutagenesis will result in a non-functional protein as exon 1 exists in the N-terminus of Nav1.4a and none of the proper protein domains will be able to form (Figure 21C).

To eliminate the need to clone and sequence CRISPR/Cas9 mutations, the sgRNA target can be selected such that there is a commercially available restriction enzyme digest site overlapping, or very near, the Cas9 cleavage site. If the sgRNA is designed in this way, it is possible to do a restriction enzyme digest on PCR amplified gDNA to test for the presence of

mutations (Shan *et al.*, 2014). WT sequence will cleave; however, InDels at the sgRNA cut site in mutated sequences will leave the restriction enzyme unable to cleave as its target is no longer present. By comparing the levels of cleaved vs whole DNA bands, a rough approximation of the mutant status can be determined. The restriction digest method is good for higher throughput mutant screening as it is fast, inexpensive, and easy to execute, but this method does not allow the researchers to know the exact sequence of the mutations. If the exact sequence needs to be known (characterizing breeding lines for example) researchers will need to clone and sequence the DNA.

A similar method to restriction enzyme digest is the T7 endonuclease-1 cleavage assay. When heteroduplexes of DNA form from PCR amplicons of a mutant individual, the mismatched DNA can be detected and cleaved by the T7 endonuclease-1. If InDel mutations are present that are too small to detect visually from the wild type sequence using gel electrophoresis, the T7 endonuclease-1 will cleave the heteroduplexes that form and multiple bands will be produced (D. Li *et al.*, 2013; Hammouda *et al.*, 2019). T7 endonuclease-1 and restriction enzyme digest are attractive methods for high throughput of screening crispants as they offer a presence/absence test for mutations.

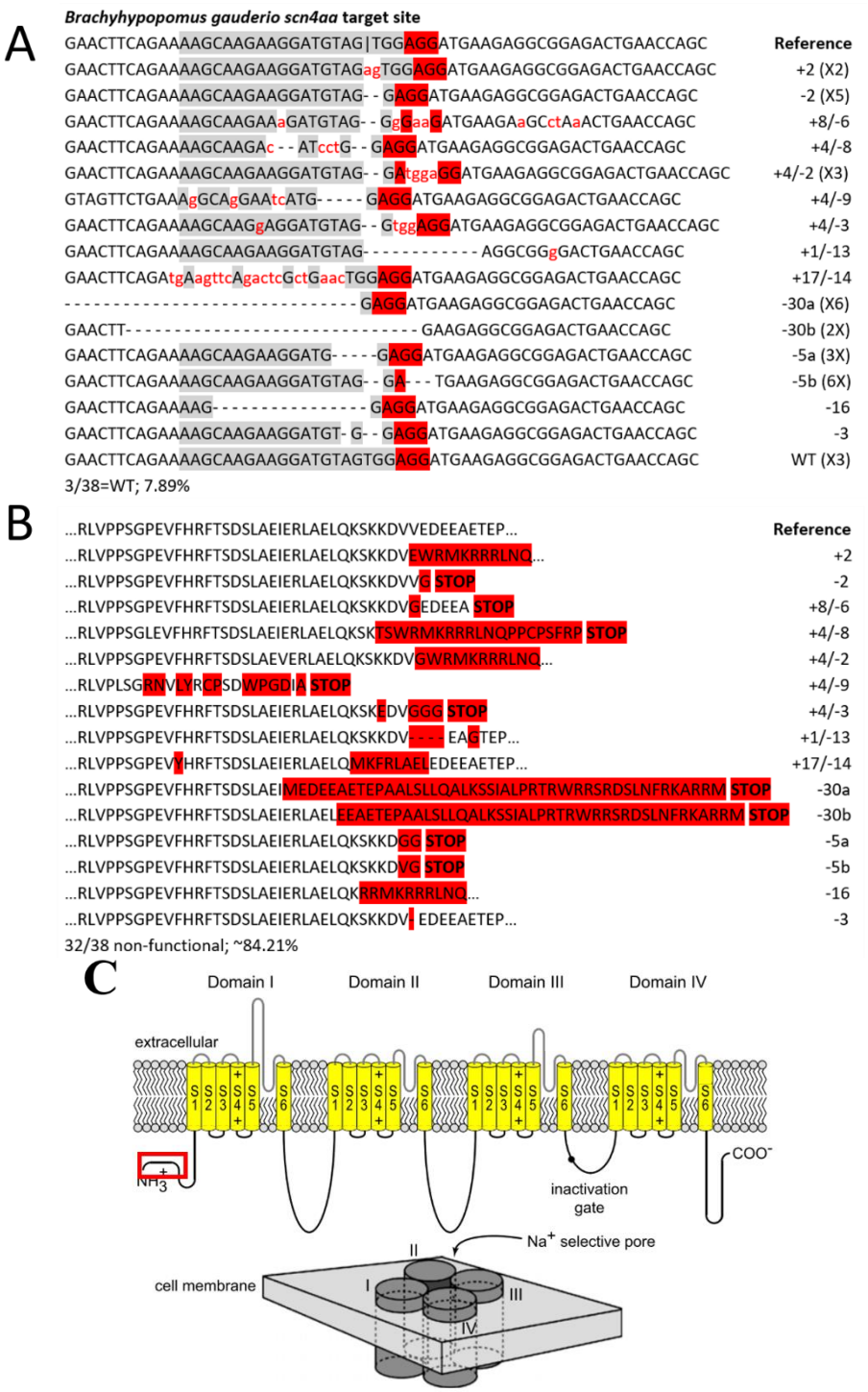

Figure 21: "CRISPR" clone sequencing results- (A) 38 clones from the gDNA of the "CRISPR" individual (Figure 20) at 16 months. The reference sequence is underlined with the sgRNA target site highlighted in gray, the protospacer-adjacent motif (PAM) sequence highlighted in red, and the Cas9 cut site marked with "|". The change from the expected wild type sequence is given and the number of clones for each sequence is given in parenthesis. (Abbreviations: + = insertion, - = deletion, ± = InDel) Any non-CRISPR associated sequence

Figure 21 (cont'd)

dissimilarities are bolded. Figure modeled after (Jao, Wente and Chen, 2013). See Table 4 for the percentage of total reads that each InDel represents in the sample. (B) Amino acid sequence predicted from sequenced clones from (A). Cas9-induced changes from the wild type sequence are highlighted in red and the nucleotide induced change number from (A) is given. (C) Nav1.4a protein domains and transmembrane structure when folded in the membrane. Exon 1 is highlighted (red box) and is part of the N-terminus. STOP mutations and frameshift mutations in exon 1 (B) will cause a completely non-functional protein as no protein domains will form and the Na^+ pore will not be present. Modified from (Arnegard *et al.*, 2010).

Although the restriction enzyme and T7 endonuclease-1 cleavage assays may be faster and less expensive than sequencing clones, these methods do not allow the actual sequence of the mutation to be known. Given the time and cost associated with sequencing PCR clones to identify the mutant genotypes present and their sequence, next generation sequencing (NGS) may be the most attractive option for laboratories moving forward. NGS can accurately predict mutation frequency to 0.01% (Gagnon *et al.*, 2014; Hendel *et al.*, 2015) and provides researchers with the specific sequence of tens of thousands of PCR amplicons. NGS can be performed commercially through a company like GENEWIZ, including the bioinformatics necessary to interpret the NGS output. GENEWIZ offers Illumina sequencing of PCR amplicons at $50-$75 per sample, a relatively low cost given the cost of sanger sequencing and cloning/transformation associated costs required to produce a fraction of the same data over many person-hours when identifying mutant sequence through cloning.

The efficacy of using NGS to identify crispants was tested using the known mutant (Figure 21) against known wild type fish and other suspected mutants. The "CRISPR" individual was allowed to regenerate the tail tip and a second tail tip was collected from the regenerate at nearly 25 months of age. Tail tips were also taken from three wild type individuals and 8 potential crispants that could not be identified as mutant or wild type using Sanger sequencing (including "CRISPR1" and "CRISPR2" from Figure 20). The gDNA was extracted and the

sgRNA target site was PCR amplified. The amplicons were submitted to GENEWIZ for Illumina sequencing. Deep sequencing of many PCR amplicons by GENEWIZ found a high level of mutations at the sgRNA target site in the regenerated tail tip of the CRISPR individual (Figure 22). 98% of amplicons showed mutations with 67% resulting in a frameshift mutation of the protein. The distribution of InDels was highest around the double-stranded break site (Figure 22A). The mutations consisted of more deletions than insertions and included large deletions (Figure 22B).

Five of the other 8 potential crispants, including CRISPR1 and CRISPR2 (Figure 20) reported 1% of reads as mutated. The number of reads in each case was ~600 out of ~100,000 (Figure 23B). The three wild type individuals, and the other 3 potential crispants, reported 0% mutated DNA; however, there are reads recovered (~300) with InDels of +/- 1 or 2 in all five of these samples that report 0% mutated DNA (Figure 23A). It is unlikely that the 1% reported mutant reads represent true CRISPR/Cas9 induced mutations. In wild type fish with a reported 0% mutant sequences, the number of sequences is not truly 0, it is 0% of sequenced reads (Figure 23A). There are actually a few hundred reads sequenced (of ~100,000) that do not match the expected sequence and are usually only +/- 1 or 2 base pairs different from the expected sequence. These reads are likely a result of replication errors in the original PCR amplification (even though the OneTaq polymerase used has an error rate of $<140x10^{-6}$ bases), or during the next-generation sequencing process itself. The 1% of mutated sequences seen in 5 of the potential crispants are likely a result of artifacts in the amplification/sequencing pipeline and not true CRISPR/Cas9 associated mutations.

Table 4: InDel percentages.

Indel Identifer	Figure #	Percent of Reads
+2	21	5.26
-2	21	13.16
+8/-6	21	2.63
+4/-8	21	2.63
+4/-2	21	7.89
+4/-9	21	2.63
+4/-3	21	2.63
+1/-13	21	2.63
+17/-14	21	2.63
-30a	21	15.79
-30b	21	5.26
-5a	21	7.89
-5b	21	15.79
-16	21	2.63
-3	21	2.63
WT	21	7.89
-42	22	0.39
-40	22	0.02
-39	22	4.70
-37	22	9.41×10^{-4}
-36	22	9.41×10^{-4}
-32	22	2.82×10^{-3}
-31	22	0.02
-30	22	2.77
-27	22	0.04
-24	22	0.07
-23	22	0.52
-22	22	5.27
-20	22	9.41×10^{-3}
-19	22	0.32
-18	22	6.59×10^{-3}
-17	22	0.71
-16	22	4.84
-15	22	1.88×10^{-3}
-14	22	3.77×10^{-3}
-13	22	0.16
-12	22	2.17
-11	22	9.41×10^{-4}
-10	22	1.88×10^{-3}
-9	22	4.71×10^{-3}
-8	22	4.71×10^{-3}
-7	22	0.49
-6	22	1.9
-5	22	22.65
-4	22	7.24
-3	22	12.01
-2	22	2.28
-1	22	0.97
WT	22	2.31

Table 4 (cont'd)

1	22	0.38
2	22	18.15
3	22	0.59
4	22	1.72
5	22	1.21
6	22	6.59×10^{-3}
8	22	4.71×10^{-3}
9	22	0.46
14	22	5.65×10^{-3}
15	22	9.41×10^{-4}
16	22	3.77×10^{-3}
17	22	0.05
18	22	5.51
21	22	2.82×10^{-3}
22	22	9.41×10^{-4}
33	22	2.82×10^{-3}
34	22	9.41×10^{-4}
35	22	1.88×10^{-3}
38	22	9.41×10^{-4}
39	22	9.41×10^{-4}
46	22	9.41×10^{-4}
47	22	9.41×10^{-4}
53	22	9.41×10^{-4}
67	22	9.41×10^{-4}
70	22	9.41×10^{-4}

The percentage of total reads that each InDel represents in the "CRISPR" individual. Figure 21 represents Sanger sequencing clones (38 total reads) and Figure 22 represents NGS (106,232 total reads).

The slight EOD amplitude reduction seen in some potential crispants versus wild type (Figure 20) does not appear to be the result of mutations in the *scn4aa* gene. There are a few hypotheses that may explain this result. It is possible that the wild type regression generated to calculate EOD amplitude from length is not represented by enough data points and does not reflect the full extent of the variance seen in EOD amplitude at a given size of the population. More measurements of wild type fish over time may alter the regression so that fish like CRISPR1 and CRISPR2 (Figure 20) fall within wild type expectations. There is also a possibility for off-target effects (see below section "Off-target effects") of the CRISPR components causing

some unknown effect on amplitude. In this case, those fish injected with CRISPR components would have mutations outside the *scn4aa* target site that could cause the slight phenotype seen.

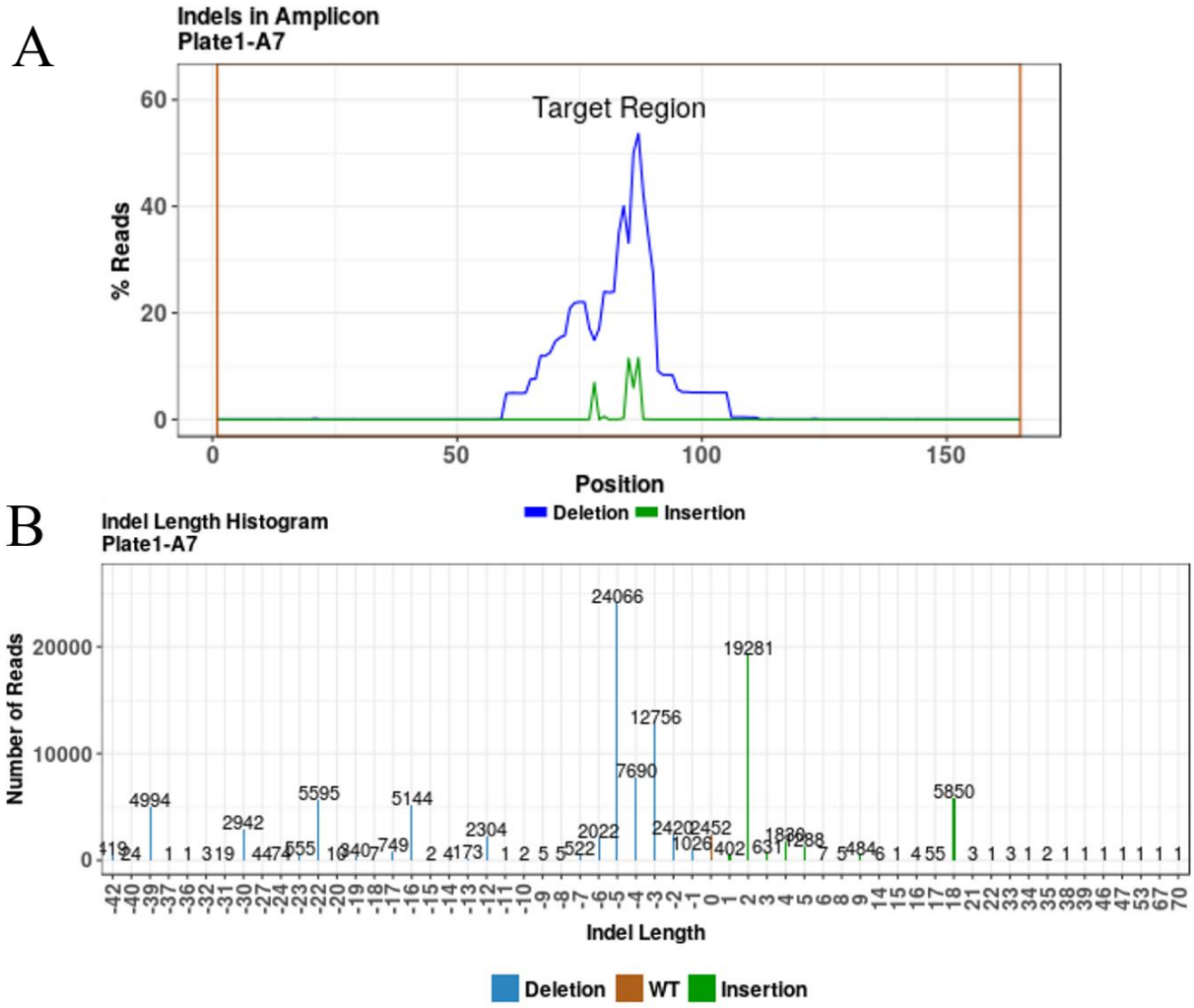

Figure 22: GENEWIZ Illumina sequencing results- Sequencing *scn4aa* from the adult "CRISPR" electrocyte gDNA. (A) A visual representation of the proportion of sequenced reads that contained either insertions (green) or deletions (blue) compared to WT reference and their location in the amplicon. The DSB site is at position 87, where a high proportion of InDels are located. (B) The number of reads (out of 106,232 total reads) that were WT (orange), had deletions (blue, negative InDel length), or had insertions (green, positive InDel length) as well as the number of bases added/removed in the InDel (Indel Length). See Table 4 for the percentage of total reads that each InDel represents in the sample.

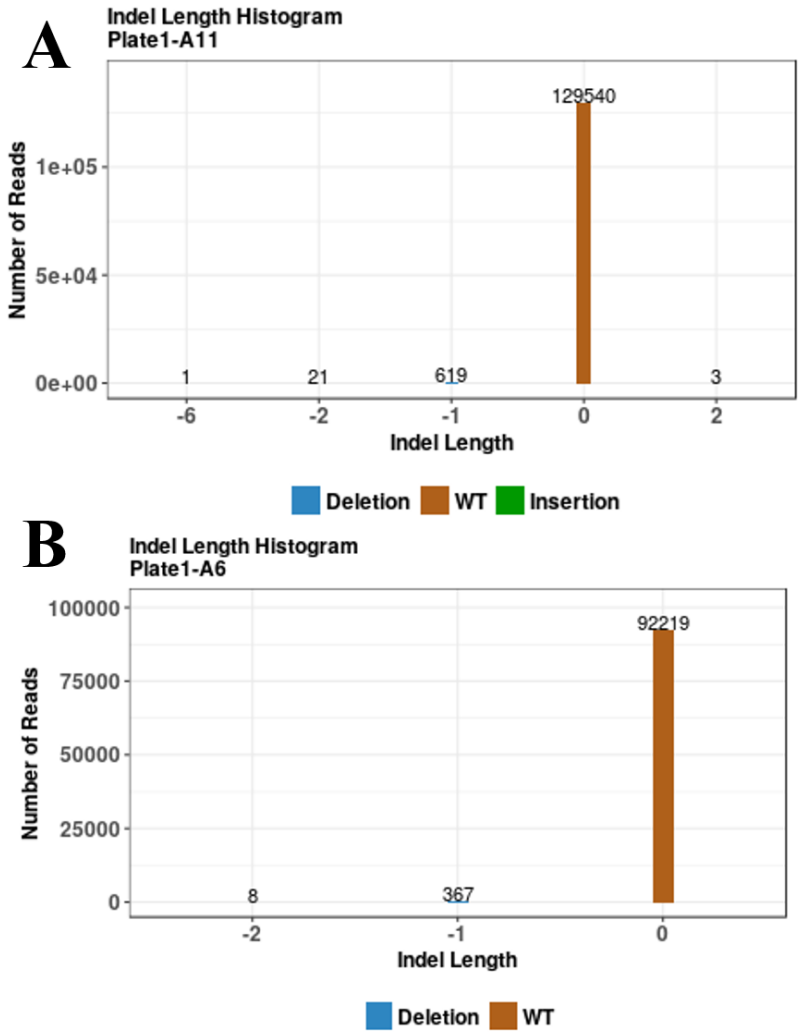

Figure 23: Non-crispant GENEWIZ Illumina sequencing results- Sequencing *scn4aa* from the adult WT and potential crispant electrocyte gDNA. Representative examples of the number of reads that were WT (orange), had deletions (blue, negative InDel length), or had insertions (green, positive InDel length) as well as the number of bases added/removed in the InDel for 0% mutated DNA (A) and 1% mutated DNA (B).

Crispant mosaicism

Genetic mosaicism occurs when differences in mutagenesis rates or success at the one-cell stage results in an organism that has a range of genotypes within and among different tissues (Mehravar *et al.*, 2019). Additionally, there is some evidence that CRISPR/Cas9 mutagenesis tends to occur following embryo cleavages (Yen *et al.*, 2014; Singh, Schimenti and Bolcun-Filas,

2015; Mianné *et al.*, 2017), multiplying genetic mosaicism concerns as different mutations may arise in subsequent daughter cells. From what is understood about how sgRNA induced double-stranded breaks repair themselves, every 4/9 cells in an injected embryo are expected to have bi-allelic out-of-frame mutations when using a single sgRNA given that 1/3 of InDels will be in frame (Shah *et al.*, 2015), thus some level of mosaicism is to be expected in CRISPR/Cas9 genome editing experiments.

Generally, mosaicism is an undesired outcome and can be problematic. When trying to establish mutant lines, mosaicism can result in an organism that has mutations in somatic tissue but not in the germline. The F_0 crispant may demonstrate a phenotype from the mutations it carries; however, these mutations are not able to be passed to offspring as they are not present in the gametes. Depending on the length of time it takes for any given electric fish species to become sexually mature, which can be more than a year in some gymnotiformes and is thought to be slightly longer in mormyrids (Kirschbaum and Schugardt, 2002), mosaicism resulting in non-mutated gametes can be a major setback. If possible, researchers should attempt to express and genotype gametes from adult crispants soon after sexual maturation. The alternative, to phenotype and genotype the F_1 individuals, will take time and resources and has challenges as previously discussed.

The other major concern with mosaicism is false positives. CRISPR/Cas9 associated mutations need to be present in the cells/tissue that produce the gene product that is targeted and being studied. Mosaicism can result in an individual that lacks mutations in the tissues that were the intended target but contains mutations in other tissues. This might be a bigger problem for non-Gymnotiform researchers. Most Gymnotiformes can easily have their electric organ verified for mutations as the organ is easily accessible (as it extends into the tail tip) and regenerates

(Unguez, 2013). As far as we are aware, no other electric organs from other electric fish species regenerate, making it difficult to genotype the electric organs directly. Fins will likely be the tissue that is used for genotyping non-Gymnotiformes as they are easy to harvest and are able to regenerate. Problems can arise if the electric organ is not mutated at all or is mosaic within the electric organ (see below for methods developed to improve rates of mutation), but the fin tissue does show a CRISPR/Cas9 associated mutation at the target gene. In this case, researchers would categorize this fish as a crispant and perform phenotypic studies, thinking that they are capturing the effects of the gene being mutated and concluding that the gene has no effect. In actuality however, the gene was not mutated in the target cells and the collection and analysis of phenotypic data, as well as housing the non-mutant fish, would have been time and funds wasted. This issue of mosaicism in non-regenerating electric fish cannot easily be addressed as biopsy from electric organs would be required to verify that the electric organ has CRISPR/Cas9 associated mutations at the target gene and the biopsy will disrupt the EOD. An ideal case would be to generate a stable mutant line and then do phenotypic studies on the F_1 or F_2; however, this should not discourage researchers from attempting to generate F_0 crispants and doing phenotypic studies before sacrificing the individual to verify the presence of a mutated genotype.

Mosaicism was identified in all confirmed crispants generated during the study (Figure 15, Figure 16, Figure 21, Figure 22). There were varying degrees of mosaicism among these crispants. The number of sequences that contained different mutations varied among the individuals that were genotyped: the larval *B. brachyistius* crispant had many more unique mutant sequences (22; Figure 16) than the larval *B. gauderio* crispant (12; Figure 15) Similarly, there seemed to be differences in the identity and number of mutated sequences recovered in the adult *B. gauderio* crispant (Figure 21, Figure 22) with the NGS approach capturing many more

unique sequences. In the adult *B. gauderio* mutant that was generated, mutations to the electrocytes in the tail tip were verified through cloning (Figure 21) and next generation sequencing (Figure 22). These two methods were done months apart and on fresh tissue as *B. gauderio* can regenerate electrocytes (Alshami *et al.*, 2020). Mutations found in newly regenerated electrocytes suggest that the Pax7 positive cells remaining after tail tip removal, which are necessary for regeneration and electrocyte development (Unguez, 2013; Alshami *et al.*, 2020), also carried mutations in *scn4aa*.

Genotyping the original tail tip through cloning showed a lower percentage of mutated clones (86.8% mutant) than the next generation sequencing done on the regenerated tail tip (98% mutant). There are two possible explanations for the higher proportion of mutated clones in the second analysis. First, it is possible that removal of the original tail tip resulted in a higher proportion of *scn4aa* mutated electrocytes following regeneration. Due to mosaicism, it is possible that not all electrocytes of the original tail tip were mutated. If these were removed for genotyping, new electrocytes would arise from the remaining Pax7 positive cells near the wound site. If a high proportion of those cells were mutated at the *scn4aa* locus most of the regenerated electrocytes would carry mutations in *scn4aa*. Alternatively, the higher proportion of mutated clones captured with NGS could be explained due to the differences in the number of clones sequenced with each method (38 with Sanger sequencing and over 100,000 with NGS). I am unable to verify if sequencing additional clones (at least 10X as many) through cloning and Sanger sequencing would cause the proportion of mutated sequences to rise to a level that is not different from the number of clones sequenced through NGS.

Reduction of mosaicism helps to improve usefulness of F_0 crispants for gene function studies and possibly increase mutations in the germline. A way to reduce mosaicism is to

increase CRISPR/Cas9 efficiency. Some methods to increase efficiency have been explored that allow nearly complete saturation across the embryo (Burger *et al.*, 2016). For example, injecting Cas9:sgRNA complexed together is preferred over injecting Cas9 mRNA, and the addition of 300 mM KCl stabilizes the complex and ensures the complex can reach the DNA in the nucleus. Removal of extra guanines at the 5' end of the sgRNA can also dramatically increase mutagenesis (Hoshijima *et al.*, 2019). Targeting multiple loci within a gene can also increase the probability of frameshift mutations and biallelic mutations above 90% (Zhou *et al.*, 2014; Sunagawa *et al.*, 2016; Zuo *et al.*, 2017; Wu *et al.*, 2018; Hoshijima *et al.*, 2019; Kroll *et al.*, 2021). Lastly, the Cas9:sgRNA complex can be fluorescently tagged, allowing researchers to visually inspect early-stage embryos for unequal Cas9/sgRNA complex distribution, which may lead to less efficient mutagenesis in those cell lineages that had less of the complex present. The fluorescently tagged complex can also be monitored in real time.

A consideration for decreasing mosaicism in CRISPR associated mutagenesis is facilitating premature stop codon addition to the target site following double stranded break repair. It is possible to co-inject a linear DNA fragment that is designed to act as a template for HDR and, in doing so, forces the addition of an in frame stop codon (Gagnon *et al.*, 2014). Even if the stop codon cassette is not added by HDR, the locus will still undergo a DSB and produce InDels; even though HDR success is low, it should not reduce the rate of DSBs occurring and can only facilitate reducing total unique sequence outcomes. By reducing the total unique outcomes for DNA following DSB repair, mosaicism will be reduced as fewer unique DNA sequences will be present. If more of the mutations that arise are non-functional, due to higher rates of premature stop codons being added, there is an increased ability to use the F_0 crispant to analyze phenotypes upon functional loss of the target gene. While this method may reduce

mosaicism, because HDR is overall less efficient than InDel formation through activation of the NHEJ pathway, this method does has drawbacks.

Off-target effects

Off-target effects are a potential limitation of CRISPR/Cas9 mutagenesis that I did not address in my experiments. Although one can estimate the possibility for off-target effects when designing sgRNAs, especially if a complete genome of the organism of study is available, crispants should be genotyped for off-target CRISPR/Cas9 mutagenesis through deep sequencing (Zischewski, Fischer and Bortesi, 2017). If a crispant is generated that is intended as a founder of a stable breeding line, deep sequencing is highly recommended. CRISPR/Cas9 is a relatively specific method for targeted mutagenesis; however, there are some known off-target effects (X. H. Zhang *et al.*, 2015) that can arise. There are several approaches that can limit off-target effects, like the double nickase method (Ran *et al.*, 2013; Mei *et al.*, 2016; Tsai and Joung, 2016).

In the double nickase method, a mutated Cas9 enzyme is used that only cuts one strand of the DNA. If a single sgRNA is used, the enzyme only cleaves one strand, and the DNA is repaired without InDels. However, if two sgRNA targets are used that are on separate strands and no more than ~30 bases apart, a double-stranded break will occur as each strand will be nicked and InDels will form as the cell repairs the damage. The benefit of this approach is that either sgRNA alone cannot cause mutations, so any off-target binding of the sgRNA will have no effect on the genome, and the probability that the sgRNAs will meet the requirements for double-stranded cleavage at a site other than the target site are nearly zero. Another promising approach to reduce off-target effects is through the use of an inactivated Cas9 fused to FokI, which has over 140-fold higher specificity than standard Cas9 and functions through a mechanism similar

to the double nickase method (Guilinger, Thompson and Liu, 2014; Tsai *et al.*, 2014). The methods to reduce off-target effects should be considered when designing a CRISPR/Cas9 mutagenesis study and the use of NGS is the best-known method to assess off-target effects, as predictions for off-targets can be made and then analyzed if the genome of the species of study is available (Gagnon *et al.*, 2014; Hendel *et al.*, 2015; Singh, Schimenti and Bolcun-Filas, 2015; Varshney *et al.*, 2015; X. H. Zhang *et al.*, 2015; Burger *et al.*, 2016; Haeussler *et al.*, 2016; Tsai and Joung, 2016; Zischewski, Fischer and Bortesi, 2017; Concordet and Haeussler, 2018).

While the breeding, husbandry, CRISPR/Cas9 protocol, and results presented here are cost-effective and valuable tools to familiarize electric fish researchers who are new to reverse genetic methods, some of the pitfalls and considerations presented here should be incorporated into future study designs for CRISPR/Cas9 in electric fish. At the very least, I strongly encourage researchers to read this "Call to the Efish Community" to become more intimate with the research around CRISPR/Cas9. I look forward to the next biological discovery from electric fish that arises from CRISPR/Cas9 mutagenesis and builds on the research presented here.

CHAPTER 3

Abstract

To investigate the feasibility of using vivo-morpholinos as a reverse genetic tool in mormyrids, *scn4aa* targeting vivo-morpholinos and control vivo-morpholinos were administered to *Brienomyrus brachyistius*. A small pilot study demonstrated that *scn4aa* targeting vivo-morpholinos can induce reduction in *scn4aa* transcripts that correlates with a reduction in electric organ discharge amplitude. However, when investigating across many individuals with various delivery locations and dosages and controlling for individual effects, there was not a difference in electric organ discharge amplitude over time between control vivo-morpholino and *scn4aa* targeting vivo-morpholino treated fish. I found a toxic effect of vivo-morpholinos in mormyrids and present my considerations for future use of vivo-morpholinos in mormyrids.

Introduction

MOs are an ideal tool to test in mormyrid weakly electric fish. Compared to gymnotiform weakly electric fish, mormyrids grow relatively slowly and are more difficult to breed in the lab (Kirschbaum and Schugardt, 2002), limiting the practicality of CRISPR. MOs circumnavigate the difficulties with obtaining embryos for single-cell CRISPR injections because they can be developed for use in the adult electric organ. MOs are transient, allowing recovery and repeat studies (Ferguson, Schmitt and Lightfoot, 2013), and can be delivered as vivo-MOs. Mormyrids have an electric organ that is restricted to the caudal peduncle (Fay *et al.*, 2005; Markham, 2013) and allows for the possibility of direct electric organ injections as well. Gymnotiformes have elongated electric organs (Markham, 2013) and, given the large size of electrocytes (lots of cell surface area covered with proteins, so presumably a relatively high transcript count), the ability

to reduce gene expression efficiently via MO may have been difficult without high doses, which are expensive and can be toxic.

A promising pilot study conducted by A. Sdao, M. Lucas, and J. Gallant (2014) suggested *scn4aa* targeting MO may reduce EOD amplitude; however, saline was used as the control instead of a control MO. I present here an extended pilot study: the goal of the work described in this chapter was to perform a pilot study to investigate the effects of *scn4aa* targeting, splice blocking vivo-MO on EOD amplitude and gene target mRNA, and to determine the effect of vivo-MO on EOD amplitude over time in a larger number of individuals. I also sought to optimize the delivery location, and consider dosage and toxic effects of the vivo-MO.

To study the effects of *scn4aa* targeting, splice blocking vivo-MO on EOD amplitude in a pilot, I injected 3 total fish, one with control vivo-MO and two with *scn4aa* targeting vivo-MO, and measured EOD amplitude over time and quantified *scn4aa* mRNA levels at the end of the experiment. To study the effects of vivo-MO over time, I injected $N = 45$ fish with either *scn4aa* targeting vivo-MO or control vivo-MO, measured EOD amplitude over time, and determined the change in EOD amplitude while controlling for repeated measures. To investigate the optimal delivery location, I considered complications and ease of injection. To study dosages and toxic effects, I injected fish with varying dosages and number of injections and quantified the appearance of toxic effects and death, including after performing vivo-MO specific toxicity reduction efforts. We found overall that *scn4aa* targeting vivo-MO can reduce EOD amplitude through *scn4aa* transcript reduction; however, that result is inconsistent when considering large numbers of *scn4aa* targeting vivo-MO and control vivo-MO injected fish. We find that intraperitoneal injections are the ideal delivery route tested and that there are significant toxic effects, including death, associated with both control and *scn4aa* targeting vivo-MOs. I conclude

the chapter by considering future applications for vivo-MO use in mormyrids for the electric fish community.

Methods

Animal husbandry

B. brachyistius were housed in small groups in 20-gallon tanks. Individuals recorded more than 1 day were housed in 10-gallon tanks which had a recording chamber that served as a hiding place. Blackworms were fed daily, and water was kept clean with regular water quality testing, constant aeration, and water changes. PVC tubes were provided in each tank to serve as shelter.

Vivo-morpholinos

A splice blocking MO (SB *scn4aa*) was designed against the *scn4aa* exon1/intron1 boundary in *Paramormyrops kingsleyae*, a close relative of *B. brachyistius*. *scn4aa* splice blocking sequence (SB *scn4aa*)- 5'-TGCATTCTGAACTGACTCTCTGTGT-3'. *P. kingsleyae scn4aa* was also used to design a translation blocking MO. *scn4aa* translation blocking MO sequence- 5'-TGCATCATATTTCATCTCTACCACC-3' (TB *scn4aa*). An additional splice blocking MO was designed against the *scn4aa* exon2/intron2 boundary in *Brienomyrus brachyistius* (SB *scn4aa* E2/I2). *scn4aa* splice blocking (E2/I2) MO sequence- 5'-AGTTTAACGTGAAGGATATGAATGT-3'. A translation blocking MO was designed against *kcna7a* in *B. brachyistius* (TB *kcna7a*). *kcna7a* translation blocking MO sequence- 5'-GTGCAACGTGCTCAGATATTAAACA-3'. control MO sequence (control)- 5'-CCTCTTACCTCAGTTACAATTTATA-3'. Vivo-MOs were purchased from Gene Tools and resuspended as per the manufacturer's instructions. A schematic of the MO binding locations and

expected outcomes from MO use are given in Figure 24.

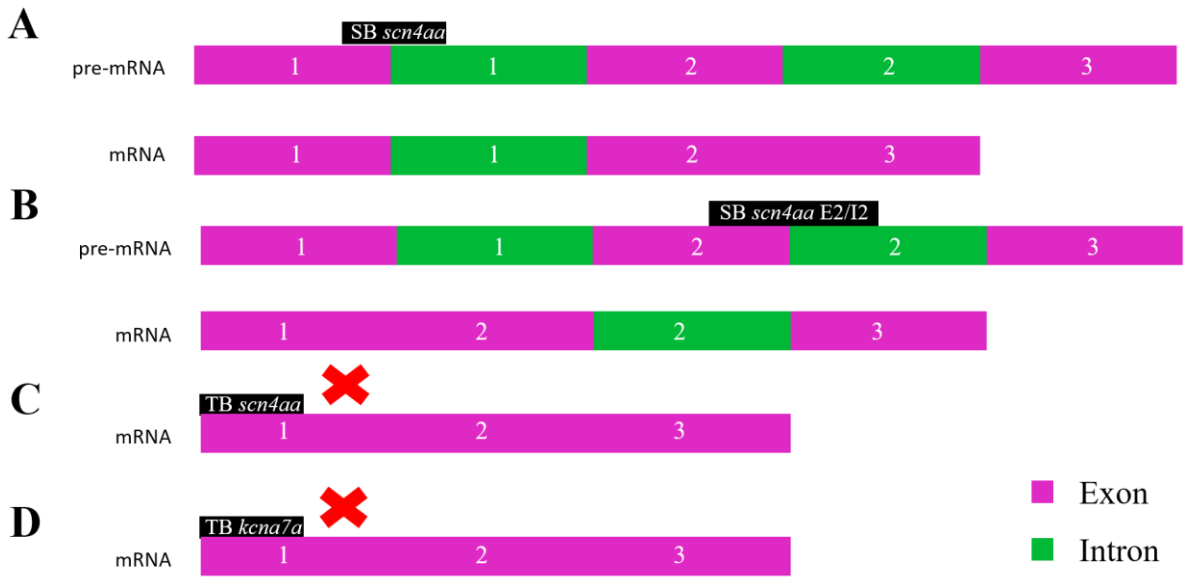

Figure 24: Morpholino binding sites- (A) *B. brachyistius scn4aa* pre-mRNA is shown with bound SB *scn4aa* MO. If bound by SB *scn4aa*, the resulting mRNA will likely retain intron 1. (B) *B. brachyistius scn4aa* pre-mRNA is shown with bound SB *scn4aa* E2/I2 MO. If bound by SB *scn4aa* E2/I2, the resulting mRNA will likely retain intron 2. (C) *B. brachyistius scn4aa* mRNA is shown with bound TB *scn4aa* MO. The red "X" indicates that the mRNA will not be translated with the translation blocking MO bound. (D) *B. brachyistius kcna7a* mRNA is shown with bound TB *kcna7a* MO. The red "X" indicates that the mRNA will not be translated with the translation blocking MO bound. There are additional introns and exons beyond exon 3 that are not depicted in both genes.

Injections

Baseline EOD recordings were taken before the fish was exposed to anesthesia. Injections were done while under the anesthetic MS-222 (Phase II in Iwama, McGreer and Pawluk, 1989), which was applied at ~0.1 g/L. Injection solutions were prepared on parafilm and drawn into the syringe/needle minimizing air bubbles. Once a fish was under the effects of anesthesia, a fresh 27.5-gauge needle was injected into the target location with the bevel facing outward, and the solution was gently expelled. Sometimes it was helpful to remove scales around the intended injection site. The needle was kept in place for a few seconds and then removed.

Immediately after removal, the site was covered by hand for 2-5 seconds before the fish was returned to system water treated with stress guard, to recover.

Intraperitoneal injections were done into the intraperitoneal cavity (Figure 25A). Fish were held ventral side up with the rostral end facing away, and the needle was injected just anterior to the pelvic fins. The needle was pushed just past the muscle wall until there was no more resistance and then the injection was gently delivered. Intramuscular injections were done into the dorsal trunk muscle anterior to the dorsal fin (Figure 25B). Direct electric organ injections were done into one column of the electric organ and the needle was injected at about a 15-30° angle (Figure 25C). Individual fish were only treated with a single MO; no single individual was present in more than one treatment group.

EOD recordings and analysis

EOD recordings were performed using bipolar silver chloride coated silver wire electrodes amplified (bandwidth= 0.0001-50 kHz) with a bioamplifier (BMB 200) and digitized at a 100 kHz sampling rate. Custom LabView-based software d2d_EOD (developed by Dr. Jason Gallant) was used for EOD signal recording. Recordings were performed in the 10-gallon tank housing the fish within a recording chamber (Figure 26) which limited movement of the fish and stabilized recording electrodes. EOD recordings were performed for 30s - 2.5 minutes before the first and at later time points following injections (up to 49 days later). If multiple injections were performed, the 1440 min (24 h) recording was taken immediately prior to the second dose and the 2880 min (48 h) recording was taken immediately prior to the third dose. If fish died or were made electrically silent from injections, they were not included in subsequent EOD amplitude changes over time. EOD recordings were analyzed by custom MATLAB code (developed by Dr. Jason Gallant).

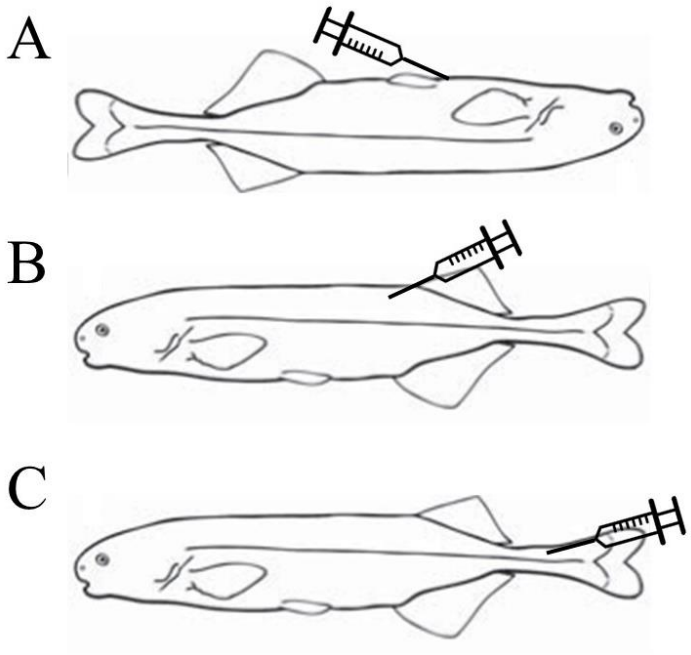

Figure 25: Injection locations- Sites of vivo-MO injection in *Brienomyrus brachyistius.* (A) Intraperitoneal injections were done just anterior to the pelvic fins. (B) Intramuscular injections were done anterior to the dorsal fin in the dorsal trunk muscle. (C) Electric organ injections were done into one column of the electric organ. Figure adapted from Carlson and Gallant, 2013.

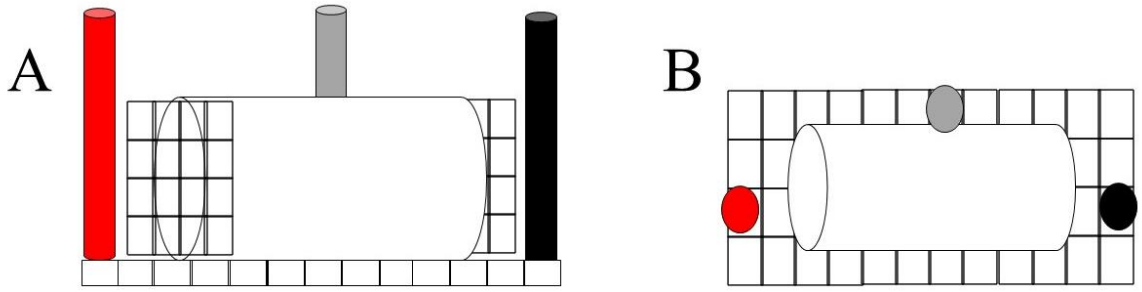

Figure 26: Recording chamber schematic- Cartoon representation of recording chamber used to measure EODs. A PVC tube is attached to a plastic egg crate and has egg crate doors lined with a mesh screen that can be opened and closed (excluded from illustration in B). Recording electrodes (red for +, black for -, and gray for ground) are inserted into the egg crate. (A) Side view. (B) Top view.

RNA extraction and cDNA synthesis

Electric organs were harvested from fish after euthanasia by MS-222 (~0.25 g/L). The entire caudal peduncle is removed, skinned, and the anterior and posterior-most electric organ was removed to reduce contamination from other tissues and placed into RNAlater. Skeletal

muscle was collected from the anterior dorsal trunk muscle and placed into RNAlater. RNA was extracted from electric organs and skeletal muscle using Qiagen RNeasy lipid tissue kit following the manufacturer's protocol. cDNA was synthesized from electric organ and skeletal muscle RNA using Takara Bio RNA to cDNA EcoDry™ Premix (Double Primed) following the manufacturer's protocol.

qPCR and relative expression analysis

qPCR was performed in triplicate using the Luna Universal qPCR Master Mix (NEB) on a CFX96 Touch Real-Time Detection System. 25 ng of cDNA were used in each 10uL reaction and the company suggested cycling parameters were used; each sample was run in triplicate along with no template controls. *scn4aa* primers: F- 5'-ATGGCCGGCCTTCTCAATAA-3', R- 5'-TCTTCCAGGGGAATATTCATAAACT-3'. *β-actin* primers: F- 5'-CCTGACCGAGAGAGGCTACA-3', R- 5'-GCCCATCAGGCAGTTCGTA-3'.

Relative expression was quantified via delta-delta Ct method (Livak and Schmittgen, 2001) using a custom R script.

PCR, gel electrophoresis, and gel extraction

acta1a was amplified using OneTaq (NEB) following the suggested cycling parameters with an annealing temperature of 53°C. PCR amplicons were verified by size using gel electrophoresis. Gels were made using 1% agarose, run at 100-140 volts, and 50 bp DNA ladders (NEB) were used to verify size. Amplicon bands were extracted from the gel using Qiagen QIAquick PCR & Gel Cleanup Kit as per the manufacturer's instructions. *acta1a* primers: F- 5'-CCAAGGCTAACCGCGAAAAG-3', R- 5'-GCGGTTGTGACGAAGGAGTA-3'

Cloning and sequencing

PCR amplicons excised from the gel had TA overhangs replaced by incubating 1 µL 10X Taq buffer, 0.5 µL 10 mM dNTP, 0.2 µL Taq polymerase (all from NEB) and 8.3 uL gel-purified *acta1a* at 68°C for 10 minutes and then moved to ice. The amplicons were then cloned into pSC-A-amp/kan vector and transformed into bacteria using the StrataClone PCR kit (Agilent) as per the manufacturer's instructions. Colony PCR was performed on blue/white screened colonies using universal M13 F and R primers to linearize clones. Linearized clones were sequenced at the Michigan State University genomics core via Sanger sequencing.

Statistics and calculations

Statistics were computed in R using custom scripts. All code mentioned is available at https://github.com/savvasjconstantinou/Chapter3 and in Appendix B. Percent baseline is calculated for each EOD as: [(amplitude/mean Baseline amplitude for that fish)*100] = Percent Baseline.

Results

Pilot study (*N*=3) to examine the effect of SB MO targeting *scn4aa* on EOD amplitude

In an initial pilot study, I compared 3 fish injected 1X daily (intraperitoneally) for 3 successive days. Two fish received splice blocking, *scn4aa* targeting MO, one fish at a 12.5 mg/kg and the other fish at 20 mg/kg dose (MOL and MOH respectively). One fish received the control MO at 20 mg/kg dose (MOC). EOD amplitude was measured during the experiment at 1440, 1800, 2880, 3240, and 4320 minutes, 24, 30, 48, 54, and 72 hours respectively. The three injections were given before the baseline recording, after the 1440 min (24 h) recording, and after the 2880 min (48 h) recording. A two-way repeated measures ANOVA was carried out on

amplitude (as percent of baseline) to determine if there are differences by time and individual. There was a statistically significant interaction between the effects of time and individual on EOD amplitude (as percent of baseline) [$F(10,1320)=431.5$, $p < 0.001$]. Tukey's HSD post-hoc tests show significant differences (adjusted p-value <0.05) between all individuals at all time points except at baseline and between MOC and MOL at 1440 minutes (Figure 27).

The control fish only differed from baseline at 4320 minutes, at which point there was a significant reduction in EOD amplitude of 6.74%. By comparison, MOL had a 23.14% reduction and MOH had a 45.96% reduction from baseline at this time point. Both experimental fish were significantly different from baseline at all time points (except MOL does not differ from MOC at 1440 min). Over time, *scn4aa* targeted MO injected fishes showed reductions in EOD amplitude.

To determine if the amplitude reductions seen with *scn4aa* targeting MOs in this pilot study were specific to the MO treatment, *scn4aa* mRNA transcripts from the electric organ were quantified. At the 4320 minute time point recording, all three fish were sacrificed. After sacrifice, the electric organs were harvested and *scn4aa* mRNA levels were assessed via qPCR. When compared to β-actin levels, *scn4aa* mRNA significantly decreased with increasing MO concentration (Figure 28). The *scn4aa* transcript levels (deltaCt) are significantly different in all three fish (each fish had mRNA levels measured in triplicate) with fewer *scn4aa* transcripts present with increasing *scn4aa* targeting MO dosage based on a one-way ANOVA [$F(2,6)=46.45$, $p<0.001$] and Tukey's HSD post hoc tests.

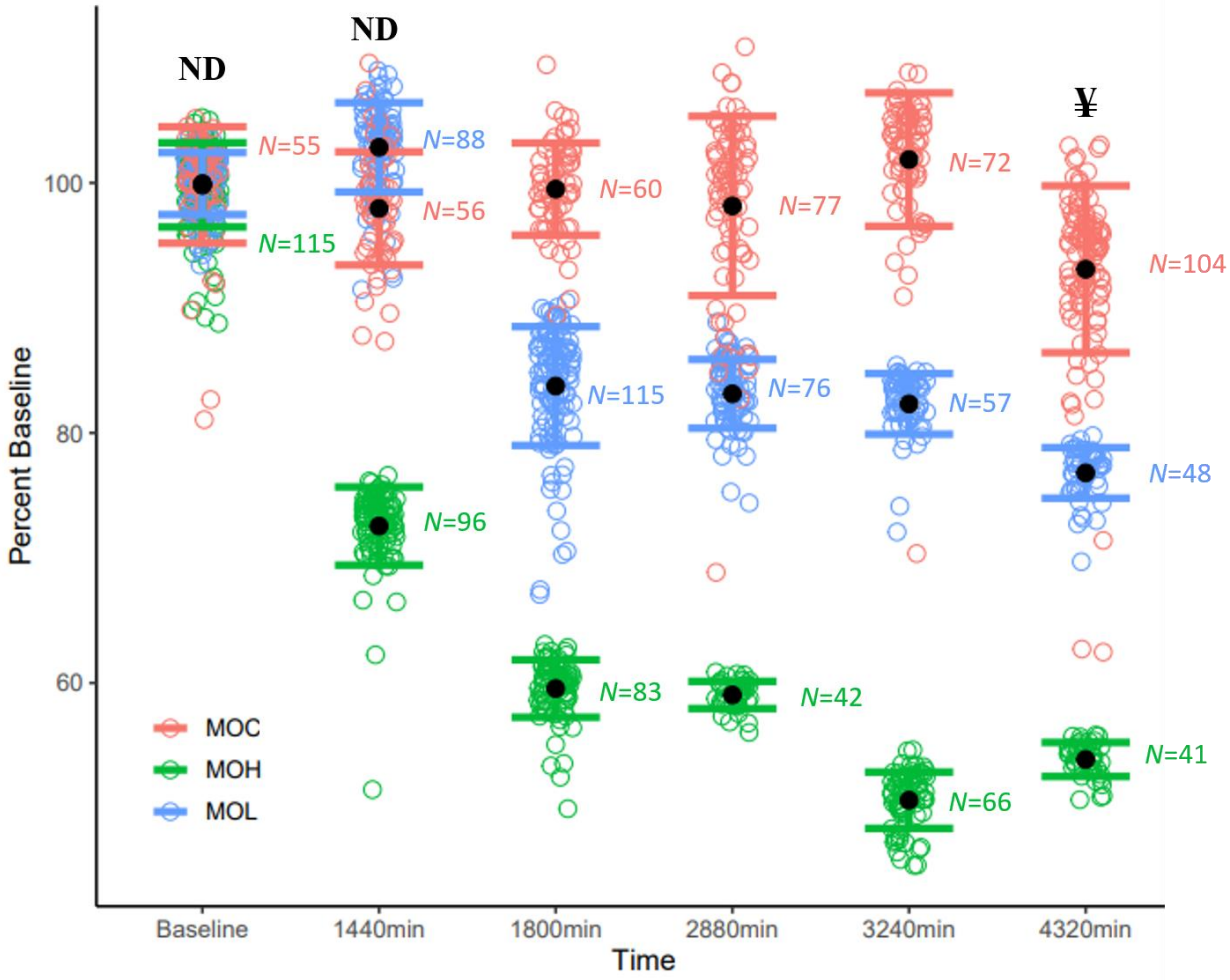

Figure 27: EOD amplitude over time following successive MO injections- EOD amplitude as a percent of baseline drops for the *scn4aa* targeting MO with very little amplitude reduction seen in the control MO. All three fish (MOC, MOL, and MOH) are significantly different from one another at all time points except Baseline and MOC and MOL at 1440 min (ND). The control fish is only significantly different from baseline at the 4320 minute time point (¥), all other control fish time points are not statistically different from baseline. Mean (black point) and standard error (colored bars) are reported as well as each individual EOD (non-filled points). Number of EODs at each time point (*N*=) for each fish is given to the right of the mean and standard error bars and is color coded following the key at bottom left. Statistics were computed using a two-way ANOVA and Tukey's HSD for post hoc comparisons. See text for statistical outputs.

scn4aa knockdown alters *acta1a* expression

Altered expression of *acta1a* was identified when *scn4aa* expression had been knocked down via vivo-MO (Figure 29). *acta1a* was originally selected as a reference gene for the qPCR

studies; however, when testing the primers to amplify this gene, fish treated with the *scn4aa* targeting splice blocking MO showed differences in *acta1a* expression in the electric organ. Three days after MO injection, an assumed isoform of *acta1a*, with a ~250 bp insertion, was produced when EOD amplitude was reduced (Figure 27) and *scn4aa* mRNA was knocked down (Figure 28). Higher levels of the *acta1a* isoform were seen with higher doses of MO which also correlated to reduced expression of the expected isoform, but this effect is only seen in the electric organ and not in skeletal muscle (Figure 29A).

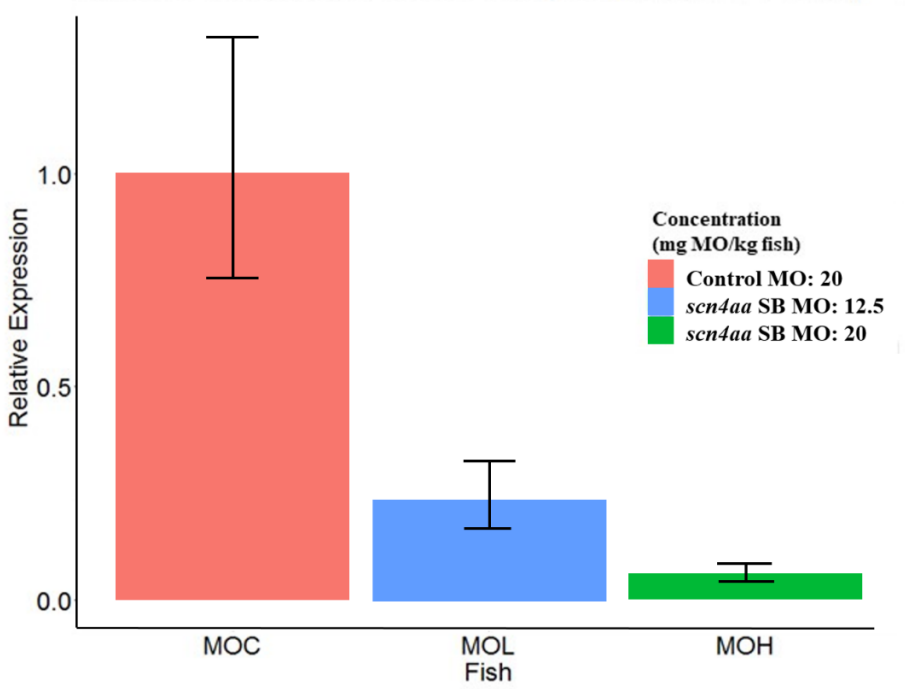

Figure 28: *scn4aa* mRNA levels after vivo-MO treatment- The relative abundance of *scn4aa* mRNA compared to *β-actin* in the electric organ 3 days after injection with control MO or a *scn4aa* specific splice blocking MO. Error bars represent standard deviation of triplicate reactions. All groups are significantly different using a one-way ANOVA and Tukey's HSD for post hoc comparisons. See text for statistical computation.

To determine the identity of the isoform produced when *scn4aa* levels are reduced, the corresponding PCR amplicon was sequenced via Sanger sequencing. The *acta1a* isoform had the same identity with ~250 bp inserted regardless of *scn4aa* targeting MO concentration (Figure

29B). The insertion caused an in-frame stop codon to be introduced. The amino acid sequence predicted from the isoform with the insert was truncated compared to the WT sequence (Figure 29C) and contains ~45% of the WT sequence length.

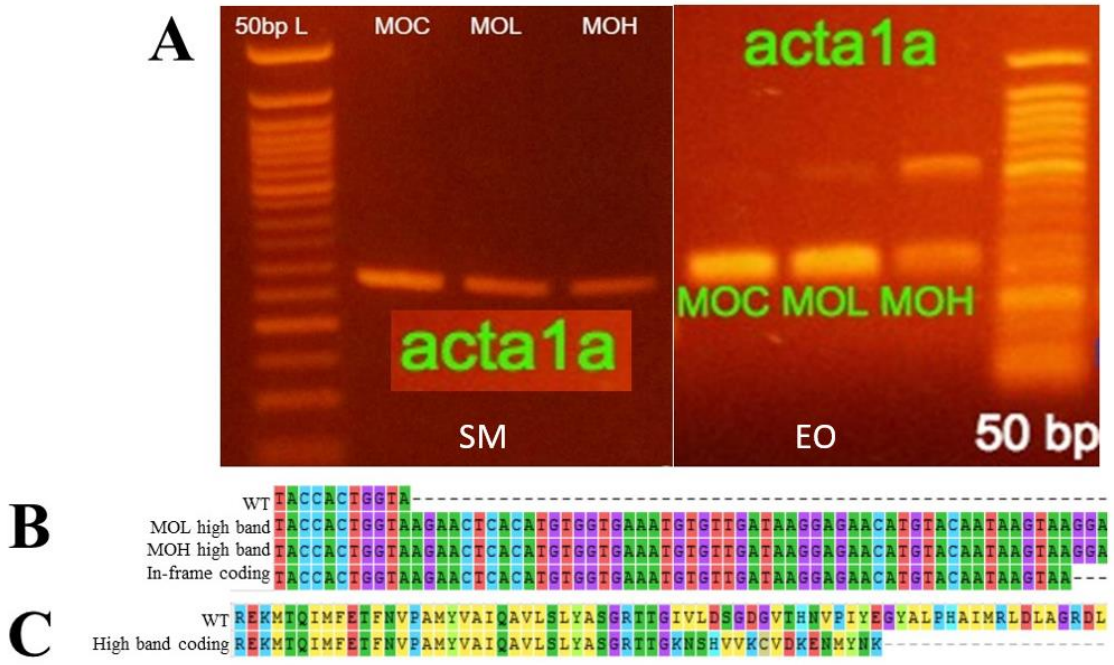

Figure 29: *acta1a* expression changes with *scn4aa* knockdown- 3 days after injection with vivo-MO against *scn4aa*, *acta1a* expression was measured in both skeletal muscle (SM) and electric organ (EO). (A) PCR amplification of cDNA from these organs showed the expected isoform in SM but an altered isoform in EO. The altered isoform, "high-band" is present at higher concentrations at higher doses of vivo-MO and subsequent *scn4aa* knockdown. (B) DNA sequencing of the "high-band" showed an insertion that produced an in-frame stop codon. (C) The predicted amino acid sequence of the "high-band" *acta1a* isoform is a truncated protein. MOC=20 mg/kg MO control, MOL= 12.5 mg/kg splice blocking *scn4aa* MO, MOH= 20 mg/kg splice blocking *scn4aa* MO.

Summary of experiments

Given the promising results of the first pilot study using MO controls and verifying that *scn4aa* targeting MOs can induce *scn4aa* transcript down regulation (Figure 27, Figure 28), I performed additional studies in attempts to replicate these initial findings in a larger group of individuals. Subsequent attempts saw variability in the amplitude of control individuals, high

death rates, and silencing of electric discharges. In attempts to mitigate these latter effects, we attempted to explore several variables to determine toxicity effects, dose-response curves, and optimal delivery location (Figure 25). These experiments are summarized in Tables 4-6 below, organized by injection location utilized.

Treatment	Dosage (mg/kg)	# of Injections	*N*	Autoclaved	1:1 saline	Behavioral issues	Deaths	Silenced EOD
Control	27.5	1	1	No	No	0	0	0
SB *scn4aa*	27.5	1	1	No	No	1	0	0
TB *kcna7a*	12.5	1	1	No	No	0	0	0
TB *kcna7a*	27.5	1	1	No	No	0	0	0

Table 5: Summary of MO experiments with intramuscular delivery. Behavioral issues indicate when a fish behaves differently after injection than during baseline recordings, see text. 1:1 saline indicates when an equal volume of saline was mixed with the treatment before injection. Injections were performed in *Brienomyrus brachyistius*. #= number, *N*= sample size, E2/I2 = Exon2/Intron2 splice blocking *scn4aa* targeting MO, SB= splice blocking.

Table 6: Summary of MO experiments with electric organ delivery.

Treatment	Dosage (mg/kg)	# of Injections	*N*	Autoclaved	1:1 saline	Behavioral issues	Deaths	Silenced EOD
Control	9.5	2	2	No	Yes	1	0	2
Control	12.5	1	7	No	No	0	0	5
Control	12.5	2	2	No	No	0	0	1
SB *scn4aa*	12.5	3	2	No	No	0	0	0
SB *scn4aa*	12.5	1	3	No	No	0	0	3
E2/I2	9.5	2	2	No	Yes	0	0	2
E2/I2	12.5	1	7	No	No	0	0	3
E2/I2	12.5	2	2	No	No	1	0	1
Saline	N/A	3	2	No	No	0	0	0

Table 6 (cont'd)

Saline	N/A	2	2	No	Yes	0	0	0

Behavioral issues indicate when a fish behaves differently after injection than during baseline recordings, see text. 1:1 saline indicates when an equal volume of saline was mixed with the treatment before injection. Multiple injections are performed 24 hours apart. Injections were performed in *Brienomyrus brachyistius*. #= number, *N*= sample size, E2/I2 = Exon2/Intron2 splice blocking *scn4aa* targeting MO, SB= splice blocking.

Table 7: Summary of MO experiments with intraperitoneal delivery.

Treatment	**Dosage (mg/kg)**	**# of Injections**	***N***	**Autoclaved**	**1:1 saline**	**Behavioral issues**	**Deaths**	**Silenced EOD**
Control	6.5	3	2	No	Yes	0	0	0
Control	9.5	1	3	No	Yes	0	0	0
Control	17.5	1	5	Yes	Yes	1	0	0
Control	20	3	1	No	No	0	0	0
Control	27.5	1	3	No	No	2	0	0
Control	27.5	2	2	No	No	0	0	0
SB *scn4aa*	12.5	3	1	No	No	0	0	0
SB *scn4aa*	12.5	1	1	No	No	0	0	0
SB *scn4aa*	17.5	1	2	No	No	2	0	0
SB *scn4aa*	17.5	1	6	Yes	Yes	4	1	0
SB *scn4aa*	20	3	1	No	No	1	0	0
SB *scn4aa*	20	1	3	No	No	2	1	0
SB *scn4aa*	22.5	1	2	No	No	2	0	0
SB *scn4aa*	25	1	2	No	No	2	0	0
SB *scn4aa*	27.5	1	4	No	No	3	2	0
E2/I2	6.5	3	2	No	Yes	1	1	0
E2/I2	9.5	1	3	No	Yes	0	0	0
TB *kcna7a*	27.5	1	4	No	No	0	0	0

Table 7 (cont'd)

TB *kcna7a*	27.5	2	2	No	No	0	0	0
TB *scn4aa*	17.5	1	4	No	No	4	4	0
Saline	N/A	3	2	No	Yes	0	0	0

sBehavioral issues indicate when a fish behaves differently after injection than during baseline recordings, see text. 1:1 saline indicates when an equal volume of saline was mixed with the treatment before injection. Multiple injections are performed 24 hours apart. Injections were performed in *Brienomyrus brachyistius*. #= number, *N*= sample size, E2/I2 = Exon2/Intron2 splice blocking *scn4aa* targeting MO, SB= splice blocking, TB= translation blocking.

Effect of vivo-morpholinos in *B. brachyistius* over time

To help understand the effects of vivo-MOs on EOD amplitude over time across all variables tested, EOD amplitude was converted to a percent of the initial baseline measure. All fish injected with control MO and *scn4aa* targeting MO (splice blocking *scn4aa* MO and E2/I2 *scn4aa*) were considered in this analysis. First, when considered as a group, there was a large amount of variance in EOD amplitude following injection in both control MO treated fish (*N*= 21; Figure 30A) and *scn4aa* targeting MO treated fish (*N*= 24; Figure 30B) over time. Second, there is a noticeable reduction in the amplitude of both experimental and control morpholino amplitudes in the time points immediately following the experiment. Third, there does not appear to be a clear difference between control MO and *scn4aa* targeting MO groups at most time points

(Figure 31).

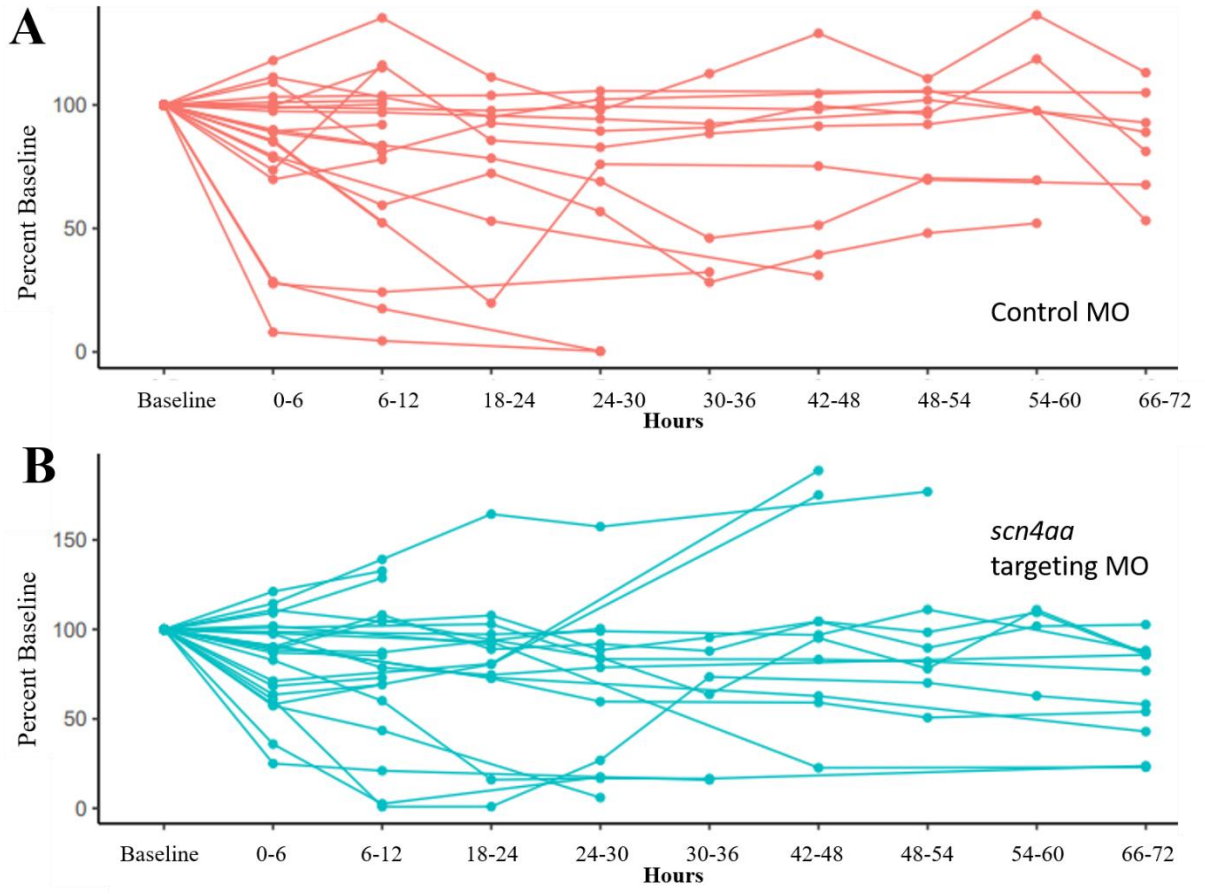

Figure 30: Individual fish EOD amplitude change over time during morpholino treatment- EODs (EOD *N= ~100-1000*), were averaged for each fish at each time point (time point *N*= 68) and then averaged together based on time bins of 6 hours for each fish. The average EOD amplitude, as percent of baseline, is shown for individual control MO treated fish (A, *N*=21) and *scn4aa* targeting MO treated fish (B, *N*=24) at each time bin. Points and lines follow a particular individual and differ between A and B; the individuals in A are not the same as in B.

To determine if there is an effect of treatment over time, a two-way repeated measures ANOVA was performed to control for the effect of individuals on amplitude as a percent of baseline measure (Dulka and Maler, 1994). There is not a significant effect of treatment ($F(1,34) = 0.004$, $p=0.95$) over binned time when controlling for individual fish differences, suggesting that the means between control MO injected and *scn4aa* targeting MO do not differ (Figure 31).

The expectation, given that the *scn4aa* targeting MOs should perform like the pilot study (Figure 27, Figure 28), would be that the treatments would differ. Additionally, controls should not change over time, so I explored how control MO treated fish EOD amplitude changed over time using a one-way repeated measures ANOVA analysis. There is a significant effect of binned time in controls ($F(9,87) = 4.289$, $p = 0.0001$), suggesting that there are differences in control amplitude means across time bins.

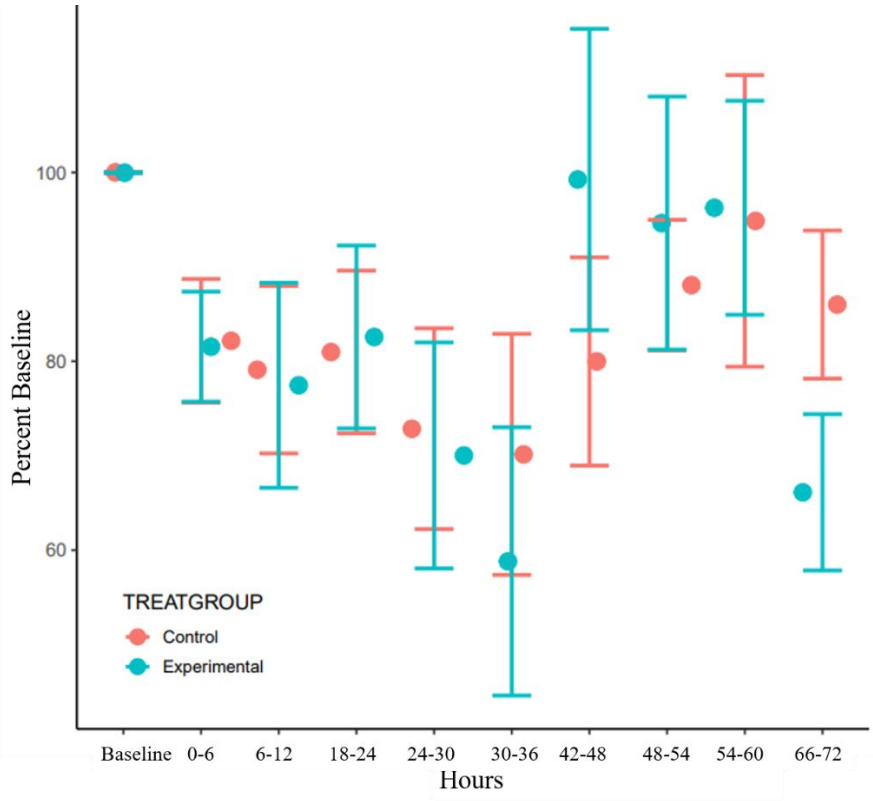

Figure 31: Morpholino effect on EOD amplitude over time- Individual EOD amplitudes (*N= ~100-1000*) as percent baseline, were averaged for each fish (*N*=45) at each time point (*N*= 68) and then averaged together based on time bins of 6 hours for each fish. Fish treated with control MO and *scn4aa* targeting MO were averaged together at each bin to estimate effects between treatments. Error bars represent standard error.

Delivery location

When discussing the effect of injection location (Figure 25), it is important to clarify issues that arise from only direct electric organ injections. Considering each time a fish was injected in a given location (including multiple injections given to the same fish), it appears that direct electric organ injections can be dangerous. In nearly 35% (17/49) of all direct electric organ injections, the fish was electrically silenced following the injection and was unable to produce measurable EODs. The damage to the electrocytes and/or the nervous system from the needle was severe enough to permanently silence electric organ discharges for at least 5 weeks following injection. The silencing rate of EODs from intramuscular and intraperitoneal injections are both 0%, 0/4, and 0/73 respectively.

Vivo-MO toxicity

Toxic effects were determined by visual inspection of fish behavior following injection and compared to baseline behavior. Following injection, if a fish displays atypical behavior (*e.g.*, resting ventral side up, loss of color, vertical body positioning within the tank, and/or diminished EOD firing rate), it was noted as having behavioral issues and was attributed to a toxic effect of the MO. Toxic effects were seen in over 21% (27/126) of injection procedures. Of those, 17 are from SB *scn4aa*, 4 from TB *scn4aa*, 4 ctrl MO, 2 E2/I2 *scn4aa* (Tables 4-6). Assuming all treatments have an equal chance of causing toxic effects, there is a significant difference in the number of fish displaying toxic effects due to morpholino treatment $X^2(5, N=27)= 45.222$, $p<0.001$. There are more fish showing toxic effects from the spice blocking *scn4aa* targeting morpholino than expected, and less in all the other four treatments. Differences in dosage and injection location are not accounted for in this analysis; however, the vivo-MO dosages administered that caused toxic effects were 6.5, 9.5, 12.5, 17.5, 20, 22.5, 25, and 27.5 mg/kg.

Death was also an outcome from injection with vivo-MO. The deaths counted here are those that resulted sometime after injection and were determined not to be due to injury sustained from the injection itself. Death was seen in just over 7% (9/126) of injection procedures. Of those, 4 were from SB *scn4aa*, 4 from TB *scn4aa*, and 1 was from E2/I2 *scn4aa* (Tables 4-6). Assuming all treatments have an equal chance of causing death, there is a significant difference in the number of fish that died due to morpholino treatment $X^2(5, N=9)= 13$, $p= 0.02$. There are more fish that died from the spice blocking *scn4aa* targeting and the translation blocking *scn4aa* targeting morpholino than expected, and less in all the other treatments. Additionally, all fish treated with the translation blocking *scn4aa* targeting morpholino died ($N=4$). Differences in dosage and injection location are not accounted for in this analysis; however, the vivo-MO dosages administered that caused death were 6.5, 17.5, 20, and 27.5 mg/kg.

GeneTools recommends that injecting the vivo-MO treatment in equal volumes to saline and autoclaving the MO solution before injection can reduce toxic effects (Ferguson, Dangott and Lightfoot, 2014). This claim was not expressively tested; however, it appears that adding saline 1:1 with the treatment volume can reduce the percentage of toxic effects as measured by behavior. 11.1% (2/18) of fish treated with MO that was not autoclaved but was mixed 1:1 with saline demonstrated toxic effects with a 5.6% (1/18) death rate. 32.8% (20/61) of fish treated with MO that was neither autoclaved nor mixed 1:1 with saline showed toxic effects, with an 11.5% (7/61) death rate. In contrast, 45.5% (5/11) of fish treated with MO that was both autoclaved and mixed 1:1 with saline demonstrated toxic effects with a 9.1% (1/11) death rate. Dosage and injection location are not accounted for in this comparison and some sample sizes are low in number, which suggests the data cannot be supported by a statistical claim of the efficacy of these treatments in reducing vivo-MO toxicity.

Discussion

Initial pilot study results

My initial pilot study focusing on three fish demonstrated that exon1/intron1 splice blocking *scn4aa* targeting MO can cause EOD amplitude reduction over time in *B. brachyistius* (Figure 27) compared to a single individual injected with control morpholino. Individuals injected with either high or low doses of SB MO in this study demonstrated decreased *scn4aa* mRNA transcripts at a time point when EOD amplitude was reduced compared to the control (Figure 28). These results are consistent with expectations of how vivo-MO function *in-vivo* (Morcos, Li and Jiang, 2008; Notch *et al.*, 2011; Ferguson, Schmitt and Lightfoot, 2013; H. Zhang *et al.*, 2015).

If the exon1/intron1 splice blocking *scn4aa* targeting vivo-MO was functioning as expected, then *scn4aa* would retain intron1 in the mRNA post splicing (Figure 24A). There are two ways of molecularly identifying MO splice blocking, either by extracting mRNA and determining if intron1 is retained through qPCR or PCR following cDNA preparation, or by quantifying *scn4aa* mRNA transcripts to find evidence of nonsense-mediated decay of the intron1 retained *scn4aa* mRNA.

When these experiments were conducted, the Gallant lab did not yet have a genome for *B. brachyistius,* only the coding sequence for *scn4aa* had been identified in this species. As such, it was unknown what the size and sequence was of intron1. Attempts to amplify intron1 using genomic DNA, or *scn4aa* targeting MO treated electrocyte cDNA, were unsuccessful. Intron 1 could not be amplified from these sources even when using primers anchored in exon1 and exon2 that successfully amplified in cDNA and when allowing extension times that would have

been able to generate a ~10,000 bp intron1 segment. Although not confirmed, we assumed that there must be a region of intron1 that is difficult to amplify such as repetitive regions, GC-rich regions, or regions that form secondary structure, or simply that intron1 was too large for the OneTaq polymerase (New England Biolabs) used.

Due to the inability to amplify intron1, primers for exon1 were used to amplify *scn4aa* in the *scn4aa* targeting MO treated electrocyte cDNA to see if there was evidence of nonsense-mediated decay (Ward *et al.*, 2014). There is evidence that nonsense-mediated decay occurred after treatment with *scn4aa* targeting splice blocking MO in *B. brachyistius* electrocytes as there were fewer *scn4aa* transcripts than in control MO *B. brachyistius* electrocytes (Figure 28). Additionally, the decrease in *scn4aa* transcripts had a direct relationship with MO dose. MOH received a higher dosage of MO than MOL and compared to MOL, showed a significantly lower amount of *scn4aa* transcripts relative to *β-actin* (Figure 28). While activation of the nonsense-mediated decay pathway was not directly measured, the results suggest that nonsense-mediated decay from *scn4aa* targeting MO intron retention is responsible for *scn4aa* transcript reduction.

When *scn4aa* mRNA levels were quantified, the EOD amplitude of *scn4aa* targeting MO treated fish was lower than that of the control MO treated fish (Figure 27) and had a direct relationship between dosage of MO and EOD amplitude reduction. Given the role of *scn4aa* on EOD amplitude in weakly electric fish broadly (Markham *et al.*, 2009; Arnegard *et al.*, 2010), this result is the expected outcome if vivo-MOs can reduce *scn4aa* expression. If there is less Nav1.4a protein, then fewer ions will pass the membrane and the amplitude will not have as great as a magnitude. The control MO in this pilot study did not have a measurable effect over time, except for a ~7% decrease from baseline at the end of the study when electric organs were harvested for mRNA. It is unclear if the control MO had a specific effect on EOD amplitude at

this time (after 3 days and 3 injections at 20 mg MO/kg fish), if there were off-target effects (Eisen and Smith, 2008), or if there is some toxic effect of the vivo-MO. While these results are only represented by three fish, these results suggest that, under certain circumstances, vivo-MO can function as intended in mormyrid electrocytes and cause transcript reduction that results in a measurable phenotype to the EOD.

Inconsistent outcomes with a larger number of individuals

While early pilots were successful in producing EOD amplitude (Figure 27) and *scn4aa* transcript reduction (Figure 28) following *scn4aa* targeting vivo-MO injections compared to controls, these results were not reproducible when attempting to increase the sample size. Given the inability to reproduce the effects seen in the pilot when injecting a larger number of individuals, subsequent experiments performed were additional small pilot studies attempting to determine effects of MO delivery location, dosage, toxic effects, and the number of injections (Tables 4-6). As such, these experiments were not completed with a full, balanced design as the intention was to find an experimental procedure that consistently produced EOD amplitude reduction in experimental but not control fish and then do a full study. However, to limit fish use (we did not want to inject fish with MO and then use them for breeding as we were unsure of the effect EOD amplitude reduction would have on natural spawning) and MO use (MOs are very expensive), we were unable to accurately estimate the effects of these various manipulations on EOD amplitude reduction and opted to pool all control MO treated fish, and all *scn4aa* targeting MO treated fish.

When considering all experimental and control fish over time, there is not an effect of treatment when correcting for individual fish differences (Figure 30) through a repeated measures ANOVA analysis (Figure 31). These results, in conjunction with the pilot study that

was verified molecularly, suggest that vivo-MOs do not have a consistent effect in mormyrid electrocytes over time. A lack of clear differences in controls and experimental may have been the result of grouping data that varied in the variables tested. Some fish received much higher doses, in more sensitive locations (Figure 25), and received multiple injections over the course of the experiment (Table 5, Table 6, Table 7). In fact, the pilot study (Figure 27, Figure 28) had 3X total injections over 3 days, where most other experiments had a single dose that was given and the multiple injections given over time may have been part of the success of the pilot.

Additionally, there was not a consistent effect of the control MO. The control MO treated fish significantly varied in their EOD amplitude over time (Figure 30A); however, if the vivo-MO itself did not affect physiology then the fishes should have experienced no effect on EOD amplitude. There seems to be some evidence that EOD amplitude is reduced in control MO treated fish over time (Figure 27, Figure 30A, Figure 31), although the mechanism is unknown.

The inconsistent effects measured may be the product of pooling together separate pilot experiments. Given constraints like cost, fish availability, and inconsistent results, we were unable to accurately estimate the effects of variables that were changed among these pilots. Any effect present may be masked by the effects of higher dosages, multiple injections over time, different morpholinos, and injection location which vary among experiments that were ultimately considered together. The effects on EOD amplitude over time may change with these variables and the results reported above should be considered in light of these limitations.

Vivo-MO delivery and toxicity issues

Although vivo-MOs are designed to enter cells and circumnavigate the problem of delivery (Morcos, Li and Jiang, 2008), the location of the initial injection could have an effect.

Direct electric organ injections would be the ideal injection route as this method would concentrate the vivo-morpholino in electrocytes, allow slower spread to other organs, and may provide a faster effect on EOD amplitude. However, EODs are highly dependent on electrocyte anatomy (Carlson and Gallant, 2013; Paul *et al.*, 2015) and it does not seem that mormyrid electric organs regenerate (Patterson and Zakon, 1993). As a result, there are risks of permanently altering the EOD by damaging the electrocytes through direct electric organ injection. Given these conflicting possibilities, intraperitoneal and intramuscular injections were performed along with direct electric organ injections (Figure 25).

While intramuscular injections are easiest to perform, there was no evidence of MO-associated EOD changes when injecting intramuscularly, even when using high doses (Table 5). Intraperitoneal injections require some practice to master as damage can be done to the internal organs during delivery but they seem to be effective in causing knockdown (Figure 27, Figure 28). Direct electric organ injections resulted in several cases of silenced fish (35% of direct electric organ injections resulted in silencing of the EOD), whereas these effects were not seen in intraperitoneal nor intramuscular injections. The silenced fish were likely the result of damage to the electromotor neuron (Carlson, 2002); however, the electromotor neuron was not explicitly investigated in silenced fish. Additionally, the extent of damage to electrocytes from the needle was not explored.

Vivo-MOs are known to have some toxic effects from the delivery motif (Ferguson, Dangott and Lightfoot, 2014; Moulton, 2016). How these toxic effects would affect mormyrids is an important consideration for future vivo-MO use in mormyrids. Control vivo-MO (supplied by GeneTools) help to give a picture of the toxic effects of vivo-MO, independent of any gene expression changes, as they are unspecific to any available mRNA (Eisen and Smith, 2008). The

lack of any mRNA targets for the vivo-MO control ensures that any effects seen on health or global gene regulation is a response to the presence of the vivo-MO itself. Even at high concentrations (27.5 mg/kg), the vivo-MO control did not cause death in *B. brachyistius*; however, fish did exhibit sickly behavior in the hour following injections so there is some toxic effect of the vivo-MO itself (Tables 1-3).

Vivo-MO can self-hybridize via complementary base pairing and cause blood thickening and clotting that can result in death (Ferguson, Dangott and Lightfoot, 2014). If a vivo-MO has a high proportion of self-complementary base pairing across its length, then the likelihood of toxic effects from the vivo-MO increases. The likelihood of these MO-related toxic issues occurring with the splice blocking *scn4aa* targeting MO is low as there are only 2 bases that self-complement. By contrast, the E2/I2 *scn4aa* targeting translation blocking MO had 10 bases that could self-complement (Figure 32).

The data collected does not support this mechanism for toxic effects. The splice blocking *scn4aa* targeting MO resulted in the most recorded toxic effects, as 62.6% of fish showed sickly behavior following injection (17/27), but had the least amount of self-complementary binding (Figure 32). The trend of increased toxicity then predicted for the splice blocking *scn4aa* targeting MO is also present when looking at toxicity-related deaths. The splice blocking *scn4aa* targeting MO was responsible for 44.4% (4/9) toxicity-related deaths. Similarly, the E2/I2 splice blocking *scn4aa* targeting MO was expected to have the highest toxic effects (10 self-complementary base pairs, Figure 32), but showed the lowest toxic effects, as 7.4% of fish showed sickly behavior following injection (2/27) and was responsible for only 11.1% (1/9) toxicity-related deaths. The self-complementary base pairing hypothesis does support the effects seen in the translation blocking *scn4aa* targeting MO (8 self-complementary base pairs, Figure

32) where all 4 fish injected with the MO showed toxicity-related behavioral changes and died within 1.5 hours.

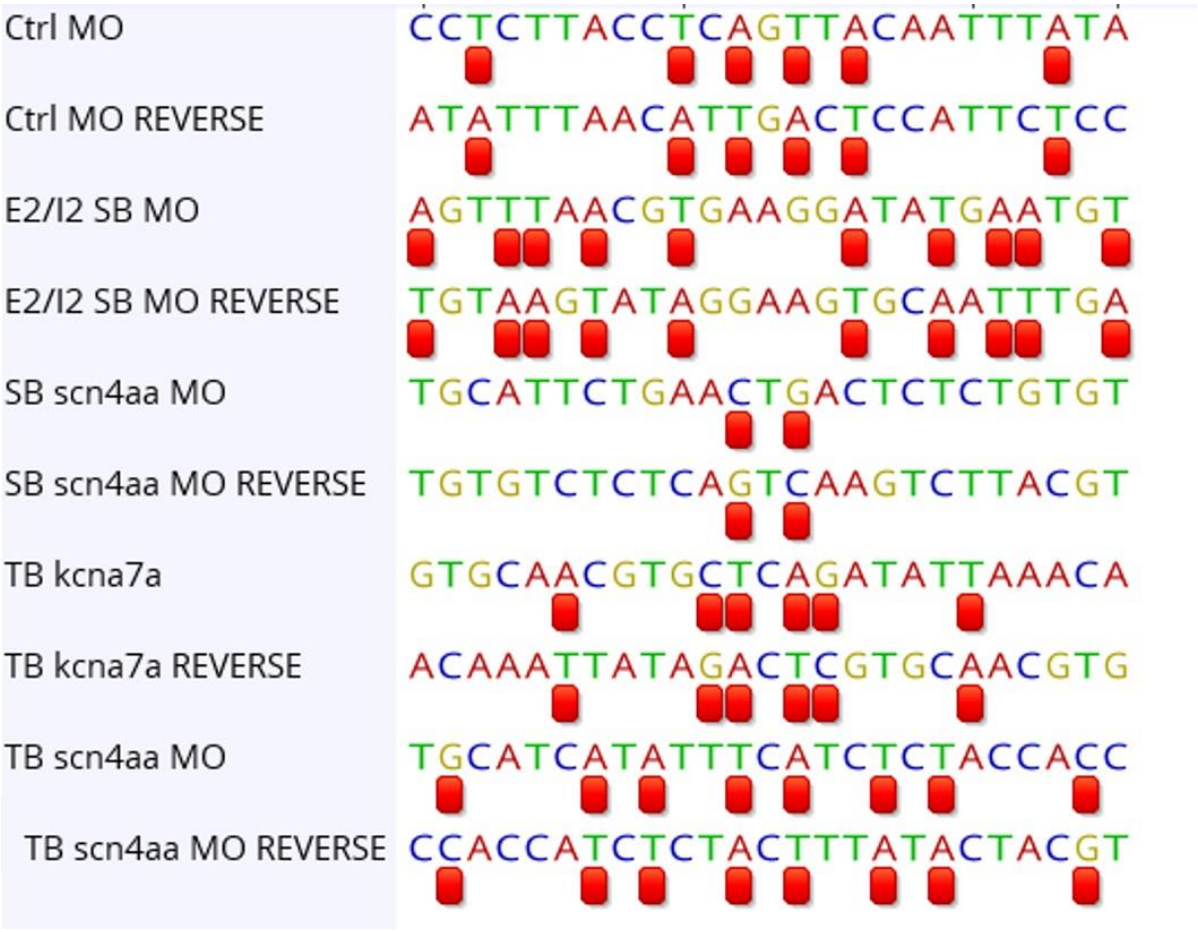

Figure 32: Self-complementary nucleotide base pairing of vivo-MO- The MOs used are displayed paired with their reverse complements. MOs self-complement at different amounts depending on the sequence. Complementary base pairs are notated by a red rectangle. E2/I2 = Exon2/Intron2 splice blocking *scn4aa* targeting MO, TB= translation blocking, SB= splice blocking.

A 1:1 physiological saline:vivo-MO injection and using autoclaved vivo-MO is thought to reduce MO toxicity (Ferguson, Dangott and Lightfoot, 2014). Autoclaving the MO may reduce the number of vivo-MOs that have self-complemented before injection and injecting the MO 1:1 with physiological saline reduces the injected concentration (while maintaining the same dosage administered) and may protect from acute toxic effects. Late during the MO pilot

experiments, when a higher number of toxic effects was seen than was expected, we began to consider autoclaving the MO before injection and injecting it 1:1 with physiological saline. The number of experiments where this was tested was not sufficiently balanced (other variables were not controlled properly) and had low sample sizes; as a result, I could not expressively test reduction of toxicity claims. However, the data may suggest that adding saline 1:1 with the treatment volume can reduce the percentage of toxic effects as measured by behavior.

The toxicity issues with MOs were seen overwhelmingly in the individuals injected with *scn4aa* targeted MO, even when known measures were taken to reduce toxicity and even though the most toxic *scn4aa* targeting MO had the lowest expectation for toxicity (Figure 32). The possibility for off-target effects is possible, as are unintended on-target effects. While *scn4aa* is a well understood, electric organ-specific gene, it is also expressed in other tissues at low levels. Brain, kidney, heart, flank skin and spleen all show some expression of *scn4aa* (Gallant *et al.*, 2017). The toxicity effects seen throughout the *scn4aa* targeting vivo-MO experiments could be unintended, on-target effects in these various other organs. Given that coloration change, mobility issues with self-righting, and EOD rate reduction were often seen when fish had toxic effects, it may suggest disruptions to brain *scn4aa* expression and death could result from kidney or heart dysfunction. The potential *scn4aa* knockdown in other tissues was not tested and mRNA from vivo-MO treated individuals was not extracted from any organs other than skeletal muscle and electric organ. Additionally, the toxic behavioral issues of *scn4aa* targeting MOs were consistent with those seen in the control MO treated fish as 14.8% of fish showed sickly behavior following injection (4/27), so it is unclear if the behavior is a result of toxicity from the vivo-MO motif or if it is an unintended, off-target effect of *scn4aa* targeting vivo-MOs.

scn4aa expression regulates *acta1a*

When *scn4aa* expression is reduced via vivo-MO (Figure 28), *acta1a* expression changes (Figure 29A). *acta1a* was first considered as a reference gene for qPCR transcript quantification. However, when amplifying the gene from control MO treated and *scn4aa* targeting MO treated electric organ and skeletal muscle, an interesting result was seen (Figure 29). Only in the electric organ of *scn4aa* targeting MO treated fish, an *acta1a* isoform with an insertion was expressed, which translates to a truncated protein due to a premature stop codon (Figure 29A-C). *acta1a* normally functions as a muscle-specific actin, a structural component of the muscle sarcomere that is involved in contraction (Sztal *et al.*, 2015). While mormyrid electric organs do not contract, they are derived from skeletal muscle cells and also contain nonfunctional sarcomeres (Gallant *et al.*, 2014), so the presence of *acta1a* is not unexpected. The truncated isoform produced when *scn4aa* levels drop is likely nonfunctional and it is unclear what function, if any, the truncated protein serves. Its function was not explored experimentally.

There is no molecular evidence to suggest that *acta1a* and *scn4aa* interact directly. However, the data presented here suggest *acta1a* and *scn4aa* may interact through intermediate proteins and be part of the gene regulatory network that impacts EOD amplitude. *acta1a* expression is not altered in skeletal muscle where *scn4aa* is expressed at near zero levels (Figure 29A). *acta1a* was not expected to be investigated, so the data and interpretations here are from limited data and a small sample size (1 control fish and 2 *scn4aa* targeting MO treated fish) but were included to demonstrate that *scn4aa* knockdown may impact more genes within the electrocyte than previously appreciated.

Recommendations for vivo-MO use in mormyrids

Vivo-morpholinos are a promising tool, however, we demonstrate highly inconsistent performance and significant non-specific effects of control morpholinos. As such, extreme caution should surround any future explorations into this method as a means for assessing gene function. In this section, I will outline my hesitations for suggesting this method to other researchers and offer suggestions for considerations of future experiments that would use vivo-MOs or plan to better test some of the variables selected for our experiments.

Vivo-MOs were shown to have the capacity to function as intended and designed from GeneTools. In a pilot experiment, vivo-MOs were able to reduce expression of the *scn4aa* target in a dose-dependent way (Figure 28) in the organ of interest, demonstrating that the molecular expectations for a splice blocking morpholino were met. In addition, the fish that were sacrificed to quantify the vivo-MO induced *scn4aa* knockdown exhibited an altered phenotype (reduced EOD amplitude) that was expected given the theorized role of the *scn4aa* target (Figure 27). There was a minimal effect of the control-MO on EOD amplitude; a significant change in EOD amplitude versus baseline was only seen after 3 days after the fish received 3 total doses of 20 mg/kg vivo-MO.

While the pilot experiment showed results that were in line with the known mechanism of vivo-MOs (Eisen and Smith, 2008; Morcos, Li and Jiang, 2008), the results only represent three individuals. When looking at all the experiments performed, these results were not reproducible in other individuals. We were unable to detect a significant difference in EOD amplitude over time between control-MOs and *scn4aa* targeting-MOs (Figure 31) and there was a large variance in the EOD amplitude change over time between individual fish (Figure 30) in both experimental and control groups. Additionally, there was a statistical difference in EOD amplitude over time

in control vivo-MO treated individuals, suggesting there was some non-specific effect of the control vivo-MO itself. These results may represent inconsistencies in the response of mormyrids to vivo-MO use.

Future researchers who are interested in vivo-MO use for gene knockdown in mormyrids should be sure to first perform a pilot study in their species of interest to determine toxic effects and dosage. Based on the data collected, there appears to be a balance in vivo-MO dose that needs to be achieved to reliably reduce the levels of the target and produce a phenotype, while minimizing off-target and toxic effects. My recommendation for future exploration in mormyrids would be first to perform a dosage response study with the control vivo-MO to see if there are any effects of the control vivo-MO and at what doses those effects are seen. It is prudent to establish the effects of the control vivo-MO as they are known to affect other systems (Ferguson, Dangott and Lightfoot, 2014; Moulton, 2016), and to see if these effects are measurable in the phenotype that the study is interested in. Without knowing if the vivo-MO itself will alter the response or cause death, it is unwise to test the efficacy of the experimental vivo-MO, as it is difficult to troubleshoot if unintended results (death, behavior to suggest toxic exposure) are from the vivo-MO target being reduced or from the delivery motif on the vivo-MO.

Another consideration for reducing toxic effects would be to use lower doses of vivo-MO but to inject multiple doses into the fish over time. Multiple injections were administered in the successful pilot experiment (Figure 27, Figure 28). If doses are too low or if low doses are not performed close enough in time, there may never be a phenotypic response that can be measured. I highly recommend that future attempts with vivo-MOs consider 2-4 low doses (between 10-15 mg/kg each to start) administered 8-12 hours apart (Morcos, Li and Jiang, 2008; Matsuda and

Shi, 2010; Notch *et al.*, 2011; Ferguson, Schmitt and Lightfoot, 2013; Park *et al.*, 2015; Suhail *et al.*, 2019; Zang *et al.*, 2019; Lu-Nguyen *et al.*, 2021)

Another consideration for future studies is delivery location. Preliminary studies suggest that intramuscular injections are not a viable method for vivo-MO administration; the highest doses, 27.5 mg/kg, when tested intraperitoneally caused death and severe EOD phenotypic change but had no effect when injected intramuscularly (Table 5, Table 7). Intraperitoneal injections are a common delivery method for vivo-MOs (Matsuda and Shi, 2010; Notch *et al.*, 2011; Park *et al.*, 2015; Suhail *et al.*, 2019; Zang *et al.*, 2019; Lu-Nguyen *et al.*, 2021) and are likely easier than intravenous injections in mormyrids, although intravenous injections were not performed. The successful pilot experiment was conducted with intraperitoneal injections of the vivo-MO (Figure 27), so there is evidence that vivo-MO injected into the peritoneal cavity can reach electrocytes and cause gene knockdown (Figure 28). Given that nearly 1/3rd of direct electric organ injections resulted in EOD silencing, electric organ injections should be avoided if possible. I strongly recommend future studies explore intraperitoneal injections.

I would highly encourage researchers to not invest in vivo-MOs as a method to knockdown gene targets to investigate gene function. If the data collected here represents the true condition, then there is a large amount of variability in individual mormyrid response to vivo-MOs (Figure 30), there is an effect over time of just the control vivo-MO, and there is a lack of clear effect of experimental vivo-MO treated fish (Figure 31). Vivo-MOs are expensive (400 nmol of custom sequence vivo-MO is $700, this equates to ~$35 per 12.5 mg MO/kg fish injections for a 15 g fish) and given my recommendation to administer multiple doses over time, the cost to conduct even pilot studies may be prohibitive for many laboratories. Even to establish the effects of control vivo-MO would take a considerable amount of time, expense, and person-

hours. Additional expense would arise in downstream molecular verification of knockdown through mRNA or protein quantification, as well as the expense to collect and house fish for the experiment in sufficient numbers to make valid claims. There will also be some amount of death or toxic effects during pilot studies to determine dose and researchers may not want to include fish previously injected with vivo-MO for other studies. Researchers must therefore weigh the ethical considerations (whether loss of life of these fish outweighs the information that may be gained), as well as account for a loss of a number of fish from the laboratory colony for a vivo-MO pilot study.

Given all these considerations and my experience working with vivo-MOs in mormyrid weakly electric fish, I cannot suggest that others attempt to utilize vivo-MOs for reverse genetic studies. A final consideration for those who want to work with vivo-MOs against my advice would be to have a target that is not an ion channel and is extremely specific in its location of expression (ideally the electric organ). There is a possibility that some of the *scn4aa* targeting vivo-MO toxic effects recorded were due to unintended on-target effects in the renal system and central nervous system. A very carefully selected target will need to be considered, in my opinion, to rationalize exploring vivo-MO use in light of the data and interpretations presented here.

APPENDIX

Coding associated with the manuscript is given in this Appendix

EODCRISPRWT_Length

```
library(AICcmodavg)
library(lsmeans)
library(ggplot2)

EODsize<-read.csv("C:/Users/Savvas Constantinou/Desktop/WTCRISPRBgFULL.csv")
head(EODsize)
EODsize$Group <-as.factor(EODsize$Group)

#subset for WT
WT <- subset(EODsize, Group == "WT")
WT <- droplevels(WT)
summary(WT)

#create data frame of averages for WT
df_summary <- data.frame(Length=unique(WT$Length), n=tapply(WT$Amplitude, WT$Length, length),
                         mean=tapply(WT$Amplitude, WT$Length, mean))
#calc standard error of mean after standard deviation
df_summary$sd <- tapply(WT$Amplitude, WT$Length, sd)
df_summary$sem <- df_summary$sd/sqrt(df_summary$n-1)
head(df_summary)
#calc 95% CI
df_summary$CI_lower <- df_summary$mean + qt((1-0.95)/2, df=df_summary$n-1)*df_summary$sem
df_summary$CI_upper <- df_summary$mean - qt((1-0.95)/2, df=df_summary$n-1)*df_summary$sem
head(df_summary)
df_summary$Amplitude<-df_summary$mean

#when I ran the above the length variable did not match up with the means, I exported the data,
#write.csv(df_summary, "C:/Users/Savvas Constantinou/Desktop/summary.csv", row.names = FALSE)
#resorted the length column from smallest to largest in excel and reuploaded to generate graph below
#df_summary<-read.csv("C:/Users/Savvas Constantinou/Desktop/summary.csv", header= TRUE)
```

```
#plot WT with 95% CI and lin reg of crispants
ggplot(df_summary, aes(x=Length, y=Amplitude)) +
  geom_point(color='black', size = 2) +
  geom_smooth(method=lm, color='black', se=TRUE, fill="lightgray") +
  #add lm predictor for crispants
  geom_point(data=subset(EODsize, Group== "CRISPR"),
             aes(x=Length, y=Amplitude, color=as.factor(Group))) +
  geom_smooth(data=subset(EODsize, Group== "CRISPR"),
              aes(x=Length, y=Amplitude, color=as.factor(Group)), method=lm, se=FALSE) +
  geom_point(data=subset(EODsize, Group== "CRISPR1"),
             aes(x=Length, y=Amplitude, color=as.factor(Group))) +
  geom_smooth(data=subset(EODsize, Group== "CRISPR1"),
              aes(x=Length, y=Amplitude, color=as.factor(Group)), method=lm, se=FALSE) +
  geom_point(data=subset(EODsize, Group== "CRISPR2"),
             aes(x=Length, y=Amplitude, color=as.factor(Group))) +
  geom_smooth(data=subset(EODsize, Group== "CRISPR2"),
              aes(x=Length, y=Amplitude, color=as.factor(Group)), method=lm, se=FALSE) +
  geom_point(data=subset(EODsize, Group== "CRISPR3"),
             aes(x=Length, y=Amplitude, color=as.factor(Group))) +
  geom_smooth(data=subset(EODsize, Group== "CRISPR3"),
              aes(x=Length, y=Amplitude, color=as.factor(Group)), method=lm, se=FALSE) +
  theme_classic()

#model
one.way <- lm(Amplitude ~ Length, data= df_summary)
summary(one.way)
```

Juvenile EOD amplitude comparisons

```
#code to visualize amplitude of CRISPR vs uninjected and run statistics - fig 7
#BB
#upload data, check
BBamp<-read.csv("C:/Users/Savvas Constantinou/Desktop/BBAmp.csv")
head(BBamp)
```

```
#group amp by individual

boxplot(BBamp[,4]~BBamp[,1])


#group amp by treatment

boxplot(BBamp[,4]~BBamp[,2], main="Brienomyrus brachyistius EOD amplitude", xlab="Treatment",
ylab="Amplitude (mV/cm)")


C<- subset(BBamp, Group== "CRISPR", select=c(Amp) )

u<-subset(BBamp, Group== "uninjected", select=c(Amp) )

t.test(u,C, paired=FALSE)


#BG

#upload data, check

BGamp<-read.csv("C:/Users/Savvas Constantinou/Desktop/BGamp.csv")

head(BGamp)


#group amp by treatment

boxplot(BGamp[,4]~BGamp[,2], main="Brachyhypopomus gauderio EOD amplitude", xlab="Treatment",
ylab="Amplitude (mV/cm)")


CBg<- subset(BGamp, Group== "CRISPR", select=c(Amp) )

uBg<-subset(BGamp, Group== "uninjected ", select=c(Amp) )

t.test(uBg,CBg, paired=FALSE)
```

Matlab tdms extraction

```
%TDMS PeakFinder With Duration  Reads TDMS Formatted Long EOD Files and Extracts Peaks.

%   Re-written for doing morpholino data analysis from new recording

%   software (dtd_eod.exe) written in LabView by JRG.

%

%   Written by J. Gallant

%   $Revision 1.00$  $Date: 2016/06/09 14:22$


final_data=[];
```

```
prompt = '     > Please Enter a Threshold Value for this Recording: ';

prompt2= '     > Please Enter the Gain for this Recording: ';

prompt3= '     > Please Enter the Average EOD Duration For this Species (seconds) ';

prompt4= '     > Please Enter the End Time for this Recording: ';

%set the directory to open data from- this needs to be 1 level up from the

%BBRACH folder you want to analyze

directory=uigetdir('C:/Users/Savvas Constantinou/Dropbox (MSU Efish Lab)/Projects/Morpholinos/','Select
directory for all individual fish');


%Look for species directories (start with B*)"  %with this code as written,

%it is looking for a directory within the directory you provide that starts

%with BBRACH -

subjectdirectory=fullfile(directory,'Che*');

listing = dir(subjectdirectory);

%Extract the Names

specieslist={listing.name};

%Count the subjects

[~,specieslistsize]=size(specieslist);

eodpreview=figure();

set(eodpreview, 'WindowStyle','docked')


%for each species directory...

for a=1:specieslistsize

    treatdirectory=fullfile(directory,specieslist(a),'*.tdms'); %create the path

    treatlisting=dir(treatdirectory{1}); % list the files with the tdms extension

   % treatlisting=treatlisting(3:end); %remove .. and . directories

    treatlist={treatlisting.name}; %get the filenames

    [~,treatlistsize]=size(treatlist); %construct a list of the files


    fprintf('Starting step %s: Analysis of %s!\n',num2str(a),specieslist{a}); %Starting step 1: Analysis of BBRACH!


    %this was off in jasons code

    %raw_data(a).name=subjectlist{a};
```

```
    for b=1:treatlistsize  %for each file....


        %filedirectory=fullfile(directory,specieslist(a),treatlist(b),'*.tdms'); %create the path

        %filelisting=dir(filedirectory{1}); % list the files with the tdms extension

        %filelist={filelisting.name}; %get the filenames

        %[~,filelistsize]=size(filelist); %construct a list of the files


        %fprintf('  Step %s.%s: Analysis of %s %s started...\n',num2str(a),num2str(b),specieslist{a},treatlist{b});
%Step 1.1 Analysis: Analysis of BBRACH CRISPR


        %for c=1:filelistsize

            fprintf('   Step %s.%s: Analysis of %s started...\n',num2str(a),num2str(b), treatlist{b});  %Step 1.1.1
%Analyis of BBRACH CRISPR file1.tdms

            eodwave=[]; %initialize variables

            wavesize=[];

            neg_peakvoltages=[];

            neg_peak_idx=[];

            pos_peakvoltages=[];

            pos_peak_idx=[];

            pos_peak_idx_size=[];

            pos_peak_idxsize=[];

            min_index=[];

            chunk=[];

            eodstart=[];

            eodend=[];

            eod_start_idxs=[];

            eod_end_idxs=[];



            filename= fullfile(directory,specieslist(a),treatlist(b));   %construct the filename

            eval(sprintf('%s_%s = TDMS_getStruct(filename{1});',specieslist{a},treatlist{b}));  %create a container
based on the filename to save data to, and open the data

            eval(sprintf('eodwave=%s_%s.Untitled.Dev1_ai0.data;',specieslist{a}, treatlist{b})); %put the data in a
variable called eodwave
```

```
        eval(sprintf('eodwaveinfo=%s_%s.Props;',specieslist{a}, treatlist{b})); %put the data in a variable called
eodwave


        j1=[1,-0.98];j2=[1,-1];

        eodwave=filtfilt(j2,j1,eodwave);


        %baseline=mean(eodwave(1:50));

        %eodwave=eodwave-baseline;


        recordlength=min(length(eodwave),1000000);

        if recordlength < 1000000

           fprintf('   Step %s.%s: Analysis of %s aborted, less than 1000000 points in recording
\n',num2str(a),num2str(b), treatlist{b});  %Step 1.1.1 %Analyis of BBRACH CRISPR file1.tdms

           continue


        end

        plot(eodwave(1:recordlength));

        gcf;

        figure(eodpreview);


        commandwindow;

        threshold=input(prompt);

        %This was on in jasons code gain=input(prompt2);

        eodwindowsize=2000; %this was the code for Jason instead of 2000

        % which is 0.02*100,000: input(prompt3)*100000;

        %t2=input(prompt4);







        %valus of 3,000,000 is 30 seconds (30 * 100,000 samples per

        %second)

[pos_peaks,pos_peak_idx]=findpeaks(eodwave(1:3000000),'MinPeakHeight',threshold,'MinPeakDistance',100);
```

```
        %[neg_peaks,neg_peak_idx]=findpeaks(-
eodwave(1:3000000),'MinPeakHeight',threshold,'MinPeakDistance',100);



        [~,pos_peak_idxsize]=size(pos_peak_idx);
        pos_peak_idx=pos_peak_idx(2:(pos_peak_idxsize-1));
        pos_peaks=pos_peaks(2:(pos_peak_idxsize-1));
        [~,pos_peak_idx_size]=size(pos_peak_idx);

        %[~,neg_peak_idxsize]=size(neg_peak_idx);
        %neg_peak_idx=neg_peak_idx(2:(neg_peak_idxsize-1));
        %neg_peaks=neg_peaks(2:(neg_peak_idxsize-1));
        %[~,neg_peak_idx_size]=size(neg_peak_idx);
        %neg_peaks=abs(neg_peaks);

        %new code finds the negative peak nearby each positive
        %peak.  use 0.02 seconds for eodwindowsize for b. brachyistius
        neg_peaks=[];
        neg_peak_idx=[];
        for e=1:length(pos_peak_idx)
           [neg_peaks(e),local_idx]=min(eodwave((pos_peak_idx(e)-
eodwindowsize):(pos_peak_idx(e)+eodwindowsize)));
           neg_peak_idx(e)=local_idx+(pos_peak_idx(e)-eodwindowsize);
        end




        all_peaks=pos_peaks+abs(neg_peaks);


        all_peaks_mean=mean(all_peaks);
        all_peaks_std=std(all_peaks);


        treatment=treatlist(b);
        fishname=strcat('fish_',num2str(b));
```

```
            raw_data.species=specieslist(a);
            raw_data.treat=treatlist(b);
            raw_data.filename=treatlist(b);
            raw_data.fish_name=fishname;
            raw_data.amplitude=all_peaks_mean;
            raw_data.peaks=all_peaks;
            raw_data.amplitidue_std=all_peaks_std;
            raw_data.threshold=threshold;
            %This was on in jasons code: raw_data.gain=gain;
            %raw_data.t1=t1;
            %raw_data.t2=t2;


            final_data=[final_data; raw_data];
        %end

    end
end
fprintf('\nAll Analysis Complete!  Enjoy your data!\n');
clearvars -except final_data

bp_data=horzcat(final_data.peaks);
[numvars,~]=size(final_data);
grp=[];
for i=1:numvars
    [~,npeaks]=size(final_data(i).peaks);
    grp=[grp,ones(1,npeaks)*i];
end
boxplot(bp_data,grp)

 for i=1:length(final_data)
     writematrix(final_data(i).peaks',char(fullfile('C:/Users/Savvas
Constantinou/Desktop/Rawvoltages',strcat(final_data(i).filename,'_raw_voltages.csv'))))
```

end

MOL MOH MOC

```
#chi square used to determine differences in behavor following MO injection and deaths


toxic <- c(17, 4, 2, 4, 0, 0)

ho <- chisq.test(toxic)

ho$expected


death <- c(4, 4, 1, 0, 0, 0)

hi <- chisq.test(death)

hi$expected

#_____________________________________

#code for anova for delta ct differences for qPCR

dCt <- c(1.42496497, 0.85455584, 1.58148445, 3.46491474, 2.97499999, 3.77181974, 4.77462939, 5.15833434, 6.13886573)

individual <- as.factor(c("control", "control", "control", "MOL", "MOL", "MOL", "MOH", "MOH", "MOH"))

new <- data.frame(dCt, individual)


testing <- aov(dCt ~ individual, data = new)

summary(testing)

TukeyHSD(testing)


#_____________________________________

#https://www.scribbr.com/statistics/anova-in-r/ - code to see if there are differences in MOL, MOH and MOC2 amp

#bring data in

library(ggpubr)

library(dplyr)

amp.data <- read.csv("C:/Users/Savvas Constantinou/Desktop/amp.data.csv", header = TRUE, colClasses = c("factor", "numeric", "factor", "numeric", "factor", "factor", "factor", "factor", "factor", "factor"))

head(amp.data)


MO <- subset(amp.data, ID == c("MOL", "MOH", "MOC2"))

#order time for plotting
```

```
MO$Time <- ordered(MO$Time, levels=c("Baseline", "1440min", "1800min", "2880min", "3240min", "4320min"
))
MO$Time <- droplevels(MO$Time)

#raw data boxplot
ggboxplot(MO, x = "Time", y = "PERBaseline", add = "point", color="ID")

#model selection- is interaction sig?
one.way <- aov(PERBaseline ~ Time + Error(ID), data= MO)
summary(one.way)
two.way <- aov(PERBaseline ~ Time + ID + Error(ID), data= MO)
summary(two.way)
interaction <- aov(PERBaseline ~ Time*ID + Error(ID), data= MO)

#post hoc tests
#Remove Error term for post hoc tests
interaction <- aov(PERBaseline ~ Time*ID, data= MO)
tukey <- TukeyHSD(interaction)
tukey

tukey.plot.aov<-aov(PERBaseline ~ Time:ID, data=MO)
tukey.plot.test<-TukeyHSD(tukey.plot.aov)
plot(tukey.plot.test, las=1)

#produce final figure

mean.data.mo <- MO %>%
 group_by(ID, Time) %>%
 summarise(
   PERBaseline = mean(PERBaseline),
   SE = sem(PERBaseline)
 )

two.way.plot <- ggplot(MO, aes(x = Time, y = PERBaseline, group=ID, color = ID)) +
```

```
  geom_point(cex = 3, pch = 1, position = position_jitter(w = 0.1, h = 0))

two.way.plot

two.way.plot <- two.way.plot +
  stat_summary(fun.y = mean,
               fun.ymin = function(x) mean(x) - sd(x),
               fun.ymax = function(x) mean(x) + sd(x),
               geom = "errorbar", size = 1.5, width=0.5)

two.way.plot

two.way.plot <- two.way.plot +
  stat_summary(fun.y= mean,
               geom= "point", color="black", size= 3)

two.way.plot

two.way.plot <- two.way.plot +
  theme_classic2() +
  labs(title = "Change in Amplitude Compared to Baseline in Response to Morpholino Treatment",
       x = "Time",
       y = "Percent Baseline")

two.way.plot

#determine number of observations in each group
label_df <- MO %>% count(ID, Time)
label_df
```

RMANOVA

```
#do repeated measures ANOVA
library(ggpubr)
```

```
library(dplyr)
library(Hmisc)
library(gridExtra)

#code to bring in file and check
threeday <- read.csv("C:/Users/Savvas Constantinou/Desktop/threeday.csv", header = TRUE, colClasses =
c("factor", "numeric", "factor", "numeric", "factor", "factor", "factor", "factor", "factor", "factor", "factor", "factor"))
head(threeday)
#order bin chronologically
threeday$bin <- ordered(threeday$bin, levels = c("0.5", "1", "2", "4", "5", "6", "8", "9","10", "12"))

#check where data lies in groups
describe(threeday)
addmargins(xtabs(~TREATGROUP + bin, data=threeday))

#check the values and their variance
aggregate(PERBaseline~bin+TREATGROUP, data = threeday, FUN = mean)
aggregate(PERBaseline~bin+TREATGROUP, data = threeday, FUN = sd)

#plot raw data in box plot (median)
ggboxplot(threeday, x = "bin", y = "PERBaseline", color = "TREATGROUP")

#spaghetti plots- are there interactions check how noisy data is

xyplot(PERBaseline~bin,data = threeday, groups=ID ,type='l')
xyplot(PERBaseline~bin,data = threeday, groups=TREATGROUP ,type='l')

##################################################
###############
#avg EOD per fish per time point to get bin averages per fish

#table with each fish, at each time point and Avg % baseline
mean.time <- threeday %>%
  group_by(TREATGROUP, ID, Time, bin) %>%
```

```
  summarise(
    PERBaseline = mean(PERBaseline)
  )
mean.time <- as.data.frame(mean.time)


#for ctrls at each bin
#subset to controls only
ctrl<- subset(mean.time, TREATGROUP == "Control")
head(ctrl)


#create summary table for means
summary <- data.frame(bin=factor(),PERBaseline=integer(), TREATGROUP=factor(), n = integer(), sd=integer(), sem=integer())


#get means for %baseline with bins and each fish ID
mean.data.ctrl <- ctrl %>%
  group_by(ID, bin) %>%
  summarise(
    PERBaseline = mean(PERBaseline)
  )
#what bins are there
unique(mean.data.ctrl$bin)
#for each bin,
#subset all individuals at a certain bin
sub<-subset(mean.data.ctrl, bin == "12")
#calculate mean, SD and Standard error for all ctrl fish at that bin
meanPB <- mean(sub$PERBaseline)
sd <- sd(sub$PERBaseline)
n <- as.integer(length(sub$PERBaseline))
sem <- sd/sqrt(n)
#put everything in summary
summary <- rbind(summary, data.frame(bin= 12, PERBaseline=meanPB, TREATGROUP="Control", n=n, sd=sd, sem=sem))
#repeat above with all bins (see unique- I couldn't get the loop to run correctly so just did manually for sake of time)
```

```
#Calculate mean and SE for exp at each bin

#subset to exp only

exp<- subset(mean.time, TREATGROUP == "Experimental")

head(exp)



#get means for % baseline with bins and each fish ID

mean.data.exp <- exp %>%

 group_by(bin,ID) %>%

 summarise(

  PERBaseline = mean(PERBaseline)

 )

#what bins are there

unique(mean.data.exp$bin)

#for each bin,

#subset all individuals at a certain bin

sub<-subset(mean.data.exp, bin == "12")

#calculate mean SD and Standard error

meanPB <- mean(sub$PERBaseline)

sd <- sd(sub$PERBaseline)

n <- as.integer(length(sub$PERBaseline))

sem <- sd/sqrt(n)

#put everything in summary

summary <- rbind(summary, data.frame(bin= 12, PERBaseline=meanPB, TREATGROUP="Experimental", n=n,
sd=sd, sem=sem))

#repeat above with all bins- (see unique- I couldn't get the loop to run correctly so just did manually for sake of
time)



#save summary

#write.csv(summary, "C:/Users/Savvas Constantinou/Desktop/summary.csv", row.names = FALSE)

#reload summary

#summary <- read.csv("C:/Users/Savvas Constantinou/Desktop/summary.csv", header = TRUE, colClasses =
c("factor", "numeric", "factor", "numeric", "numeric", "numeric"))
```

```
#summary$bin <- ordered(summary$bin, levels = c("0.5", "1", "2", "4", "5", "6", "8", "9","10", "12"))

#plot data of avg EOD of exp and ctrls over time
plot <- ggplot(summary, aes(x=bin, y=PERBaseline, group=TREATGROUP, color = TREATGROUP))+
  geom_point(position= "jitter", data=summary, size=4, aes(x=bin, y=PERBaseline)) +
  geom_errorbar(aes(ymin=PERBaseline-summary$sem, ymax=PERBaseline+summary$sem), width=0.5, size=1) +
  theme_classic2()
plot

#code to figure out color codes from graph
#ggplot_build(plot)$data
#[[1]]

#plot average EOD per fish over bins
#controls
plotctrl <- ggplot(mean.data.ctrl, aes(x=bin, y=PERBaseline, group=ID), show.legend = FALSE) +
  geom_line(color="#F8766D") +
  geom_point(color="#F8766D") +
  theme_classic2() +
  guides (color=FALSE) +
  labs(x = "Hours", y= " ")

#exp
plotexp <- ggplot(mean.data.exp, aes(x=bin, y=PERBaseline, group=ID)) +
  geom_line(colour="#00BFC4") +
  geom_point(colour="#00BFC4") +
  theme_classic2() +
  guides (color=FALSE) +
  labs(x = "Hours", y= " ")

grid.arrange(plotctrl, plotexp, nrow=2)

#determine number of fish in ctrl group
```

```
mean.data.ctrl <- droplevels(mean.data.ctrl)
unique(mean.data.ctrl$ID)

#determine number of fish in ctrl group
mean.data.exp <- droplevels(mean.data.exp)
unique(mean.data.exp$ID)

#do repeated measures ANOVA 2 way for time and treatment

#find avg baseline at each bin for ctrl/exp and each fish
mean.data <- threeday %>%
  group_by(TREATGROUP, ID, bin) %>%
  summarise(
    PERBaseline = mean(PERBaseline)
  )
#convert tibble to dataframe
mean.data<- as.data.frame(mean.data)
mean.data <-droplevels(mean.data)
head(mean.data)

#Repeated measures (include ID error as random effect) two way (time and treatment) anova

repanova <- aov(PERBaseline~TREATGROUP + bin + Error(ID), data=mean.data)
#is treatment sig?
summary(repanova)

#Do controls differ over time? RM one way analysis with just ctrls.
#Would expect ctrl mean to not differ over time if ctrls working as expected
#subset to just controls
onewayRMctrl <- subset(mean.data, TREATGROUP == "Control")

#one way RM anova
ctrlanova <- aov(PERBaseline~bin + Error(ID), data=onewayRMctrl)
```

```
#is bin sig (within effect)?
summary(ctrlanova)
```

codeforMOanalysis_mostrecentBbrachy.m

```
%TDMS PeakFinder With Duration  Reads TDMS Formatted Long EOD Files and Extracts Peaks.
%   Re-written for doing morpholino data analysis from new recording
%   software (dtd_eod.exe) written in LabView by JRG.
%
%   Written by J. Gallant
%   $Revision 1.00$  $Date: 2016/06/09 14:22$

final_data=[];
prompt = '     > Please Enter a Threshold Value for this Recording: ';
prompt2= '     > Please Enter the Gain for this Recording: ';
prompt3= '     > Please Enter the Average EOD Duration For this Species (seconds) ';
prompt4= '     > Please Enter the End Time for this Recording: ';
%set the directory to open data from- this needs to be 1 level up from the
%BBRACH folder you want to analyze
directory=uigetdir('C:/Users/Savvas Constantinou/Dropbox (MSU Efish Lab)/Projects/Morpholinos/','Select
directory for all individual fish');

%Look for species directories (start with B*)"  %with this code as written,
%it is looking for a directory within the directory you provide that starts
%with BBRACH -
subjectdirectory=fullfile(directory,'BBRACH*');
listing = dir(subjectdirectory);
%Extract the Names
specieslist={listing.name};
%Count the subjects
[~,specieslistsize]=size(specieslist);
eodpreview=figure();
set(eodpreview, 'WindowStyle','docked')

%for each species directory...
```

```
for a=1:specieslistsize
    treatdirectory=fullfile(directory,specieslist(a),'*.tdms'); %create the path
    treatlisting=dir(treatdirectory{1}); % list the files with the tdms extension
   % treatlisting=treatlisting(3:end); %remove .. and . directories
    treatlist={treatlisting.name}; %get the filenames
    [~,treatlistsize]=size(treatlist); %construct a list of the files

    fprintf('Starting step %s: Analysis of %s!\n',num2str(a),specieslist{a}); %Starting step 1: Analysis of BBRACH!

    %this was off in jasons code
    %raw_data(a).name=subjectlist{a};

    for b=1:treatlistsize  %for each file....

        %filedirectory=fullfile(directory,specieslist(a),treatlist(b),'*.tdms'); %create the path
        %filelisting=dir(filedirectory{1}); % list the files with the tdms extension
        %filelist={filelisting.name}; %get the filenames
        %[~,filelistsize]=size(filelist); %construct a list of the files

        %fprintf('  Step %s.%s: Analysis of %s %s started...\n',num2str(a),num2str(b),specieslist{a},treatlist{b});
%Step 1.1 Analysis: Analysis of BBRACH CRISPR

        %for c=1:filelistsize
            fprintf('   Step %s.%s: Analysis of %s started...\n',num2str(a),num2str(b), treatlist{b});  %Step 1.1.1
%Analyis of BBRACH CRISPR file1.tdms
            eodwave=[]; %initialize variables
            wavesize=[];
            neg_peakvoltages=[];
            neg_peak_idx=[];
            pos_peakvoltages=[];
            pos_peak_idx=[];
            pos_peak_idx_size=[];
            pos_peak_idxsize=[];
            min_index=[];
```

```
chunk=[];

eodstart=[];

eodend=[];

eod_start_idxs=[];

eod_end_idxs=[];



filename= fullfile(directory,specieslist(a),treatlist(b));   %construct the filename

eval(sprintf('%s_%s = TDMS_getStruct(filename{1});',specieslist{a},treatlist{b}));  %create a container based on the filename to save data to, and open the data

eval(sprintf('eodwave=%s_%s.Untitled.Dev1_ai0.data;',specieslist{a}, treatlist{b})); %put the data in a variable called eodwave

eval(sprintf('eodwaveinfo=%s_%s.Props;',specieslist{a}, treatlist{b})); %put the data in a variable called eodwave


j1=[1,-0.98];j2=[1,-1];

eodwave=filtfilt(j2,j1,eodwave);


%baseline=mean(eodwave(1:50));

%eodwave=eodwave-baseline;


recordlength=min(length(eodwave),1000000);

if recordlength < 1000000

   fprintf('   Step %s.%s: Analysis of %s aborted, less than 1000000 points in recording \n',num2str(a),num2str(b), treatlist{b});  %Step 1.1.1 %Analyis of BBRACH CRISPR file1.tdms

   continue


end

plot(eodwave(1:recordlength));

gcf;

figure(eodpreview);


commandwindow;

threshold=input(prompt);

%This was on in jasons code gain=input(prompt2);
```

```
eodwindowsize=2000; %this was the code for Jason instead of 2000
% which is 0.02*100,000: input(prompt3)*100000;
%t2=input(prompt4);




%valus of 3,000,000 is 30 seconds (30 * 100,000 samples per
%second)

[pos_peaks,pos_peak_idx]=findpeaks(eodwave(1:3000000),'MinPeakHeight',threshold,'MinPeakDistance',100);
%[neg_peaks,neg_peak_idx]=findpeaks(-
eodwave(1:3000000),'MinPeakHeight',threshold,'MinPeakDistance',100);



[~,pos_peak_idxsize]=size(pos_peak_idx);
pos_peak_idx=pos_peak_idx(2:(pos_peak_idxsize-1));
pos_peaks=pos_peaks(2:(pos_peak_idxsize-1));
[~,pos_peak_idx_size]=size(pos_peak_idx);

%[~,neg_peak_idxsize]=size(neg_peak_idx);
%neg_peak_idx=neg_peak_idx(2:(neg_peak_idxsize-1));
%neg_peaks=neg_peaks(2:(neg_peak_idxsize-1));
%[~,neg_peak_idx_size]=size(neg_peak_idx);
%neg_peaks=abs(neg_peaks);

%new code finds the negative peak nearby each positive
%peak.  use 0.02 seconds for eodwindowsize for b. brachyistius
neg_peaks=[];
neg_peak_idx=[];
for e=1:length(pos_peak_idx)
   [neg_peaks(e),local_idx]=min(eodwave((pos_peak_idx(e)-
eodwindowsize):(pos_peak_idx(e)+eodwindowsize)));
   neg_peak_idx(e)=local_idx+(pos_peak_idx(e)-eodwindowsize);
```

```
        end



        all_peaks=pos_peaks+abs(neg_peaks);

        all_peaks_mean=mean(all_peaks);
        all_peaks_std=std(all_peaks);

        treatment=treatlist(b);
        fishname=strcat('fish_',num2str(b));

        raw_data.species=specieslist(a);
        raw_data.treat=treatlist(b);
        raw_data.filename=treatlist(b);
        raw_data.fish_name=fishname;
        raw_data.amplitude=all_peaks_mean;
        raw_data.peaks=all_peaks;
        raw_data.amplitidue_std=all_peaks_std;
        raw_data.threshold=threshold;
        %This was on in jasons code: raw_data.gain=gain;
        %raw_data.t1=t1;
        %raw_data.t2=t2;


        final_data=[final_data; raw_data];
      %end

   end
end
fprintf('\nAll Analysis Complete!  Enjoy your data!\n');
clearvars -except final_data
```

```
bp_data=horzcat(final_data.peaks);
[numvars,~]=size(final_data);
grp=[];
for i=1:numvars
   [~,npeaks]=size(final_data(i).peaks);
   grp=[grp,ones(1,npeaks)*i];
end
boxplot(bp_data,grp)

 for i=1:length(final_data)
    writematrix(final_data(i).peaks',char(fullfile('C:/Users/Savvas
Constantinou/Desktop/Rawvoltages',strcat(final_data(i).filename,'_raw_voltages.csv'))))
 end
```

qPCR

```
#code for qPCR

#writing a script to analyze qPCR data

#install and load libraries and functions
install.packages("data.table")
install.packages("ggplot2")
install.packages("Hmisc")
library(data.table)
library(Hmisc)
library(ggplot2)



MakeDCQ <- function( MyData, AvgCq=AvgCq, Ref, GOI="GOI" ) {
  input <- MyData[ MyData$GeneID == GOI ,]
  DeltaCQ <- numeric( length=nrow( input ) )
  DeltaSD <- numeric( length=nrow( input ) )

  for( i in 1:nlevels( input$Sample )) {
```

```
   thissample <- levels( input$Sample )[i]
   thisGOI <- input$AvgCq[ input$Sample == thissample ]
   thisREF <- MyData$AvgCq[ MyData$GeneID == Ref & MyData$Sample == thissample ]
   GOISD <- input$SD[ input$Sample == thissample ]
   RefSD <- MyData$SD[ MyData$GeneID==Ref & MyData$Sample == thissample]
   DeltaCQ[i] <- thisGOI - thisREF
   DeltaSD[i] <- sqrt(GOISD^2+RefSD^2)
  }
 return( data.frame( cbind( input, DeltaCQ, DeltaSD ) ))
}

#upload data and check, #make sure to change file path for current analysis
qPCR<-read.csv("C:/Users/Savvas Constantinou/Downloads/sjc 3-3-17 EO, scn4aa Bact,
rps11.csv",stringsAsFactors=F)
head(qPCR)
unique(qPCR$Gene)
unique(qPCR$Sample)

#calculate average Cq and SD for each sample: make a dataframe to put it into
AvgCq = data.frame(Gene=character(0), GeneID=character(0), Sample=character(0), SampleID=character(0),
AvgCq=numeric(0), SD=numeric(0) )
for(i in unique(qPCR$Gene)) {
  currentGene = qPCR[qPCR$Gene==i,]
  for(j in unique(currentGene$Sample)) {
    currentSample = currentGene[currentGene$Sample==j,]
    AvgCq = rbind(AvgCq, data.frame(Gene=i, GeneID=unique(currentSample$GeneID), Sample=j,
SampleID=unique(currentSample$SampleID), AvgCq=mean(currentSample$Cq), SD=sd(currentSample$Cq)))
  }
}
print(AvgCq)
MyData=AvgCq

#calculate deltaCq values and delta SD
DCq1 <- MakeDCQ( AvgCq, AvgCq, "Ref1" )
```

```
DCq1
#can use below code if wanting the second Ref gene
#DCq1 <- MakeDCQ( AvgCq, AvgCq, "Ref2" )

#calculate DDCq.
#specify control DCq value
control <- DCq1[DCq1$SampleID=="control", 7]
#Calculate DDCq = DCq - DCq of control
DDCq<-DCq1$DeltaCQ - control
#add DDCq to data frame with gene, gene ID, sample, Sample ID
DDCq<-cbind(DCq1, DDCq)
#calculate Relative Quantity and add to dataframe
RelQuant<- 2^(-DDCq$DDCq)
DDCq<-cbind(DDCq, RelQuant)
#Calculate Upper Error and add to dataframe
UpperError <- (2^-(DDCq$DDCq-DDCq$DeltaSD))-DDCq$RelQuant
LowerError <- DDCq$RelQuant-(2^-(DDCq$DDCq+DDCq$DeltaSD))
DDCq<-cbind(DDCq, UpperError, LowerError)

#Set limits of error bars.
limits <- aes(ymax=DDCq$RelQuant + DDCq$UpperError,ymin=DDCq$RelQuant - DDCq$LowerError)

#the below code restructures the graph to put in a different order. Remove for other datasets
DDCq$Sample <-factor(DDCq$Sample, levels=c("MOC","MOL","MOH"))

#plot the data
p <- ggplot(data=DDCq, aes(x=Sample, y=RelQuant, fill=Sample))
p + geom_col(position=position_dodge()) +
  #change the size and color of text to make more legable (changed for poster, defaults may be good for papers)
  theme(title=element_text(size=20), axis.text = element_text(size=18,color="black"), axis.title =
element_text(size=18),
        legend.title = element_text(size=14),legend.text = element_text(size=14)) +
  #add errorbars
```

```
  geom_errorbar( aes(ymax=RelQuant + UpperError,ymin=RelQuant - LowerError), width=0.2,
position=position_dodge(0.9))+

  #add labels

  ggtitle(expression(paste("Relative Abundance of ", italic("scn4aa"), "(compared to B-actin) after MO treatment")))
+

  xlab("Fish") +

  ylab("Relative Expression") +

  #change title of legend

  scale_fill_hue(name="MO concentration

  (mg MO/kg fish)", # Legend label, use darker colors

            breaks=c("MOC", "MOL","MOH"),

            labels=c("Control MO; 20.0", "scn4aa SB; 12.5 (low)","scn4aa SB; 20.0 (high)"))


########################


analysis of ct differences-

#code for anova for delta ct differences for qPCR

dCt <- c(1.42496497, 0.85455584, 1.58148445, 3.46491474, 2.97499999, 3.77181974, 4.77462939, 5.15833434,
6.13886573)

individual <- as.factor(c("control", "control", "control", "MOL", "MOL", "MOL", "MOH", "MOH", "MOH"))

new <- data.frame(dCt, individual)


testing <- aov(dCt ~ individual, data = new)

summary(testing)

TukeyHSD(testing)
```

Toxicity&deaths

```
#chi square used to determine differences in behavor following MO injection and deaths

toxic <- c(17, 4, 2, 4, 0, 0)

ho <- chisq.test(toxic)

ho$expected

death <- c(4, 4, 1, 0, 0, 0)

hi <- chisq.test(death)

hi$expected
```

WORKS CITED

WORKS CITED

Ablain, J. *et al.* (2015) 'A CRISPR/Cas9 Vector System for Tissue-Specific Gene Disruption in Zebrafish', *Developmental Cell*, 32, pp. 756–764. doi: 10.1016/j.devcel.2015.01.032.

Adli, M. (2018) 'The CRISPR tool kit for genome editing and beyond.', *Nature communications*. Nature Publishing Group, 9(1911), pp. 1–13. doi: 10.1038/s41467-018-04252-2.

Alagia, A. and Eritja, R. (2016) 'siRNA and RNAi optimization', *Wiley Interdisciplinary Reviews: RNA*. Blackwell Publishing Ltd, 7(3), pp. 316–329. doi: 10.1002/wrna.1337.

Alshami, I. J. J. *et al.* (2020) 'Development of the electric organ in embryos and larvae of the knifefish, Brachyhypopomus gauderio', *Developmental Biology*. Elsevier Inc. doi: 10.1016/j.ydbio.2020.06.010.

Altschul, S. F. *et al.* (1997) 'Gapped BLAST and PSI-BLAST: A new generation of protein database search programs', *Nucleic Acids Research*. Oxford University Press, pp. 3389–3402. doi: 10.1093/nar/25.17.3389.

Alves-Gomes, J. A. (2001) 'The evolution of electroreception and bioelectrogenesis in teleost fish: A phylogenetic perspective', *Journal of Fish Biology*, 58(6), pp. 1489–1511. doi: 10.1006/jfbi.2001.1625.

Amanze, D. and Iyengar, A. (1990) 'The micropyle: A sperm guidance system in teleost fertilization', *Development*, 109(2), pp. 495–500.

Amsterdam, A., Varshney, G. K. and Burgess, S. M. (2011) 'Retroviral-mediated insertional mutagenesis in zebrafish', in *Methods in Cell Biology*. Academic Press Inc., pp. 59–82. doi: 10.1016/B978-0-12-374814-0.00004-5.

Andrews, O. E. *et al.* (2014) 'RNAi-mediated gene silencing in zebrafish triggered by convergent transcription', *Scientific Reports*. Nature Publishing Groups, 4(1), pp. 1–8. doi: 10.1038/srep05222.

Arnegard, M. E. *et al.* (2010) 'Old gene duplication facilitates origin and diversification of an innovative communication system--twice.', *Proceedings of the National Academy of Sciences of the United States of America*, 107(51), pp. 22172–22177. doi: 10.1073/pnas.1011803107.

Arnegard, M. E., Jackson, B. S. and Hopkins, C. D. (2006) 'Time-domain signal divergence and discrimination without receptor modification in sympatric morphs of electric fishes.', *The Journal of experimental biology*, 209(Pt 11), pp. 2182–2198.

Artegiani, B. *et al.* (2020) 'Fast and efficient generation of knock-in human organoids using homology-independent CRISPR–Cas9 precision genome editing', *Nature Cell Biology*. Nature

Research, 22(3), pp. 321–331. doi: 10.1038/s41556-020-0472-5.

Auer, T. O. *et al.* (2014) 'Highly efficient CRISPR/Cas9-mediated knock-in in zebrafish by homology-independent DNA repair', *Genome Research*, 24(1), pp. 142–153. doi: 10.1101/gr.161638.113.

Baillet-Derbin, C. (1978) 'Cytodifferentiation of regenerating electrocyte in an electric fish', *Biol. Cell*, 33, pp. 15–24.

Baker, C. V. H., Modrell, M. S. and Gillis, J. A. (2013) 'The evolution and development of vertebrate lateral line electroreceptors', *The Journal of experimental biology*, 216(13), pp. 2515–2522. doi: 10.1242/jeb.082362.

Ban, Y., Smith, B. E. and Markham, M. R. (2015) 'A highly polarized excitable cell separates sodium channels from sodium-activated potassium channels by more than a millimeter', *Journal of Neurophysiology*. American Physiological Society, 114(1), pp. 520–530. doi: 10.1152/jn.00475.2014.

Barrangou, R. and Doudna, J. A. (2016) 'Applications of CRISPR technologies in research and beyond', *Nature Biotechnology*, 34(9), pp. 933–941. doi: 10.1038/nbt.3659.

Bartlett, A. *et al.* (2017) 'Mapping genome-wide transcription-factor binding sites using DAP-seq', *Nature Protocols*. Nature Publishing Group, 12(8), pp. 1659–1672. doi: 10.1038/nprot.2017.055.

Bass, A. H. (1986) 'Electric organs revisited: evolution of a vertebrate communication and orientation system', in Bullock, T. H. and Heiligenberg, W. (eds) *Electroreception*. New York: Wiley, pp. 13–70.

Beirão, J. *et al.* (2019) 'Sperm handling in aquatic animals for artificial reproduction', *Theriogenology*. Elsevier Inc., 133, pp. 161–178. doi: 10.1016/j.theriogenology.2019.05.004.

Bell, C. C. *et al.* (1997) 'Synaptic plasticity in a cerebellum-like structure depends on temporal order', *Nature*, 387, pp. 278–281.

Benetta, E. D. *et al.* (2020) 'Pupal and adult injections for rnai and crispr gene editing in nasonia vitripennis', *Journal of Visualized Experiments*. Journal of Visualized Experiments, 2020(166), pp. 1–15. doi: 10.3791/61892.

Bengtson, D. A., Léger, P. and Sorgeloos, P. (1991) 'Use of Artemia As a Food Source for Aquaculture', in Browne, R. A., Sargeloos, P., and Trotman, C. N. A. (eds) *Artemia Biology*. Boca Raton, Florida: CRC Press Inc., pp. 255–286. doi: 10.1201/9781351069892-11.

Best, J. *et al.* (2010) 'A Novel Method for Rearing First-Feeding Larval Zebrafish: Polyculture with Type L Saltwater Rotifers (Brachionus plicatilis)', *Zebrafish*. Mary Ann Liebert, Inc. 140 Huguenot Street, 3rd Floor New Rochelle, NY 10801 USA , 7(3), pp. 289–295. doi:

10.1089/zeb.2010.0667.

Bi, H. and Yang, B. (2017) ‘Gene Editing With TALEN and CRISPR/Cas in Rice’, in *Progress in Molecular Biology and Translational Science*. Elsevier B.V., pp. 81–98. doi: 10.1016/bs.pmbts.2017.04.006.

Brinkman, E. K. *et al.* (2014) ‘Easy quantitative assessment of genome editing by sequence trace decomposition’, *Nucleic Acids Research*. Oxford University Press, 42(22), p. e168. doi: 10.1093/nar/gku936.

Brüggemann, J. (2012) ‘Nematodes as Live Food in Larviculture - A Review’, *Journal of the World Aquaculture Society*. John Wiley & Sons, Ltd, 43(6), pp. 739–763. doi: 10.1111/j.1749-7345.2012.00608.x.

Brusick, D. (1983) ‘MUTAGENICITY AND CARCINOGENICITY CORRELATIONS BETWEEN BACTERIA AND RODENTS’, *Annals of the New York Academy of Sciences*. John Wiley & Sons, Ltd, 407(1), pp. 164–176. doi: 10.1111/j.1749-6632.1983.tb47822.x.

Brzuska, E. (2021) ‘Reproduction effectiveness of carp (Cyprinus carpio L.) from the Hungarian W breeding line after stimulating ovulation with spawning inducing agents of natural (CPH, hCG, PMSG) and/or synthetic origin (Ovopel, Dagin, Ovaprim, mGnRH-a)’, *Aquaculture*. Elsevier B.V., 532, p. 736023. doi: 10.1016/j.aquaculture.2020.736023.

Burger, A. *et al.* (2016) ‘Maximizing mutagenesis with solubilized CRISPR-Cas9 ribonucleoprotein complexes’, *Development (Cambridge)*. Company of Biologists Ltd, 143(11), pp. 2025–2037. doi: 10.1242/dev.134809.

Capecchi, M. R. (2005) ‘Gene targeting in mice: Functional analysis of the mammalian genome for the twenty-first century’, *Nature Reviews Genetics*. Nature Publishing Group, pp. 507–512. doi: 10.1038/nrg1619.

Carlson, B. A. (2002) ‘Neuroanatomy of the mormyrid electromotor control system’, *Journal of Comparative Neurology*, 454(4), pp. 440–455. doi: 10.1002/cne.10462.

Carlson, B. A. (2009) *Encyclopedia of Neuroscience*. Edited by M. Binder et al. Springer.

Carlson, B. a and Gallant, J. R. (2013) ‘From sequence to spike to spark: evo-devo-neuroethology of electric communication in mormyrid fishes.’, *Journal of neurogenetics*, 27(3), pp. 106–29. doi: 10.3109/01677063.2013.799670.

Catania, K. C. (2019) ‘The Astonishing Behavior of Electric Eels’, *Frontiers in Integrative Neuroscience*. Frontiers Media S.A., 13, p. 23. doi: 10.3389/fnint.2019.00023.

Cejko, B. I. *et al.* (2018) ‘Multiple collections of common carp Cyprinus carpio L. semen during the reproductive period and its effects on sperm quality’, *Animal Reproduction Science*. Elsevier B.V., 188, pp. 178–188. doi: 10.1016/j.anireprosci.2017.12.002.

Char, S. N. *et al.* (2017) 'An Agrobacterium-delivered CRISPR/Cas9 system for high-frequency targeted mutagenesis in maize', *Plant Biotechnology Journal*. Blackwell Publishing Ltd, 15(2), pp. 257–268. doi: 10.1111/pbi.12611.

Chaverra-Rodriguez, D. *et al.* (2020) 'Germline mutagenesis of Nasonia vitripennis through ovarian delivery of CRISPR-Cas9 ribonucleoprotein', *Insect Molecular Biology*. Blackwell Publishing Ltd, 29(6), pp. 569–577. doi: 10.1111/imb.12663.

Chen, Z. *et al.* (2021) 'Neurodevelopmental and transcriptomic effects of CRISPR/Cas9-induced somatic orco mutation in honey bees.', *Journal of neurogenetics*. J Neurogenet, pp. 1–13. doi: 10.1080/01677063.2021.1887173.

Chilcoat, D., Liu, Z. Bin and Sander, J. (2017) 'Use of CRISPR/Cas9 for Crop Improvement in Maize and Soybean', in *Progress in Molecular Biology and Translational Science*. Elsevier B.V., pp. 27–46. doi: 10.1016/bs.pmbts.2017.04.005.

Colbert, T. *et al.* (2001) 'High-throughput screening for induced point mutations', *Plant Physiology*. Plant Physiol, 126(2), pp. 480–484. doi: 10.1104/pp.126.2.480.

Concordet, J. P. and Haeussler, M. (2018) 'CRISPOR: Intuitive guide selection for CRISPR/Cas9 genome editing experiments and screens', *Nucleic Acids Research*. Oxford University Press, 46(W1), pp. W242–W245. doi: 10.1093/nar/gky354.

Constantinou, S. J. *et al.* (2019) 'Silencing the Spark : CRISPR / Cas9 Genome Editing in Weakly Electric Fish', *Journal of visualized experiments*, 152(October), pp. 1–16. doi: 10.3791/60253.

Cooley, L., Kelley, R. and Spradling, A. (1988) 'Insertional mutagenesis of the Drosophila genome with single P elements', *Science*. American Association for the Advancement of Science, 239(4844), pp. 1121–1128. doi: 10.1126/science.2830671.

Crampton, W. G. R. (1998) 'Effects of anoxia on the distribution, respiratory strategies and electric signal diversity of gymnotiform fishes', *Journal of Fish Biology*. Academic Press, 53(sA), pp. 307–330. doi: 10.1111/j.1095-8649.1998.tb01034.x.

Crampton, W. G. R. (2019) 'Electroreception, electrogenesis and electric signal evolution', *Journal of Fish Biology*. Blackwell Publishing Ltd, 95(1), pp. 92–134. doi: 10.1111/jfb.13922.

Crebelli, R. *et al.* (1986) 'A comparative study on selected chemical carcinogens for chromosome malsegregation, mitotic crossing-over and forward mutation induction in Aspergillus nidulans', *Mutation Research/Genetic Toxicology*. Elsevier, 172(2), pp. 139–149. doi: 10.1016/0165-1218(86)90070-4.

Crispo, M. *et al.* (2015) 'Efficient generation of myostatin knock-out sheep using CRISPR/Cas9 technology and microinjection into zygotes', *PLoS ONE*. Public Library of Science, 10(8). doi: 10.1371/journal.pone.0136690.

Cuellar, H., Kim, J. A. and Unguez, G. A. (2006) ‘Evidence of post-transcriptional regulation in the maintenance of a partial muscle phenotype by electrogenic cells of S. macrurus.’, *The FASEB journal : official publication of the Federation of American Societies for Experimental Biology*, 20, pp. E1856–E1865. doi: 10.1096/fj.06-6474fje.

Curtis, C. C. and Stoddard, P. K. (2003) ‘Mate preference in female electric fish, Brachyhypopomus pinnicaudatus’, *Animal Behaviour*. Academic Press, 66(2), pp. 329–336. doi: 10.1006/ANBE.2003.2216.

Davies, L. and Ratcliffe, G. G. (1994) ‘Development rates of some pre-adult stages in blowflies with reference to low temperatures’, *Medical and Veterinary Entomology*, 8(3), pp. 245–254. doi: 10.1111/j.1365-2915.1994.tb00506.x.

Değirmenci, L. *et al.* (2020) ‘CRISPR/Cas9 mediated mutations as a new tool for studying taste in honeybees’, *bioRxiv*. Cold Spring Harbor Laboratory, p. 2020.03.26.009696. doi: 10.1101/2020.03.26.009696.

Denizot, J. P. *et al.* (1978) ‘The larval electric organ of the weakly electric fish Pollimyrus (Marcusenius) isidori (Mormyridae, Teleostei)’, *Journal of Neurocytology*, 7(2), pp. 165–181.

Dhont, J. *et al.* (2013) ‘Rotifers, Artemia and copepods as live feeds for fish larvae in aquaculture’, in Allan, G. and Burnell, G. (eds) *Advances in Aquaculture Hatchery Technology*. Woodhead Publishing Limited, pp. 157–202. doi: 10.1533/9780857097460.1.157.

Dietrich, M. R. *et al.* (2020) ‘How to choose your research organism’, *Studies in History and Philosophy of Science Part C :Studies in History and Philosophy of Biological and Biomedical Sciences*. Elsevier Ltd, 80, p. 101227. doi: 10.1016/j.shpsc.2019.101227.

DiMaggio, M. A., Broach, J. S. and Ohs, C. L. (2013) ‘Evaluation of Ovaprim and human chorionic gonadotropin doses on spawning induction and egg and larval quality of pinfish, Lagodon rhomboides’, *Aquaculture*. Elsevier, 414–415, pp. 9–18. doi: 10.1016/j.aquaculture.2013.07.012.

Diogo, P. *et al.* (2019) ‘Selection Criteria of Zebrafish Male Donors for Sperm Cryopreservation’, *Zebrafish*. Mary Ann Liebert Inc., 16(2), pp. 189–196. doi: 10.1089/zeb.2018.1660.

Doench, J. G. *et al.* (2014) ‘Rational design of highly active sgRNAs for CRISPR-Cas9-mediated gene inactivation’, *Nature Biotechnology*. Nature Publishing Group, 32(12), pp. 1262–1267. doi: 10.1038/nbt.3026.

Doitsidou, M. *et al.* (2010) ‘C. elegans Mutant Identification with a One-Step Whole-Genome-Sequencing and SNP Mapping Strategy’, *PLoS ONE*. Public Library of Science, 5(11), p. 15435. doi: 10.1371/JOURNAL.PONE.0015435.

Draper, B. W., Morcos, P. A. and Kimmel, C. B. (2001) ‘Inhibition of zebrafish fgf8 pre-mRNA

splicing with morpholino oligos: A quantifiable method for gene knockdown', *Genesis*. Genesis, 30(3), pp. 154–156. doi: 10.1002/gene.1053.

Dulka, J. G. and Maler, L. (1994) 'Testosterone modulates female chirping behavior in the weakly electric fish, Apteronotus leptorhynchus', *Journal of Comparative Physiology A*, 174(3), pp. 331–343. doi: 10.1007/BF00240215.

Duverger, Y. *et al.* (2007) 'A semi-automated high-throughput approach to the generation of transposon insertion mutants in the nematode Caenorhabditis elegans', *Nucleic Acids Research*. Oxford University Press, 35(2), p. e11. doi: 10.1093/nar/gkl1046.

Edgley, M. *et al.* (2002) 'Improved detection of small deletions in complex pools of DNA', *Nucleic acids research*. Oxford University Press, 30(12), p. e52. doi: 10.1093/nar/gnf051.

Eisen, J. S. and Smith, J. C. (2008) 'Controlling morpholino experiments: Don't stop making antisense', *Development*. The Company of Biologists Ltd, pp. 1735–1743. doi: 10.1242/dev.001115.

von der Emde, G. (1999) 'Active Electrolocation of Objects in Weakly Electric Fish', *The Journal of experimental biology*, 202, pp. 1205–15.

von der Emde, G. and Fetz, S. (2007) 'Distance, shape and more: recognition of object features during active electrolocation in a weakly electric fish.', *The Journal of experimental biology*, 210(Pt 17), pp. 3082–95. doi: 10.1242/jeb.005694.

Farhat, S. *et al.* (2019) 'CRISPR-Cas9 directed genome engineering for enhancing salt stress tolerance in rice', *Seminars in Cell and Developmental Biology*. Elsevier Ltd, pp. 91–99. doi: 10.1016/j.semcdb.2019.05.003.

Farnworth, M. S. *et al.* (2020) 'The Red Flour Beetle as Model for Comparative Neural Development: Genome Editing to Mark Neural Cells in Tribolium Brain Development', in *Methods in Molecular Biology*. Humana Press Inc., pp. 191–217. doi: 10.1007/978-1-4939-9732-9_11.

Fauser, F., Schiml, S. and Puchta, H. (2014) 'Both CRISPR/Cas-based nucleases and nickases can be used efficiently for genome engineering in Arabidopsis thaliana', *Plant Journal*. Blackwell Publishing Ltd, 79(2), pp. 348–359. doi: 10.1111/tpj.12554.

Favreau, E. *et al.* (2018) 'Genes and genomic processes underpinning the social lives of ants', *Current Opinion in Insect Science*. Elsevier Inc., pp. 83–90. doi: 10.1016/j.cois.2017.12.001.

Fay, R. R. *et al.* (2005) *Electroreception*. New York: Springer.

Ferguson, D. P., Dangott, L. J. and Lightfoot, T. J. (2014) 'Lessons learned from vivo-morpholinos: How to avoid vivo-morpholino toxicity', *BioTechniques*, 56(5), pp. 251–256. doi: 10.2144/000114167.

Ferguson, D. P., Schmitt, E. E. and Lightfoot, J. T. (2013) 'Vivo-Morpholinos Induced Transient Knockdown of Physical Activity Related Proteins', *PLoS ONE*, 8(4). doi: 10.1371/journal.pone.0061472.

Ferrari, M. B. and Zakon, H. H. (1993) *Conductances contributing to the action potential of Sternopygus electrocytes, J Comp Physiol A.*

Ferrarla, M. B., Mcanelly, M. L. and Zakon, H. H. (1995) *Individual Variation in and Androgen-Modulation of the Sodium Current in Electric Organ, The Journal of Neuroscience*.

Fire, A. *et al.* (1998) 'Potent and specific genetic interference by double-stranded RNA in caenorhabditis elegans', *Nature*. Nature Publishing Group, 391(6669), pp. 806–811. doi: 10.1038/35888.

Franchina, C. R. (1997) 'Ontogeny of the electric organ discharge and the electric organ in the weakly electric pulse fish Brachyhypopomus pinnicaudatus (Hypopomidae, Gymnotiformes)', *Journal of Comparative Physiology - A Sensory, Neural, and Behavioral Physiology*, 181(2), pp. 111–119. doi: 10.1007/s003590050098.

Friedman, D. A., Gordon, D. M. and Luo, L. (2017) 'The MutAnts Are Here', *Cell*. Cell Press, pp. 601–602. doi: 10.1016/j.cell.2017.07.046.

Fritz, J. H., Girardin, S. E. and Philpott, D. J. (2006) 'Innate immune defense through RNA interference.', *Science's STKE : signal transduction knowledge environment*, 2006(339). doi: 10.1126/stke.3392006pe27.

Futuyma, D. J. (2013) *Evolution*. Sinauer Associates Incorporated.

Gagnon, J. a. *et al.* (2014) 'Efficient mutagenesis by Cas9 protein-mediated oligonucleotide insertion and large-scale assessment of single-guide RNAs', *PLoS ONE*, 9(5), pp. 1–8. doi: 10.1371/journal.pone.0098186.

Gallant, J. R. *et al.* (2014) 'Genomic basis for the convergent evolution of electric organs', *Science*, 344(6191), pp. 1522–1525.

Gallant, J. R. *et al.* (2017) 'The genome and adult somatic transcriptome of the mormyrid electric fish paramormyrops kingsleyae', *Genome Biology and Evolution*. Oxford University Press, 9(12), pp. 3525–3530. doi: 10.1093/gbe/evx265.

Gallant, J. R. (2019) 'The Evolution and Development of Electric Organs', in Carlson B., Sisneros J., Popper A., F. R. (ed.) *Electroreception: Fundamental Insights from Comparative Approaches*. Springer, Cham, pp. 91–123. doi: 10.1007/978-3-030-29105-1_4.

Gallant, J. R. and O'Connell, L. A. (2020) 'Studying convergent evolution to relate genotype to behavioral phenotype', *Journal of Experimental Biology*. Company of Biologists Ltd. doi: 10.1242/jeb.213447.

Gavassa, S. and Stoddard, P. K. (2012) ‘Food restriction promotes signaling effort in response to social challenge in a short-lived electric fish’, *Hormones and Behavior*. Academic Press, 62(4), pp. 381–388. doi: 10.1016/j.yhbeh.2012.07.003.

Gebski, B. L. *et al.* (2003) ‘Morpholino antisense oligonucleotide induced dystrophin exon 23 skipping in mdx mouse muscle’, *Human Molecular Genetics*. Hum Mol Genet, 12(15), pp. 1801–1811. doi: 10.1093/hmg/ddg196.

Gilbert, L. A. *et al.* (2013) ‘CRISPR-mediated modular RNA-guided regulation of transcription in eukaryotes’, *Cell*. Elsevier B.V., 154(2), p. 442. doi: 10.1016/j.cell.2013.06.044.

Gilles, A. F., Schinko, J. B. and Averof, M. (2015) ‘Efficient CRISPR-mediated gene targeting and transgene replacement in the beetle Tribolium castaneum’, *Development (Cambridge)*. Company of Biologists Ltd, 142(16), pp. 2832–2839. doi: 10.1242/dev.125054.

Goldstein, B. and King, N. (2016) ‘The Future of Cell Biology: Emerging Model Organisms’, *Trends in Cell Biology*. Elsevier Ltd, pp. 818–824. doi: 10.1016/j.tcb.2016.08.005.

Gottwald, M. *et al.* (2018) ‘Electric-Color Sensing in Weakly Electric Fish Suggests Color Perception as a Sensory Concept beyond Vision’, *Current biology : CB*, 28(22), pp. 3648–3653. doi: 10.1016/j.cub.2018.09.036.

Granger, L., Martin, E. and Ségalat, L. (2004) ‘Mos as a tool for genome-wide insertional mutagenesis in Caenorhabditis elegans: results of a pilot study.’, *Nucleic acids research*. Oxford University Press, 32(14), p. e117. doi: 10.1093/nar/gnh111.

Gregory, T. R. (2008) ‘The Evolution of Complex Organs’, *Evolution: Education and Outreach*. Springer US, 1(4), pp. 358–389. doi: 10.1007/s12052-008-0076-1.

Grimes, A. C. and Kirby, M. L. (2009) ‘The outflow tract of the heart in fishes: anatomy, genes and evolution’, *Journal of Fish Biology*. John Wiley & Sons, Ltd (10.1111), 74(5), pp. 983–1036. doi: 10.1111/j.1095-8649.2008.02125.x.

Gui, S. *et al.* (2020) ‘First report on CRISPR/Cas9-targeted mutagenesis in the Colorado potato beetle, Leptinotarsa decemlineata’, *Journal of Insect Physiology*. Elsevier Ltd, 121. doi: 10.1016/j.jinsphys.2020.104013.

Guilinger, J. P., Thompson, D. B. and Liu, D. R. (2014) ‘Fusion of catalytically inactive Cas9 to FokI nuclease improves the specificity of genome modification’, *Nature Biotechnology*. Nature Publishing Group, 32(6), pp. 577–582. doi: 10.1038/nbt.2909.

Haeussler, M. *et al.* (2016) ‘Evaluation of off-target and on-target scoring algorithms and integration into the guide RNA selection tool CRISPOR’, *Genome Biology*. BioMed Central Ltd., 17(1), p. 148. doi: 10.1186/s13059-016-1012-2.

Hagedorn, M. and Carter, V. L. (2011) ‘Zebrafish reproduction: Revisiting in vitro fertilization

to increase sperm cryopreservation success', *PLoS ONE*. Public Library of Science, 6(6). doi: 10.1371/journal.pone.0021059.

Hammouda, O. T. *et al.* (2019) 'Swift Large-scale Examination of Directed Genome Editing', *PLOS ONE*. Edited by S. C. F. Neuhauss. Public Library of Science, 14(3), p. e0213317. doi: 10.1371/journal.pone.0213317.

Hardy, S. *et al.* (2010) 'Reverse genetics in eukaryotes', *Biology of the Cell*. Wiley-Blackwell, 102(10), pp. 561–580. doi: 10.1042/bc20100038.

Hashimoto, M. and Takemoto, T. (2015) 'Electroporation enables the efficient mRNA delivery into the mouse zygotes and facilitates CRISPR/Cas9-based genome editing', *Scientific Reports*. Nature Publishing Group, 5(May), p. 11315. doi: 10.1038/srep11315.

Heiligenberg, W. (1991) *Neural Nets in Electric Fish*. Cambridge: MIT Press.

Hendel, A. *et al.* (2015) 'Quantifying on- and off-target genome editing', *Trends in Biotechnology*. Elsevier Ltd, pp. 132–140. doi: 10.1016/j.tibtech.2014.12.001.

Hilton, I. B. *et al.* (2015) 'Epigenome editing by a CRISPR-Cas9-based acetyltransferase activates genes from promoters and enhancers', *Nature Biotechnology*. Nature Publishing Group, 33(5), pp. 510–517. doi: 10.1038/nbt.3199.

Hopkins, C. D. (1974) 'Electric communication: functions in the social behavior of Eigenmannia virescens', *BEHAVIOUR*. Brill, 50(3–4), pp. 270–305. doi: 10.1163/156853974x00499.

Hopkins, C. D. (1988) 'Neuroethology of electric communication.', *Annual review of neuroscience*, 11(1), pp. 497–535. doi: 10.1146/annurev.ne.11.030188.002433.

Hopkins, Carl D (1999) 'Design features for electric communication', *Journal of Experimental Biology*. Co Biol, 202(10), pp. 1217–1228.

Hopkins, C D (1999) 'Signal evolution in electric communication', in Hauser, M. and Konishi, M. (eds) *The Design of Animal Communication*. Cambridge: M.I.T. Press, pp. 461–491. Available at: http://www.nbb.cornell.edu/neurobio/hopkins/Reprints/Ch16.pdf.

Hopkins, C. D. and Bass, A. H. (1981) 'Temporal coding of species recognition signals in an electric fish', *Science*. AAAS, 212(4490), pp. 85–87. doi: 10.1126/science.7209524.

Horvath, P. and Barrangou, R. (2010) 'CRISPR/Cas, the Immune System of Bacteria and Archaea', *Science*, 327(5962), pp. 167–170. doi: 10.1126/science.1179555.

Hoshijima, K. *et al.* (2019) 'Highly Efficient CRISPR-Cas9-Based Methods for Generating Deletion Mutations and F0 Embryos that Lack Gene Function in Zebrafish', *Developmental Cell*. Cell Press, 51(5), pp. 645-657.e4. doi: 10.1016/j.devcel.2019.10.004.

Hua, Y. *et al.* (2017) 'A simple and efficient method for CRISPR/Cas9-induced mutant screening', *Journal of Genetics and Genomics*. Institute of Genetics and Developmental Biology, 44(4), pp. 207–213. doi: 10.1016/j.jgg.2017.03.005.

Hwang, W. Y. *et al.* (2013) 'Heritable and Precise Zebrafish Genome Editing Using a CRISPR-Cas System', *PLoS ONE*, 8(7), pp. 1–9. doi: 10.1371/journal.pone.0068708.

Hyde, D. R., Godwin, A. R. and Thummel, R. (2012) 'In vivo electroporation of morpholinos into the regenerating adult zebrafish tail fin.', *Journal of visualized experiments : JoVE*. MyJoVE Corporation, 61(61), p. 3632. doi: 10.3791/3632.

Iovine, M. K. and Johnson, S. L. (2000) 'Genetic analysis of isometric growth control mechanisms in the zebrafish caudal fin', *Genetics*, 155(3), pp. 1321–1329. doi: 10.1093/genetics/155.3.1321.

Irion, U., Krauss, J. and Nusslein-Volhard, C. (2014) 'Precise and efficient genome editing in zebrafish using the CRISPR/Cas9 system', *Development*, 141(24), pp. 4827–4830. doi: 10.1242/dev.115584.

Iwama, G. K., McGreer, J. C. and Pawluk, M. P. (1989) 'The effects of five fish anaesthetics on acid-base balance, hematocrit, blood gases, cortisol, and adrenaline in rainbow trout', *Candian Journal of Zoology*, 67(8), pp. 2065–2073. doi: 10.1016/j.paid.2011.03.037.

Jacot, D. and Soldati-Favre, D. (2020) 'CRISPR/Cas9-Mediated Generation of Tetracycline Repressor-Based Inducible Knockdown in Toxoplasma gondii', in *Methods in Molecular Biology*. Humana Press Inc., pp. 125–141. doi: 10.1007/978-1-4939-9857-9_7.

Jansen, G. *et al.* (1997) 'Reverse genetics by chemical mutagenesis in Caenorhabditis elegans', *Nature Genetics*. Nat Genet, 17(1), pp. 119–121. doi: 10.1038/ng0997-119.

Jao, L.-E., Wente, S. R. and Chen, W. (2013) 'Efficient multiplex biallelic zebrafish genome editing using a CRISPR nuclease system.', *Proceedings of the National Academy of Sciences of the United States of America*, 110(34), pp. 13904–9. doi: 10.1073/pnas.1308335110.

Jinek, M. *et al.* (2012) 'A programmable dual-RNA-guided DNA endonuclease in adaptive bacterial immunity.', *Science (New York, N.Y.)*. Howard Hughes Medical Institute, 337(6096), pp. 816–21. doi: 10.1126/science.1225829.

Jones, M. R. *et al.* (2007) 'Oligonucleotide Array Comparative Genomic Hybridization (oaCGH) based characterization of genetic deficiencies as an aid to gene mapping in Caenorhabditis elegans', *BMC Genomics 2007 8:1*. BioMed Central, 8(1), pp. 1–10. doi: 10.1186/1471-2164-8-402.

Jung, C. J. *et al.* (2017) 'Efficient gene targeting in mouse zygotes mediated by CRISPR/Cas9-protein', *Transgenic Research*. Springer, 26(2), pp. 263–277. doi: 10.1007/s11248-016-9998-5.

Katz, L., Baltz, R. and Baltz, R. H. (2016) 'Natural product discovery: past, present, and future', *Article in Journal of Industrial Microbiology*, 43, pp. 155–176. doi: 10.1007/s10295-015-1723-5.

Kawasaki, M. (1997) 'Sensory hyperacuity in the jamming avoidance response of weakly electric fish', *Current Opinion in Neurobiology*. Elsevier Ltd, 7(4), pp. 473–479. doi: 10.1016/S0959-4388(97)80025-6.

Kawasaki, M. (2009) 'Evolution of Time-Coding Systems in Weakly Electric Fishes', *Zoological Science*. Zoological Society of Japan, 26(9), pp. 587–599. doi: 10.2108/zsj.26.587.

Khan, M. H. U. *et al.* (2018) 'Induced mutation and epigenetics modification in plants for crop improvement by targeting CRISPR/Cas9 technology', *Journal of Cellular Physiology*. John Wiley & Sons, Ltd, 233(6), pp. 4578–4594. doi: 10.1002/jcp.26299.

Kim, D., Alptekin, B. and Budak, H. (2018) 'CRISPR/Cas9 genome editing in wheat', *Functional and Integrative Genomics*. Springer Verlag, 18(1), pp. 31–41. doi: 10.1007/s10142-017-0572-x.

Kim, H. *et al.* (2018) 'Mouse Cre-LoxP system: general principles to determine tissue-specific roles of target genes Cre-loxP System', *Lab Anim Res*, 34(4), pp. 147–159. doi: 10.5625/lar.2018.34.4.147.

Kim, J. H. *et al.* (2011) 'High Cleavage Efficiency of a 2A Peptide Derived from Porcine Teschovirus-1 in Human Cell Lines, Zebrafish and Mice', *Zebrafish and Mice. PLoS ONE*, 6(4), pp. 18556–70204. doi: 10.1371/journal.pone.0018556.

Kim, V. N., Han, J. and Siomi, M. C. (2009) 'Biogenesis of small RNAs in animals', *Nature Reviews Molecular Cell Biology*. Nature Publishing Group, pp. 126–139. doi: 10.1038/nrm2632.

Kirschbaum, F. (1975) 'Environmental factors control the periodical reproduction of tropical electric fish', *Experientia*. Birkhäuser-Verlag, 31(10), pp. 1159–1160.

Kirschbaum, F. (1977) 'Electric-Organ ontogeny: Distinct Larval organ precedes the Adult organ in weakly electric fish', *Naturwissenschaften*, 64(7), pp. 387–388.

Kirschbaum, F. (1983) 'Myogenic electric organ precedes the neurogenic organ in apteronotid fish', *Naturwissenschaften*, 70(4), pp. 205–207.

Kirschbaum, F. (1987) 'Reproduction and development of the weakly electric fish, Pollimyrus isidori (Mormyridae, Teleostei) in captivity', *Environmental Biology Of Fishes*, 20(1), pp. 11–31.

Kirschbaum, F. *et al.* (2016) 'Intragenus (Campylomormyrus) and intergenus hybrids in mormyrid fish: Physiological and histological investigations of the electric organ ontogeny', *Journal of Physiology Paris*. Elsevier Ltd, 110(3), pp. 281–301. doi: 10.1016/j.jphysparis.2017.01.003.

Kirschbaum, F. and Denizot, J. P. (2011) *Detection and generation of electric signals | Development of Electroreceptors and Electric Organs*, *Encyclopedia of Fish Physiology*. Elsevier Inc. doi: 10.1016/B978-0-12-374553-8.00132-5.

Kirschbaum, F. and Schugardt, C. (2002) 'Reproductive strategies and developmental aspects in mormyrid and gymnotiform fishes', *Journal of Physiology Paris*, 96(5–6), pp. 557–566. doi: 10.1016/S0928-4257(03)00011-1.

Kirschbaum, F. and Schwassmann, H. O. (2008) 'Ontogeny and evolution of electric organs in gymnotiform fish', *Journal of Physiology Paris*. Elsevier Ltd, 102(4–6), pp. 347–356. doi: 10.1016/j.jphysparis.2008.10.008.

Kirschbaum, F. and Westby, G. W. M. (1975) 'Development of the electric discharge in mormyrid and gymnotid fish (Marcusenius sp. and Eigenmannia virescens)', *Experientia*, 31(11), pp. 1290–1294.

Kok, F. O. *et al.* (2015) 'Reverse Genetic Screening Reveals Poor Correlation between Morpholino-Induced and Mutant Phenotypes in Zebrafish', *Developmental Cell*. Cell Press, 32(1), pp. 97–108. doi: 10.1016/J.DEVCEL.2014.11.018.

Kolesnik, N. *et al.* (2019) 'The cultivation of the nematodes Panagrellus, Turbatrix (Anguillula) and Rhabditis for using in fish feeding', *Ribogospodars'ka nauka Ukraïni.*, (3(49)), pp. 16–31. doi: 10.15407/fsu2019.02.016.

Kotb, A. M. *et al.* (2016) 'Knockdown of ApoL1 in Zebrafish Larvae Affects the Glomerular Filtration Barrier and the Expression of Nephrin', *PLOS ONE*. Edited by C. Chatziantoniou. Public Library of Science, 11(5), p. e0153768. doi: 10.1371/journal.pone.0153768.

Kroll, F. *et al.* (2021) 'A simple and effective f0 knockout method for rapid screening of behaviour and other complex phenotypes', *eLife*. eLife Sciences Publications Ltd, 10, pp. 1–34. doi: 10.7554/eLife.59683.

Kutscher, L. M. and Shaham, S. (2014) 'Forward and reverse mutagenesis in C. elegans', *WormBook : the online review of C. elegans biology*. NIH Public Access, pp. 1–26. doi: 10.1895/wormbook.1.167.1.

Lamanna, F. *et al.* (2015) 'Cross-tissue and cross-species analysis of gene expression in skeletal muscle and electric organ of African weakly-electric fish (Teleostei; Mormyridae)', *BMC Genomics*. BioMed Central, 16(668), pp. 1–17. doi: 10.1186/s12864-015-1858-9.

Lamanna, F., Kirschbaum, F. and Tiedemann, R. (2014) 'De novo assembly and characterization of the skeletal muscle and electric organ transcriptomes of the African weakly electric fish Campylomormyrus compressirostris (Mormyridae, Teleostei)', *Molecular Ecology Resources*. Blackwell Publishing Ltd, 14(6), pp. 1222–1230. doi: 10.1111/1755-0998.12260.

Lawrence, C. *et al.* (2016) 'The complete and updated "rotifer polyculture method" for rearing first feeding zebrafish', *Journal of Visualized Experiments*. Journal of Visualized Experiments, 2016(107), p. e53629. doi: 10.3791/53629.

Lee, R. C., Feinbaum, R. L. and Ambrost, V. (1993) *The C. elegans Heterochronic Gene lin-4 Encodes Small RNAs with Antisense Complementarity to &II-14*, *Cell*.

Lewis, J. E. *et al.* (2014) 'Action potential energetics at the organismal level reveal a trade-off in efficiency at high firing rates', *Journal of Neuroscience*. Society for Neuroscience, 34(1), pp. 197–201. doi: 10.1523/JNEUROSCI.3180-13.2014.

Li, D. *et al.* (2013) 'Heritable gene targeting in the mouse and rat using a CRISPR-Cas system', *Nature Biotechnology*. Nature Publishing Group, pp. 681–683. doi: 10.1038/nbt.2661.

Li, K. *et al.* (2014) 'Optimization of Genome Engineering Approaches with the CRISPR/Cas9 System', *PLoS ONE*. Edited by K. Yu. Public Library of Science, 9(8), p. e105779. doi: 10.1371/journal.pone.0105779.

Li, Y. *et al.* (2013) 'RNA interference functions as an antiviral immunity mechanism in mammals', *Science*, 342(6155), pp. 231–234. doi: 10.1126/science.1241911.

Liang, X. *et al.* (2015) 'Rapid and highly efficient mammalian cell engineering via Cas9 protein transfection', *Journal of Biotechnology*. Elsevier, 208, pp. 44–53. doi: 10.1016/J.JBIOTEC.2015.04.024.

Lissmann, H. W. (1951) 'Continuous electrical signals from the tail of a fish, gymnarchus niloticus Cuv', *Nature*. Nature Publishing Group, 167(4240), pp. 201–202. doi: 10.1038/167201a0.

Liu, J. *et al.* (2019) 'Genome editing in soybean with CRISPR/Cas9', in *Methods in Molecular Biology*. Humana Press Inc., pp. 217–234. doi: 10.1007/978-1-4939-8991-1_16.

Liu, K. *et al.* (2019) 'Expanding the CRISPR Toolbox in Zebrafish for Studying Development and Disease', *Frontiers in Cell and Developmental Biology*. Frontiers, 7(13), pp. 1–15. doi: 10.3389/fcell.2019.00013.

Liu, M. *et al.* (2018) 'Methodologies for Improving HDR Efficiency.', *Frontiers in genetics*. Frontiers Media SA, 9(691), pp. 1–9. doi: 10.3389/fgene.2018.00691.

Livak, K. J. and Schmittgen, T. D. (2001) 'Analysis of relative gene expression data using real-time quantitative PCR and the 2(-Delta Delta C(T)) Method.', *Methods (San Diego, Calif.)*, 25(4), pp. 402–8. doi: 10.1006/meth.2001.1262.

Lu-Nguyen, N. *et al.* (2021) 'Systemic antisense therapeutics inhibiting DUX4 expression improves muscle function in an FSHD mouse model', *bioRxiv*. Cold Spring Harbor Laboratory, p. 2021.01.14.426659. doi: 10.1101/2021.01.14.426659.

Lu, Y. *et al.* (2020) 'Safety and feasibility of CRISPR-edited T cells in patients with refractory non-small-cell lung cancer', *Nature Medicine*. Nature Research, 26(5), pp. 732–740. doi: 10.1038/s41591-020-0840-5.

Macesic, L. J. and Kajiura, S. M. (2009) 'Electric organ morphology and function in the lesser electric ray, Narcine brasiliensis', *Zoology*. Urban & Fischer, 112(6), pp. 442–450. doi: 10.1016/j.zool.2009.02.002.

Marchetti, G. *et al.* (2012) 'Functional genetics', *Thrombosis Research*. Pergamon, pp. 336–340. doi: 10.1016/j.thromres.2011.10.028.

Markert, M. J. *et al.* (2016) 'Genomic access to monarch migration using TALEN and CRISPR/Cas9-mediated targeted mutagenesis', *G3: Genes, Genomes, Genetics*, 6(4), pp. 905–915. doi: 10.1534/g3.116.027029.

Markham, M. R. *et al.* (2009) 'Circadian and Social Cues Regulate Ion Channel Trafficking', *PLoS biology*, 7(9), p. e1000203.

Markham, M. R. (2013) 'Electrocyte physiology: 50 years later', *Journal of Experimental Biology*, 216(13), pp. 2451–2458. doi: 10.1242/jeb.082628.

Markham, M. R., Kaczmarek, L. K. and Zakon, H. H. (2013) 'A sodium-activated potassium channel supports high-frequency firing and reduces energetic costs during rapid modulations of action potential amplitude', *Journal of Neurophysiology*. American Physiological Society, 109(7), pp. 1713–1723. doi: 10.1152/jn.00875.2012.

Martín, B. *et al.* (2009) 'A high-density collection of EMS-induced mutations for TILLING in Landsberg erecta genetic background of Arabidopsis', *BMC Plant Biology*. BioMed Central, 9(1), pp. 1–9. doi: 10.1186/1471-2229-9-147.

Mate, S. E., Brown, K. J. and Hoffman, E. P. (2011) 'Integrated genomics and proteomics of the Torpedo californica electric organ: concordance with the mammalian neuromuscular junction', *Skeletal Muscle*. BioMed Central, 1(20), pp. 1–17. doi: 10.1186/2044-5040-1-20.

Matsuda, H. and Shi, Y.-B. (2010) 'An Essential and Evolutionarily Conserved Role of Protein Arginine Methyltransferase 1 for Adult Intestinal Stem Cells During Postembryonic Development', *STEM CELLS*. John Wiley & Sons, Ltd, 28(11), pp. 2073–2083. doi: 10.1002/stem.529.

Matsuoka, Y. and Monteiro, A. (2018) 'Melanin Pathway Genes Regulate Color and Morphology of Butterfly Wing Scales', *Cell Reports*. Elsevier B.V., 24(1), pp. 56–65. doi: 10.1016/j.celrep.2018.05.092.

Matthews, J. L. *et al.* (2018) 'Changes to extender, cryoprotective medium, and in vitro fertilization improve zebrafish sperm cryopreservation', *Zebrafish*. Mary Ann Liebert Inc., 15(3), pp. 279–290. doi: 10.1089/zeb.2017.1521.

Maydan, J. S. *et al.* (2009) 'De Novo Identification of Single Nucleotide Mutations in Caenorhabditis elegans Using Array Comparative Genomic Hybridization', *Genetics*. Oxford Academic, 181(4), pp. 1673–1677. doi: 10.1534/GENETICS.108.100065.

Mazo-Vargas, A. *et al.* (2017) 'Macroevolutionary shifts of WntA function potentiate butterfly wing-pattern diversity', *Proceedings of the National Academy of Sciences of the United States of America*. National Academy of Sciences, 114(40), pp. 10701–10706. doi: 10.1073/pnas.1708149114.

McCallum, C. M. *et al.* (2000) 'Targeting induced local lesions IN genomes (TILLING) for plant functional genomics', *Plant Physiology*. Plant Physiol, pp. 439–442. doi: 10.1104/pp.123.2.439.

Mehravar, M. *et al.* (2019) 'Mosaicism in CRISPR/Cas9-mediated genome editing', *Developmental Biology*. Academic Press, 445(2), pp. 156–162. doi: 10.1016/J.YDBIO.2018.10.008.

Mei, Y. *et al.* (2016) 'Recent Progress in CRISPR/Cas9 Technology', *Journal of Genetics and Genomics*. Institute of Genetics and Developmental Biology, pp. 63–75. doi: 10.1016/j.jgg.2016.01.001.

Mianné, J. *et al.* (2017) 'Analysing the outcome of CRISPR-aided genome editing in embryos: Screening, genotyping and quality control', *Methods*. Academic Press Inc., pp. 68–76. doi: 10.1016/j.ymeth.2017.03.016.

Miki, D. *et al.* (2018) 'CRISPR/Cas9-mediated gene targeting in Arabidopsis using sequential transformation', *Nature Communications*. Nature Publishing Group, 9(1), pp. 1–9. doi: 10.1038/s41467-018-04416-0.

Modrell, M. S. and Baker, C. V. H. (2012) 'Evolution of electrosensory ampullary organs: Conservation of Eya4 expression during lateral line development in jawed vertebrates', *Evolution and Development*. Europe PMC Funders, 14(3), pp. 277–285. doi: 10.1111/j.1525-142X.2012.00544.x.

Morcos, P. A. (2007) 'Achieving targeted and quantifiable alteration of mRNA splicing with Morpholino oligos', *Biochemical and Biophysical Research Communications*. Biochem Biophys Res Commun, 358(2), pp. 521–527. doi: 10.1016/j.bbrc.2007.04.172.

Morcos, P. A., Li, Y. and Jiang, S. (2008) 'Vivo-Morpholinos: A non-peptide transporter delivers Morpholinos into a wide array of mouse tissues', *BioTechniques*. Future Science Ltd London, UK , 45(6), pp. 613–623. doi: 10.2144/000113005.

Morcos, P. A., Vincent, A. C. and Moulton, J. D. (2015) 'Gene Editing Versus Morphants', *Zebrafish*, 12(5), p. 319. doi: 10.1038/nature14580.

Moriyama, Y. *et al.* (2016) 'Evolution of the fish heart by sub/neofunctionalization of an elastin gene.', *Nature communications*. Nature Publishing Group, 7, p. 10397. doi:

10.1038/ncomms10397.

Moulton, J. (2016) ‘Guide for Morpholino Users: Towards Therapeutics’, *Journal of Drug Discovery, Development and Delivery*, 3(2), pp. 1–13.

Moulton, J. D. and Shan, J. (2009) ‘Gene knockdowns in adult animals: PPMOs and vivo-morpholinos’, *Molecules*. Molecular Diversity Preservation International, pp. 1304–1323. doi: 10.3390/molecules14031304.

Mylonas, C. C., Hinshaw, J. M. and Sullivan, C. V. (1992) ‘GnRHa-induced ovulation of brown trout (Salmo trutta) and its effects on egg quality’, *Aquaculture*. Elsevier, 106(3–4), pp. 379–392. doi: 10.1016/0044-8486(92)90268-P.

Mylonas, C. C. and Zohar, Y. (2007) ‘Promoting oocyte maturation, ovulation and spawning in farmed fish’, in *The Fish Oocyte: From Basic Studies to Biotechnological Applications*. Springer Netherlands, pp. 437–474. doi: 10.1007/978-1-4020-6235-3_15.

Nagayoshi, S. *et al.* (2008) ‘Insertional mutagenesis by the Tol2 transposon-mediated enhancer trap approach generated mutations in two developmental genes: tcf7 and synembryn-like’, *Development*. The Company of Biologists, 135(1), pp. 159–169. doi: 10.1242/dev.009050.

Nakazawa, T. *et al.* (2020) ‘Effect of CRISPR/Cas9-Mediated PD-1-Disrupted Primary Human Third-Generation CAR-T Cells Targeting EGFRvIII on In Vitro Human Glioblastoma Cell Growth’, *Cells*. NLM (Medline), 9(4). doi: 10.3390/cells9040998.

Napoli, C., Lemieux, C. and Jorgensen, R. (1990) *lntroduction of a Chimeric Chalcone Synthase Gene into Petunia Results in Reversible Co-Suppression of Homologous Genes Ín trans*, *The Plant Cell*. American Society of Plant Physiologists.

Nguyen, L. *et al.* (2020) ‘Ontogeny of electric organ and electric organ discharge in Campylomormyrus rhynchophorus (Teleostei: Mormyridae)’, *Journal of Comparative Physiology A*, 206(3), pp. 453–466. doi: 10.1007/s00359-020-01411-z.

Nguyen, M. D. L. *et al.* (2017) ‘Reproduction and Development in some species of the weakly electric genus Campylomormyrus (Mormyridae, Teleostei)’, *Environmental Biology of Fishes*. Environmental Biology of Fishes, pp. 49–68. doi: 10.1007/s10641-016-0554-1.

Nord, A. S. *et al.* (2006) ‘The International Gene Trap Consortium Website: a portal to all publicly available gene trap cell lines in mouse.’, *Nucleic acids research*. Oxford University Press, 34(Database issue), p. D642. doi: 10.1093/nar/gkj097.

Notch, E. G. *et al.* (2011) ‘Morpholino Gene Knockdown in Adult Fundulus heteroclitus: Role of SGK1 in Seawater Acclimation’, *PLoS ONE*. Edited by V. Laudet. Public Library of Science, 6(12), p. e29462. doi: 10.1371/journal.pone.0029462.

Nuraini, N. *et al.* (2017) ‘Induced spawning of siban fish Cyclocheilichthys apogon using

Ovaprim', *F1000Research*. Faculty of 1000 Ltd, 6(1855). doi: 10.12688/f1000research.12885.1.

Obholzer, N. *et al.* (2012) 'Rapid positional cloning of zebrafish mutations by linkage and homozygosity mapping using whole-genome sequencing', *Development (Cambridge)*. Development, 139(22), pp. 4280–4290. doi: 10.1242/dev.083931.

Okedi, J. (1970) 'A Study of the Fecundity of Some Mormyrid Fishes from Lake Victoria', *East African Agricultural and Forestry Journal*, 35(4), pp. 436–442. doi: 10.1080/00128325.1970.11662433.

De Oliveira, V. C. *et al.* (2019) 'Edition of TFAM gene by CRISPR/Cas9 technology in bovine model', *PLoS ONE*. Public Library of Science, 14(3). doi: 10.1371/journal.pone.0213376.

Palatnik, J. F. *et al.* (2003) 'Control of leaf morphogenesis by miRNAs Evolution of LEAFY View project Chloroplast quality control View project', *Article in Nature*. doi: 10.1038/nature01958.

Park, S.-A. *et al.* (2015) 'E2F8 as a Novel Therapeutic Target for Lung Cancer', *JNCI: Journal of the National Cancer Institute*. Oxford University Press, 107(9). doi: 10.1093/jnci/djv151.

Parks, A. L. *et al.* (2004) 'Systematic generation of high-resolution deletion coverage of the Drosophila melanogaster genome', *Nature Genetics 2004 36:3*. Nature Publishing Group, 36(3), pp. 288–292. doi: 10.1038/ng1312.

Patterson, J. M. and Zakon, H. H. (1993) 'Bromodeoxyuridine labeling reveals a class of satellite-like cells within the electric organ', *Journal of Neurobiology*, 24(5), pp. 660–674.

Patterson, J. M. and Zakon, H. H. (1997) 'Transdifferentiation of muscle to electric organ: Regulation of muscle-specific proteins is independent of patterned nerve activity', *Developmental Biology*. Elsevier, 186(1), pp. 115–126.

Paul, C. *et al.* (2015) 'Comparative histology of the adult electric organ among four species of the genus Campylomormyrus (Teleostei: Mormyridae)', *Journal of Comparative Physiology A*. Springer Berlin Heidelberg, 201(4), pp. 357–374. doi: 10.1007/s00359-015-0995-6.

Paul, C. *et al.* (2016) 'Evidence for Non-neutral Evolution in a Sodium Channel Gene in African Weakly Electric Fish (Campylomormyrus, Mormyridae)', *Journal of Molecular Evolution*. Springer US, 83(1–2), pp. 61–77. doi: 10.1007/s00239-016-9754-8.

Pinch, M. *et al.* (2016) ' The myogenic electric organ of Sternopygus macrurus : a non-contractile tissue with a skeletal muscle transcriptome ', *PeerJ*, 4, p. e1828. doi: 10.7717/peerj.1828.

Pitchers, W. R. *et al.* (2016) 'Electric fish genomics: Progress, prospects, and new tools for neuroethology'. doi: 10.1016/j.jphysparis.2016.10.003.

Prince, V. E. and Pickett, F. B. (2002) 'Splitting pairs: the diverging fates of duplicated genes', *Nature Reviews Genetics*. Nature Publishing Group, 3(11), pp. 827–837. doi: 10.1038/nrg928.

Qi, L. S. *et al.* (2013) 'Repurposing CRISPR as an RNA-γuided platform for sequence-specific control of gene expression', *Cell*. Elsevier B.V., 152(5), pp. 1173–1183. doi: 10.1016/j.cell.2013.02.022.

Qin, W. *et al.* (2015) 'Efficient CRISPR/Cas9-Mediated Genome Editing in Mice by Zygote Electroporation of Nuclease', *Genetics*, 200(June), pp. 423–430. doi: 10.1534/genetics.115.176594.

Rach, J. J., Marks, J. A. and Dawson, V. K. (1995) 'Effect of Water Flow Rates in Hatching Jars to Control Fungal Infections of Rainbow Trout Eggs', *The Progressive Fish-Culturist*. John Wiley & Sons, Ltd, 57(3), pp. 226–230. doi: 10.1577/1548-8640(1995)057<0226:EOWFRI>2.3.CO;2.

Ramharack, P. and Soliman, M. E. S. (2018) 'Bioinformatics-based tools in drug discovery: the cartography from single gene to integrative biological networks', *Drug Discovery Today*, 23(9). doi: 10.1016/j.drudis.2018.05.041.

Ran, F. A. *et al.* (2013) 'Double nicking by RNA-guided CRISPR cas9 for enhanced genome editing specificity', *Cell*. NIH Public Access, 154(6), pp. 1380–1389. doi: 10.1016/j.cell.2013.08.021.

Rana, A. A. *et al.* (2006) 'Defining Synphenotype Groups in Xenopus tropicalis by Use of Antisense Morpholino Oligonucleotides', *PLoS Genetics*. Public Library of Science, 2(11), p. e193. doi: 10.1371/journal.pgen.0020193.

Rasys, A. M. *et al.* (2019) 'CRISPR-Cas9 Gene Editing in Lizards through Microinjection of Unfertilized Oocytes', *Cell Reports*. Elsevier B.V., 28(9), pp. 2288-2292.e3. doi: 10.1016/j.celrep.2019.07.089.

Roth, A. *et al.* (2019) 'A genetic switch for worker nutritionmediated traits in honeybees', *PLoS Biology*. Public Library of Science, 17(3), p. e3000171. doi: 10.1371/journal.pbio.3000171.

Rubin, B. E. *et al.* (2015) 'The essential gene set of a photosynthetic organism', *Proceedings of the National Academy of Sciences of the United States of America*. National Academy of Sciences, 112(48), pp. e6634–e6643. doi: 10.1073/pnas.1519220112.

Russell, J. J. *et al.* (2017) 'Non-model model organisms', *BMC Biology*. BioMed Central Ltd., 15(1), pp. 1–31. doi: 10.1186/s12915-017-0391-5.

Salazar, V. L., Krahe, R. and Lewis, J. E. (2013) 'The energetics of electric organ discharge generation in gymnotiform weakly electric fish.', *The Journal of experimental biology*. The Company of Biologists Ltd, 216(Pt 13), pp. 2459–68. doi: 10.1242/jeb.082735.

Salazar, V. L. and Stoddard, P. K. (2008) 'Sex differences in energetic costs explain sexual dimorphism in the circadian rhythm modulation of the electrocommunication signal of the gymnotiform fish Brachyhypopomus pinnicaudatus', *Journal of Experimental Biology*. The Company of Biologists Ltd, 211(6), pp. 1012–1020. doi: 10.1242/jeb.014795.

Salisbury, J. P. *et al.* (2015) 'The central nervous system transcriptome of the weakly electric brown ghost knifefish (Apteronotus leptorhynchus): De novo assembly, annotation, and proteomics validation', *BMC Genomics*. BioMed Central Ltd., 16(1), p. 166. doi: 10.1186/s12864-015-1354-2.

Sánchez-León, S. *et al.* (2018) 'Low-gluten, nontransgenic wheat engineered with CRISPR/Cas9', *Plant Biotechnology Journal*. Blackwell Publishing Ltd, 16(4), pp. 902–910. doi: 10.1111/pbi.12837.

Sanchez, N. E. *et al.* (2017) 'Whole genome sequencing-based mapping and candidate identification of mutations from fixed zebrafish tissue', *G3: Genes, Genomes, Genetics*. G3 (Bethesda), 7(10), pp. 3415–3425. doi: 10.1534/g3.117.300212.

Sarin, S. *et al.* (2008) 'Caenorhabditis elegans mutant allele identification by whole-genome sequencing', *Nature methods*. NIH Public Access, 5(10), p. 865. doi: 10.1038/NMETH.1249.

Savy, V. *et al.* (2020) 'CRISPR-on for activation of endogenous SMARCA4 and TFAP2C expression in bovine embryos', *Reproduction*. BioScientifica Ltd., 159(6), pp. 767–778. doi: 10.1530/REP-19-0517.

Schreier, T. M., Rach, J. J. and Howe, G. E. (1996) 'Efficacy of formalin, hydrogen peroxide, and sodium chloride on fungal-infected rainbow trout eggs', *Aquaculture*. Elsevier, 140(4), pp. 323–331. doi: 10.1016/0044-8486(95)01182-X.

Schugardt, C. and Kirschbaum, F. (2004) 'Control of gonadal maturation and regression by experimental variation of environmental factors in the mormyrid fish, Mormyrus rume proboscirostris', *Environmental Biology of Fishes*, 70, pp. 227–233.

Schulman, S. *et al.* (2016) 'Extracellular Thiol Isomerases and Their Role in Thrombus Formation', *Antioxidants and Redox Signaling*. Mary Ann Liebert Inc., pp. 1–5. doi: 10.1089/ars.2015.6530.

Schwassmann, H. O., Assunção, M. I. S. and Kirschbaum, F. (2014) 'Ontogeny of the Electric Organs in the Electric Eel, Electrophorus electricus : Physiological, Histological, and Fine Structural Investigations', *Brain, Behavior and Evolution*, 84, pp. 288–302. doi: 10.1159/000367884.

Shah, A. N. *et al.* (2015) 'Rapid reverse genetic screening using CRISPR in zebrafish', *Nature Methods*. Nature Publishing Group, 12(6), pp. 535–540. doi: 10.1038/nmeth.3360.

Shan, Q. *et al.* (2014) 'Genome editing in rice and wheat using the CRISPR/Cas system', *Nature*

Protocols. Nature Publishing Group, 9(10), pp. 2395–2410. doi: 10.1038/nprot.2014.157.

Shenkel, S. and Sigworth, F. J. (1991) 'Patch recordings from the electrocytes electrophorus electricus: Na currents and PNa/PK variability', *Journal of General Physiology*. The Rockefeller University Press, 97(5), pp. 1013–1041. doi: 10.1085/jgp.97.5.1013.

Shestopalov, I. A., Pitt, C. L. W. and Chen, J. K. (2012) 'Spatiotemporal resolution of the Ntla transcriptome in axial mesoderm development', *Nature Chemical Biology*. Nature Publishing Group, 8(3), pp. 270–276. doi: 10.1038/nchembio.772.

Shrimp, J. H. *et al.* (2018) 'Chemical Control of a CRISPR-Cas9 Acetyltransferase', *ACS Chemical Biology*. American Chemical Society, 13(2), pp. 455–460. doi: 10.1021/acschembio.7b00883.

Sifa, L. and Mathias, J. A. (1987) 'The critical period of high mortality of larvae fish -A discussion based on current research', *Chinese Journal of Oceanology and Limnology*. Springer, 5(1), pp. 80–96. doi: 10.1007/BF02848526.

Singh, P., Schimenti, J. C. and Bolcun-Filas, E. (2015) 'A mouse geneticist's practical guide to CRISPR applications', *Genetics*. Genetics, 199(1), pp. 1–15. doi: 10.1534/genetics.114.169771.

Sinnett, P. M. and Markham, M. R. (2015) 'Food deprivation reduces and leptin increases the amplitude of an active sensory and communication signal in a weakly electric fish', *Hormones and Behavior*. Academic Press Inc., 71, pp. 31–40. doi: 10.1016/j.yhbeh.2015.03.010.

Sivasubbu, S. *et al.* (2007) 'Insertional mutagenesis strategies in zebrafish', *Genome Biology*. BioMed Central, p. S9. doi: 10.1186/gb-2007-8-s1-s9.

Small, B. C. (2006) 'Managing Hatch Rate and Diseases in Catfish Eggs', *Southern Regional Aquaculture Center*, (1804).

Smith, G. T., Schniederjan, S. and Nguyenkim, J. (2013) 'Evolution and hormonal regulation of sex differences in the electrocommunication behavior of ghost knifefishes (Apteronotidae).', *The Journal of experimental biology*. The Company of Biologists Ltd, 216(Pt 13), pp. 2421–33. doi: 10.1242/jeb.082933.

Sorgeloos, P., Dhert, P. and Candreva, P. (2001) 'Use of the brine shrimp, Artemia spp., in marine fish larviculture', in *Aquaculture*. Elsevier, pp. 147–159. doi: 10.1016/S0044-8486(01)00698-6.

Stickney, H. L. *et al.* (2002) 'Rapid Mapping of Zebrafish Mutations With SNPs and Oligonucleotide Microarrays', *Genome Research*. Cold Spring Harbor Laboratory Press, 12(12), p. 1929. doi: 10.1101/GR.777302.

Stoddard, P. K. (2002) 'The evolutionary origins of electric signal complexity', *Journal of Physiology Paris*, 96(5–6), pp. 485–491. doi: 10.1016/S0928-4257(03)00004-4.

Sudova, E. *et al.* (2007) 'Negative effects of malachite green and possibilities of its replacement in the treatment of fish eggs and fish: A review', *Veterinarni Medicina*. Czech Academy of Agricultural Sciences, pp. 527–539. doi: 10.17221/2027-VETMED.

Suhail, A. *et al.* (2019) 'DeSUMOylase SENP7-Mediated Epithelial Signaling Triggers Intestinal Inflammation via Expansion of Gamma-Delta T Cells', *Cell Reports*. Elsevier B.V., 29(11), pp. 3522-3538.e7. doi: 10.1016/j.celrep.2019.11.028.

Sullivan, J. P. *et al.* (2004) 'AFLPs resolve phylogeny and reveal mitochondrial introgression within a species flock of African electric fish (Mormyroidea: Teleostei).', *Evolution; international journal of organic evolution*, 58(4), pp. 825–841.

Sun, D. *et al.* (2017) 'Progress and Prospects of CRISPR/Cas Systems in Insects and Other Arthropods', *Frontiers in Physiology*. Frontiers, 8(608), pp. 1–22. doi: 10.3389/fphys.2017.00608.

Sunagawa, G. A. *et al.* (2016) 'Mammalian Reverse Genetics without Crossing Reveals Nr3a as a Short-Sleeper Gene', *Cell Reports*. Elsevier B.V., 14(3), pp. 662–677. doi: 10.1016/j.celrep.2015.12.052.

Suquet, M. *et al.* (1992) 'Assessment of sperm concentration and motility in turbot (Scophthalmus maximus)', *Aquaculture*. Elsevier, 101(1–2), pp. 177–185. doi: 10.1016/0044-8486(92)90241-C.

Swapna, I. *et al.* (2018) 'Electrostatic Tuning of a Potassium Channel in Electric Fish', *Current Biology*. Cell Press, 28(13), pp. 2094-2102.e5. doi: 10.1016/j.cub.2018.05.012.

Sztal, T. E. *et al.* (2015) 'Zebrafish models for nemaline myopathy reveal a spectrum of nemaline bodies contributing to reduced muscle function', *Acta Neuropathologica*. Springer Verlag, 130(3), pp. 389–406. doi: 10.1007/s00401-015-1430-3.

Tang, X. J. *et al.* (2007) 'Regulating gene expression in zebrafish embryos using light-activated, negatively charged peptide nucleic acids', *Journal of the American Chemical Society*. American Chemical Society , 129(36), pp. 11000–11001. doi: 10.1021/ja073723s.

'Targeting zebrafish' (2000) *Nature Genetics*. Nature Publishing Group, pp. 129–130. doi: 10.1038/79826.

Thompson, A. *et al.* (2014) 'Expression evolution facilitated the convergent neofunctionalization of a sodium channel gene', *Molecular Biology and Evolution*, 31(8), pp. 1941–1955. doi: 10.1093/molbev/msu145.

Till, B. J. *et al.* (2003) 'Large-scale discovery of induced point mutations with high-throughput TILLING', *Genome Research*. Genome Res, 13(3), pp. 524–530. doi: 10.1101/gr.977903.

Traeger, L. L. *et al.* (2015a) 'Unique patterns of transcript and miRNA expression in the South

American strong voltage electric eel (Electrophorus electricus)', *BMC Genomics*, 16(243), pp. 1–13. doi: 10.1186/s12864-015-1288-8.

Traeger, L. L. *et al.* (2015b) 'Unique patterns of transcript and miRNA expression in the South American strong voltage electric eel (Electrophorus electricus)', *BMC Genomics*. BioMed Central, 16(1), p. 243. doi: 10.1186/s12864-015-1288-8.

Trible, W. *et al.* (2017) 'orco Mutagenesis Causes Loss of Antennal Lobe Glomeruli and Impaired Social Behavior in Ants', *Cell*. Cell Press, 170(4), pp. 727-735.e10. doi: 10.1016/j.cell.2017.07.001.

Le Trionnaire, G. *et al.* (2019) 'An integrated protocol for targeted mutagenesis with CRISPR-Cas9 system in the pea aphid', *Insect Biochemistry and Molecular Biology*. Elsevier Ltd, 110, pp. 34–44. doi: 10.1016/j.ibmb.2019.04.016.

Tsai, S. Q. *et al.* (2014) 'Dimeric CRISPR RNA-guided FokI nucleases for highly specific genome editing', *Nature Biotechnology*. Nature Publishing Group, 32(6), pp. 569–576. doi: 10.1038/nbt.2908.

Tsai, S. Q. and Joung, J. K. (2016) 'Defining and improving the genome-wide specificities of CRISPR-Cas9 nucleases', *Nature Reviews Genetics*. Nature Publishing Group, 17(5), pp. 300–312. doi: 10.1038/nrg.2016.28.

Turetzek, N. *et al.* (2016) 'Neofunctionalization of a Duplicate *dachshund* Gene Underlies the Evolution of a Novel Leg Segment in Arachnids', *Molecular Biology and Evolution*. Oxford University Press, 33(1), pp. 109–121. doi: 10.1093/molbev/msv200.

Tye, M. *et al.* (2015) 'Nonhatching decapsulated artemia cysts as a replacement to artemia nauplii in juvenile and adult zebrafish culture', *Zebrafish*. Mary Ann Liebert Inc., 12(6), pp. 457–461. doi: 10.1089/zeb.2014.1031.

Unguez, G. A. (2013) 'Electric fish: new insights into conserved processes of adult tissue regeneration', *Journal of Experimental Biology*, 216(13), pp. 2478–2486. doi: 10.1242/jeb.082396.

Unguez, G. A. and Zakon, H. H. (2002) 'Skeletal muscle transformation into electric organ in S. macrurus depends on innervation', *Journal of Neurobiology*, 53(3), pp. 391–402.

Varshney, G. K. *et al.* (2015) 'High-throughput gene targeting and phenotyping in zebrafish using CRISPR/Cas9.', *Genome research*. Cold Spring Harbor Laboratory Press, 25(7), pp. 1030–42. doi: 10.1101/gr.186379.114.

Venken, K. J. T. and Bellen, H. J. (2014) 'Chemical mutagens, transposons, and transgenes to interrogate gene function in Drosophila melanogaster', *Methods*. Academic Press Inc., 68(1), pp. 15–28. doi: 10.1016/j.ymeth.2014.02.025.

Wang, T. *et al.* (2014) 'Genetic screens in human cells using the CRISPR-Cas9 system.', *Science (New York, N.Y.)*. NIH Public Access, 343(6166), pp. 80–4. doi: 10.1126/science.1246981.

Wang, X. H. *et al.* (2006) 'RNA interference directs innate immunity against viruses in adult Drosophila', *Science*. American Association for the Advancement of Science, 312(5772), pp. 452–454. doi: 10.1126/science.1125694.

Ward, A. J. *et al.* (2014) 'Nonsense-mediated decay as a terminating mechanism for antisense oligonucleotides', *Nucleic Acids Research*. Oxford University Press, 42(9), pp. 5871–5879. doi: 10.1093/nar/gku184.

Westby, G. W. M. and Kirschbaum, F. (1977) 'Emergence and development of the electric organ discharge in the mormyrid fish, Pollimyrus isidori I. the larval discharge', *Journal of Comparative Physiology*, 122(2), pp. 251–271. doi: 10.1007/BF00611894.

Westby, G. W. M. and Kirschbaum, F. (1978) 'Emergence and development of the electric organ discharge in the mormyrid fish, Pollimyrus isidori II. Replacement of the larval by the adult discharge', *Journal of comparative physiology*, 127(1), pp. 45–59.

Westerfield, M. (2000) *The zebrafish book. A guide for the laboratory use of zebrafish (Danio rerio)*. 4th ed. Oregon Press.

Whipps, C. M. and Kent, M. L. (2019) 'Bacterial and fungal diseases of zebrafish', in *The Zebrafish in Biomedical Research: Biology, Husbandry, Diseases, and Research Applications*. Elsevier, pp. 495–508. doi: 10.1016/B978-0-12-812431-4.00041-5.

Wicks, S. R. *et al.* (2001) 'Rapid gene mapping in Caenorhabditis elegans using a high density polymorphism map', *Nature Genetics*. Nat Genet, 28(2), pp. 160–164. doi: 10.1038/88878.

Widmark, J. *et al.* (2011) 'Differential evolution of voltage-gated sodium channels in tetrapods and teleost fishes', *Molecular Biology and Evolution*. Oxford Academic, 28(1), pp. 859–871. doi: 10.1093/molbev/msq257.

Wong, T. T. and Zohar, Y. (2015) 'Production of reproductively sterile fish by a non-transgenic gene silencing technology', *Scientific Reports*. Nature Publishing Group, 5(1), pp. 1–8. doi: 10.1038/srep15822.

Wu, J. L. *et al.* (2005) 'Chemical- and irradiation-induced mutants of indica rice IR64 for forward and reverse genetics', *Plant Molecular Biology*. Springer, pp. 85–97. doi: 10.1007/s11103-004-5112-0.

Wu, M. *et al.* (2020) 'CRISPR/Cas9 mediated genetic resource for unknown kinase and phosphatase genes in Drosophila', *Scientific Reports*. Nature Research, 10(1), pp. 1–6. doi: 10.1038/s41598-020-64253-4.

Wu, R. S. *et al.* (2018) 'A Rapid Method for Directed Gene Knockout for Screening in G0

Zebrafish', *Developmental Cell*. Cell Press, 46(1), pp. 112-125.e4. doi: 10.1016/j.devcel.2018.06.003.

Xie, Z. *et al.* (2020) 'Generation of pRSAD2 gene knock-in pig via CRISPR/Cas9 technology', *Antiviral Research*. Elsevier B.V., 174. doi: 10.1016/j.antiviral.2019.104696.

Xu, J. *et al.* (2020) 'A cytokine screen using CRISPR-Cas9 knock-in reporter pig iPS cells reveals that Activin A regulates NANOG', *Stem Cell Research and Therapy*. BioMed Central Ltd., 11(1). doi: 10.1186/s13287-020-1588-z.

Yamazoe, S. *et al.* (2012) 'Cyclic Caged Morpholinos: Conformationally Gated Probes of Embryonic Gene Function', *Angewandte Chemie*. Wiley, 124(28), pp. 7014–7017. doi: 10.1002/ange.201201690.

Yang, H. *et al.* (2013) 'One-step generation of mice carrying reporter and conditional alleles by CRISPR/Cas mediated genome engineering', *Cell*, 154(6), pp. 1370–1379. doi: 10.1016/j.cell.2013.08.022.One-step.

Yen, S. T. *et al.* (2014) 'Somatic mosaicism and allele complexity induced by CRISPR/Cas9 RNA injections in mouse zygotes', *Developmental Biology*. Academic Press Inc., 393(1), pp. 3–9. doi: 10.1016/j.ydbio.2014.06.017.

Zadmajid, V. *et al.* (2017) 'Hormonal induction of ovulation using Ovaprim™ [(D-Arg6, Pro9NEt)-sGnRH + domperidone] and its impact on embryonic development of wild-caught Longspine scraper, Capoeta trutta (Heckel, 1843)', *Animal Reproduction Science*, 187, pp. 79–90. doi: 10.1016/j.anireprosci.2017.10.009.

Zakon, H. H. *et al.* (2006) 'Sodium channel genes and the evolution of diversity in communication signals of electric fishes: convergent molecular evolution.', *Proc Natl Acad Sci U S A*, 103(10), pp. 3675–3680.

Zakon, H. H. *et al.* (2008) 'Molecular evolution of communication signals in electric fish', *Journal of Experimental Biology*. Co Biol, 211(11), p. 1814.

Zang, L. *et al.* (2019) 'Therapeutic Silencing of Centromere Protein X Ameliorates Hyperglycemia in Zebrafish and Mouse Models of Type 2 Diabetes Mellitus', *Frontiers in Genetics*. Frontiers Media S.A., 10(JUL), p. 693. doi: 10.3389/fgene.2019.00693.

Zhang, H. *et al.* (2015) 'Time point-based integrative analyses of deep-transcriptome identify four signal pathways in blastemal regeneration of zebrafish lower jaw', *Stem Cells*, 33(3), pp. 806–818. doi: 10.1002/stem.1899.

Zhang, L., Mazo-Vargas, A. and Reed, R. D. (2017) 'Single master regulatory gene coordinates the evolution and development of butterfly color and iridescence', *Proceedings of the National Academy of Sciences of the United States of America*. National Academy of Sciences, 114(40), pp. 10707–10712. doi: 10.1073/pnas.1709058114.

Zhang, L. and Reed, R. D. (2017) ‘A Practical Guide to CRISPR/Cas9 Genome Editing in Lepidoptera’, in *Diversity and Evolution of Butterfly Wing Patterns: An Integrative Approach*. Springer, Singapore, pp. 155–172. doi: 10.1007/978-981-10-4956-9_8.

Zhang, X. H. *et al.* (2015) ‘Off-target effects in CRISPR/Cas9-mediated genome engineering’, *Molecular Therapy - Nucleic Acids*. Nature Publishing Group, p. e264. doi: 10.1038/mtna.2015.37.

Zhou, J. *et al.* (2014) ‘Dual sgRNAs facilitate CRISPR/Cas9-mediated mouse genome targeting’, *FEBS Journal*. Blackwell Publishing Ltd, pp. 1717–1725. doi: 10.1111/febs.12735.

Zischewski, J., Fischer, R. and Bortesi, L. (2017) ‘Detection of on-target and off-target mutations generated by CRISPR/Cas9 and other sequence-specific nucleases’, *Biotechnology Advances*. Elsevier Inc., pp. 95–104. doi: 10.1016/j.biotechadv.2016.12.003.

Zu, Y. *et al.* (2016) ‘Biallelic editing of a lamprey genome using the CRISPR/Cas9 system’, *Scientific Reports*. Nature Publishing Group, 6(23496), pp. 1–9. doi: 10.1038/srep23496.

Zuo, E. *et al.* (2017) ‘One-step generation of complete gene knockout mice and monkeys by CRISPR/Cas9-mediated gene editing with multiple sgRNAs’, *Cell Research*. Nature Publishing Group, 27(7), pp. 933–945. doi: 10.1038/cr.2017.81.

Zuryn, S. *et al.* (2010) ‘A Strategy for Direct Mapping and Identification of Mutations by Whole-Genome Sequencing’, *Genetics*. Oxford University Press, 186(1), p. 427. doi: 10.1534/GENETICS.110.119230.

Zwaal, R. R. *et al.* (1993) ‘Target-selected gene inactivation in Caenorhabditis elegans by using a frozen transposon insertion mutant bank’, *Proceedings of the National Academy of Sciences of the United States of America*. National Academy of Sciences, 90(16), pp. 7431–7435. doi: 10.1073/pnas.90.16.7431.